BIOTIC RESPONSE TO PALEOCEANOGRAPHIC CHANGES IN THE MIDDLE EOCENE OF BLAKE NOSE, WESTERN NORTH ATLANTIC

A Dissertation

by

CHIOMA UCHE OKAFOR

Submitted to the Office of Graduate Studies of
Texas A&M University
in partial fulfillment of the requirements for the degree of

DOCTOR OF PHILOSOPHY

May 2009

Major Subject: Geology

BIOTIC RESPONSE TO PALEOCEANOGRAPHIC CHANGES IN THE MIDDLE EOCENE OF BLAKE NOSE, WESTERN NORTH ATLANTIC

A Dissertation

by

CHIOMA UCHE OKAFOR

Submitted to the Office of Graduate Studies of
Texas A&M University
in partial fulfillment of the requirements for the degree of

DOCTOR OF PHILOSOPHY

Approved by:

Co-Chairs of Committee,	Deborah Thomas
	John Firth
Committee Members,	Thomas Olszewski
	Bridget Wade
	Niall Slowey
Head of Department,	Andreas Kronenberg

May 2009

Major Subject: Geology

ABSTRACT

Biotic Response to Paleoceanographic Changes in the Middle Eocene of Blake Nose, Western North Atlantic. (May 2009)

Chioma Uche Okafor, B.S., University of Nigeria Nsukka;

M.S., University of Missouri Rolla

Co-Chairs of Advisory Committee: Dr. Deborah Thomas
Dr. John Firth

Geochemical proxy records of sea surface environmental conditions at Blake Nose indicate short-term high amplitude variations. In order to investigate the response of calcareous nannoplankton to these short-term sea-surface environmental changes, we developed a high-resolution Eocene planktonic foraminifera Mg/Ca record and calcareous nannofossil absolute abundance record for ODP Site 1052 spanning the late middle Eocene (37.85 to 37.45 Ma). These data enable direct comparison of the absolute nannofossil abundance data to geochemical paleoenvironmental proxies (Mg/Ca, $\delta^{18}O$ and $\delta^{13}C$) to determine the phytoplankton response to paleoenvironmental change and whether temperature or nutrient levels exerted primary control.

The nannofossil absolute abundances were estimated using a combination of the random settling technique (RST) and spiking method (SM), which are two independent methods. Both methods yielded similar and reproducible results.

The calculated Mg/Ca paleotemperature record indicates a decrease in SSTs from ~33 to 28°C, while the $\delta^{18}O_{sw}$ values calculated from the Mg/Ca paleotemperature also decreased from ~3‰ at 37.83 Ma to ~2‰ at 37.6 Ma. The combined trends of the SST and $\delta^{18}O_{sw}$ suggest that continental ice did not have a major influence on the climate during the study interval. Variations in the Gulf Stream (e.g. track of proto-Gulf stream, number and transit of eddies, and Gulf Stream related upwelling), may have contributed to the reconstructed sea surface hydrographical changes at Blake Nose. However, overall weakening of the hydrological cycle as global climate transitioned from a greenhouse to an icehouse could be the major factor controlling the hydrographical changes at Blake Nose.

Approximately 48 nannofossil taxa were identified in this study. These taxa have been grouped into major, minor and rare taxa based on their abundance in any given sample. Results of the statistical analyses (canonical correspondence analysis CCA, Cluster analysis, and correspondence analysis CA) used to relate the nannofossil abundance to environmental parameters did not show expected relationships between the nannofossil absolute abundance and environmental parameters. There are several explanations for this which includes dominance of biotic control over abiotic control, difference in depth habitats between the planktonic foraminifera used for the

geochemical proxies and the calcareous nannoplankton, and changing combinations of environmental controls operating during the ~400 ky interval. This suggests that these factors should be taken into account when making conclusions about nannofossil environmental preferences.

ACKNOWLEDGEMENTS

I would like to thank my committee co-chairs, Dr. Thomas and Dr. Firth, and my committee members, Dr. Olszewski, Dr. Wade, and Dr. Slowey for their guidance and support throughout the course of this research.

Thanks also go to my friends and colleagues and the department faculty and staff for making my time at Texas A&M University a great experience. I also want to extend my gratitude to Texas A&M University, which provided the major part of the funding I needed for successful completion of my program.

Thanks to my family for their encouragement, especially my husband for his patience and love. Finally I would like to thank God for making all this possible. I could not have made it through without Him.

TABLE OF CONTENTS

Page

LIST OF FIGURES

FIGURE Page

LIST OF TABLES

1. INTRODUCTION: RESEARCH OVERVIEW

Significant short-term, cyclic variations have been identified in the $\delta^{18}O$ record of Middle Eocene planktonic foraminifera from Blake Nose, western North Atlantic. The causes of the variations are not well understood and the response of marine microorganisms to these climatic changes is also not clear. The main aim of this research is to document the response of marine phytoplankton (calcareous nannoplankton), which are major primary producers in the ocean, to short-term climatic changes identified in the Middle Eocene of Blake Nose, western North Atlantic.

The Eocene was chosen for this study because it is the only period during the Cenozoic that has pCO_2 values similar to the values projected by IPCC. Geochemistry, paleontology, and sedimentology have revealed that the Eocene climate was much warmer than any other time during the Cenozoic. Eocene high latitude SSTs (15-18°C, Sluijs et al., 2008) were warmer than present. Such warm high-latitude SSTs imply that large scale polar ice sheets did not exist. Estes and Hutchinson (1980) and Wolfe (1980) documented evidence of subtropical fauna and flora existing in sub-polar regions during the Eocene.

_____

This dissertation follows the style of *Paleoceanography*.

Starting from the Early Eocene (~50 Ma), global mean temperatures began to cool and by the earliest Oligocene, there was a rapid expansion of ice-sheets in Antarctica (Zachos et al., 2001; Lear et al., 2000; Coxall et al., 2005). Oxygen isotope values increased for both benthic and planktonic foraminifera which indicates cooling of deeper waters as well as surface waters (Zachos et al., 1994). The long-term cooling of the climate from the Eocene has been attributed to decreasing pCO_2 levels, from about 2000 ppmv in the Paleocene and early Eocene to about 350 ppmv in the latest Oligocene, based on alkenone and boron isotope reconstructions (Pearson and Palmer, 2000; Pagani et al., 2005).

Superimposed on the long-term cooling of the climate during the Eocene are short-term, high amplitude changes (Bohaty and Zachos, 2003; Wade and Kroon, 2002; Lourens et al., 2005; Röhl et al., 2005). The long-term cooling that started during the Eocene is well documented but the mechanism and causes of the short-term climatic changes that occurred during this switch from a warm climate to a cooler climate are still not well understood. Higher resolution paleoceanographic studies of the Middle Eocene, including those by Diester-Haass and Zhan (1996) and Bohaty and Zachos (2003), revealed short-term fluctuations in the isotopic records.

Diester-Haass and Zhan (1996) studied the carbon and oxygen isotopes and benthic foraminiferal accumulation rates from the Eocene-Oligocene interval of Maud Rise, Weddell Sea. They identified short-term orbitally-driven fluctuations with periodicities of 100-400 ka in the isotope and benthic foraminiferal abundance records

and a major increase in productivity at 37 Ma. At Kerguelen Plateau and Maud Rise, Bohaty and Zachos (2003) recognized a distinct negative $\delta^{18}O$ shift (~1‰) at 41.5 Ma (middle Eocene Climatic Optimum). They interpreted this short-term climatic change as a temperature signal with a transient warming of 4°C over 600 k.y. and suggested an increase in atmospheric pCO_2 as the mechanism for this warming.

Wade et al. (2001) and Wade and Kroon (2002) generated high resolution benthic and planktonic foraminiferal stable isotope records from ODP Sites 1051 and 1052, western North Atlantic (Fig. A1), in the interval between ~38.0-38.5 Ma and 37.3-39.6 Ma, respectively. They recognized significant (up to 1.4‰ in about 2500 to 4000 yrs) variability in the oxygen isotope records from middle Eocene mixed-layer dwelling planktonic foraminifera. Based on the absence of large ice-volume effect during the late middle Eocene (the $\delta^{18}O$ seawater component of the total $\delta^{18}O$ record, which is a function of the ice-volume effect, is -0.5‰, Lear et al., 2000) and small salinity variations across Blake Nose in the present day (0.27 ppt, Levitus et al., 1994b), Wade and Kroon (2002) attributed most of this variability to large shifts in temperature of about 4-6°C which could reflect variations in the position of the Gulf Stream or variations in upwelling. This temperature change agrees with temperature anomalies (up to 4°C) in upwelling regions during El Niño events (e.g. McPhaden, 1999) assuming upwelling is the main cause of the temperature change.

In order to understand the response of nannoplankton to the environmental changes at Blake Nose, we need to first understand what was going on in the

environment. Stable oxygen isotope data, such as that generated by Wade and Kroon (2002), may record more than one environmental parameter (temperature and sea water $\delta^{18}O$). This may prevent clear understanding of the causes and consequences of the climatic variability recognized and how microplankton responded to these climatic changes. Hence, there is a need to incorporate other geochemical data (Mg/Ca) which are known to record changes in one environmental parameter and which, when combined with the oxygen isotope data, will give a clear picture of the prevailing environmental conditions. Using these geochemical proxies will help constrain the environmental parameters the nannoplankton assemblages are responding to and the magnitude of that response which is the main focus of this study.

Calcareous nannoplankton (coccolithophorids and nannoliths) are marine, unicellular, flagellate phytoplankton belonging to the phylum Haptophyta and division Prymnesiophyceae. Extant coccolithophorids are known to have a widespread oceanic distribution and are most diverse at low latitudes. Their presence is primarily limited to latitudes below 70° and they thrive in warm, stratified, open-ocean oligotrophic environments (Street and Bown, 2000). The test of a coccolithophore is called a coccosphere and the coccosphere consists of plates called coccoliths. Coccoliths have been a major component of pelagic carbonates above the calcite compensation depth (CCD) since the Cretaceous (Bramlette, 1958; Roth, 1986) and their sedimentation is enhanced by transportation in fecal pellets of zooplankton.

Calcareous nannoplankton were chosen for this study because 1) they dwell in the photic zone and are sensitive to environmental factors such as temperature and nutrient levels, 2) they are one of the major primary producers in the ocean, and 3) their calcite plates may record geochemical variations in surface water related to paleoproductivity.

This research involves a multi-proxy investigation using planktonic foraminifera Mg/Ca ratios and calcareous nannofossil absolute abundances corresponding to the record of $\delta^{18}O$ changes in surface waters at Blake Nose, ODP Site 1052 in order to 1) Extract the sea surface temperature (SST) signal using Mg/Ca of planktonic foraminifera as a paleotemperature proxy, 2) Calculate $\delta^{18}O_{sw}$ using the Mg/Ca paleotemperatures and $\delta^{18}O$ records and 3) Document the response of calcareous nannoplankton assemblages to environmental change during the Middle Eocene (37.85-37.45 Ma) using a new method for absolute abundance estimates (Udeze et al., 2005a, b) and comparing the absolute abundance data to geochemical data using multivariate statistical analyses.

2. CALCULATING CALCAREOUS NANNOFOSSIL ABSOLUTE ABUNDANCES AND UNCERTAINTIES FOR PALEOCEANOGRAPHIC STUDIES

2.1 INTRODUCTION

Calcareous nannofossils are useful for reconstructing past oceanographic conditions by using their known environmental preferences and changes in their abundances as proxies to reflect changes in paleoenvironmental parameters, such as temperature and nutrient levels. In order to estimate the abundance of nannoplankton in the photic zone and their flux from the photic zone into ocean-bottom sediments, it is necessary to calculate their absolute abundances (nannofossils per gram of sediment N/Sg) in sediment samples.

Traditional smear slides used for most nannofossil investigations are easy to make but provide only data on relative abundance (i.e. percent abundance). This is because smear-slide preparation does not include using a known weight of sediment, and without this information the absolute abundance of nannofossils in a sample cannot be calculated. In addition, the distribution of nannofossils on a smear slide is often clumped, making it difficult to count the exact number of specimens in a particular field of view (FOV).

Relative-abundance data can be misleading when used to reconstruct paleoceanographic conditions. A high relative abundance of one species, in an assemblage may reflect an increase in total flux of that species but it does not

necessarily mean that the total flux of other species decreased. For example, in Williams and Bralower (1995) the absolute abundance peak of *Biscutum constans* at ~ 30 m in British geological survey (BGS) borehole 81/43 within the *S. comptus* zone is recorded as a decrease in relative abundance owing to the large absolute and relative abundance peaks of *Watznaueria barnesae* at the same level. To overcome the limitations of the smear-slide technique, various authors (Backman and Shackleton, 1983; Beaufort, 1991; Flores and Sierro, 1998; Baumann et al., 1999; Geisen et al., 1999; Bollmann et al., 1999) have applied different methods, including random settling techniques, spiking techniques, and filtration techniques to try to calculate the absolute abundance of nannofossils.

The objectives of this section are to use two methods (RST and SM) to determine nannofossil absolute abundances, to compare the results of both methods, and to calculate the errors or uncertainties associated with each method. The application and accuracy of these methods will be demonstrated by using them to analyze middle Eocene samples from Blake Nose, North Atlantic Ocean.

2.1.1 Study Area

Blake Nose, a salient on the eastern margin of the Blake Plateau, was cored during ODP Leg 171B (Fig. A1; Norris et al., 1998). Paleogene to Cretaceous sediments are shallowly buried in present water depths of about 1200 m to 2700 m across the edge of the plateau and have very good preservation of calcareous and siliceous

microfossils (Norris et al., 1998; SanFilippo and Blome, 2001; Self-Trail, 2001; Kulhanek and Watkins, 2002). These conditions make the study area suitable to test the quantitative methods described in this study.

2.1.2 Previous Work

Several studies have tried to improve the quantitative study of calcareous nannofossils. The RST was proposed by Beaufort (1991) and modified by different authors (Williams and Bralower, 1995; Su, 1996; Flores and Sierro, 1998). Beaufort (1991) described a RST in which a known weight of sample was mixed and homogenized with a known volume of water. A small amount of the sediment–water suspension was then taken and oven dried, leaving behind the nannofossils that settled on a cover slip placed at a height of 25 mm above the bottom of the settling chamber. Beaufort (1991) showed the reproducibility and accuracy of the method by preparing sixteen slides from one sample and obtaining an r^2 (coefficient of correlation) of 0.97 when he plotted the weight of sediment used for each slide against the number of *Sphenolithus* counted per 30 fields of view. The samples used by Beaufort (1991) were lower Pliocene marly limestone, and he obtained values of up to126 million N/Sg.

Williams and Bralower (1995) calculated the absolute abundance of nannofossils from Lower Cretaceous North Sea sediments using a modified version of Beaufort's (1991) RST. They obtained values as high as 10 billion N/Sg and showed reproducibility of their RST by making duplicate slides of each of the samples used.

Their results showed that the percentages of major taxa in the duplicate slides were ≤ ± 5% compared to the original slides.

Flores and Sierro (1998) also used a RST to estimate the absolute abundance of nannofossils in Pliocene samples from ODP Hole 852; they obtained values as high as 1.48 billion N/Sg.

Bollmann et al. (1999) applied a combination of a SM and a spraying technique on two different sediment types: a pure coccolith ooze, dominated by *Gephyrocapsa* from the mid-Pleistocene of DSDP Hole 607, and a hemipelagic Holocene sample with low carbonate content (Blagnac sample off Cape Verde). They were able to estimate the error in calculated N/Sg by adding the errors associated with weighing of microbeads and sediments, calculating the total number of microbeads per sample, and counting the number of coccoliths and microbeads.

Geisen et al. (1999) used a combination of the RST and SM to calculate N/Sg. Their RST is based on the assumption that the number of particles, whether coccoliths or microbeads, collected per unit area of the cover slip is proportional to the volume of suspension originally present above the cover slip (Geisen et al., 1999). Their SM involves adding microbeads as a spike in order to provide information on absolute abundances of coccoliths. Their results showed that the RST yielded values that were consistently 1.82 times higher than the SM values. They recalculated the known weight of the beads using their equation for the RST and found that the estimated weight from the slide counts was 2.5 times higher than the known weight of microbeads added in

the settling chamber. Additionally, the values Geisen et al. (1999) obtained with the SM were closer to the values they obtained using the spiking with microbeads and spraying (SMS) method of Bollmann et al. (1999). Based on these results, Geisen et al. (1999) concluded that the RST gave incorrect values. The methods used in this study are similar to those of Geisen et al. (1999) but were improved by modifying the settling chamber and by calculating the errors involved in all the measured quantities.

2.2 MATERIALS AND METHODS

2.2.1 Microbeads

The size of the microbeads used in this study is ~ 6 µm with a CV (coefficient of variation) ≤ 10% according to the manufacturer, Polysciences, Inc. The microbeads come suspended in latex, and every 100 ml of the latex suspension contains 2.5 grams of polymer spheres. Thus the number of ~ 6 µm microbeads per milliliter of latex solution is approximately 2.20×10^8 ($\pm 4.61 \times 10^7$, ± 21%). This can be calculated using the following equation provided by Polysciences, Inc., $N = \frac{6W \times 10^{12}}{\rho \times \pi \times \phi^3}$ where N is the number of microbeads per ml of solution, W is the grams of polymer per ml in latex (0.025g), ρ is the density of polymer in grams per ml (1.05 for polystyrene), and ϕ is the diameter in microns of the microbeads (ranged from 5.658 ± 0.413 µm to 6.156 ± 0.413 µm). These microbeads are good for this study because they are stable in buffered water (pH 8.4) and they are resistant to ultrasonic treatment, which is used to

disaggregate clumps or strings of microbeads. The size was chosen because 6 µm represents a middle size range for nannofossils.

2.2.2 The Settling Chamber

The settling chamber consists of a Plexiglas container, a platform on which the cover slip is placed, a glass tube that passes through the platform, and a rubber hose attached to the glass tube (Fig. A2). The glass tube and rubber hose were used to siphon out the water after the nannofossils and microbeads settled on the cover slip. A three way stopcock was used to control the amount of water flow during siphoning. The siphoning was done below the platform to avoid disturbance of the particles on the platform and also to make sure that most of the water is removed from the chamber. Extra care was taken during the making of the chamber and the platform surface on which the cover slips were placed to ensure that they were flat because tilting can cause bias as the particles settle on the cover slip. Measurement of the legs of the platform using a high-precision caliper revealed that the platform was at an angle of less than 0.4°.

2.2.3 Sediment Samples

Nineteen samples from ODP Site 1052 (81.38–83.18 rmcd, revised meters composite depth, from Palike et al., 2001) were analyzed. The sediments consist predominantly of calcareous nannofossil ooze and have a diverse assemblage of well

preserved nannofossils. Common species used for this study are *Coccolithus pelagicus*, *Reticulofenestra reticulatum*, *Discoaster barbadiensis*, and *Reticulofenestra bisecta*.

2.2.4. Analytical Methods

In this study, we combined the RST and SM to determine two independent estimates of nannofossil absolute abundance. The basic assumption of the RST is that nannofossils that are allowed to settle out from a suspension onto a cover slip will be more uniformly distributed than those prepared by the smear slide technique. The absolute abundance of the nannofossils is calculated using the weight of sediment put into the overall suspension and the ratio of the volume of water above the cover slip to the total volume of water in the settling chamber (Fig. A2).

The SM adds a known quantity of tracer particles to a weighed sample in order to calculate the unknown amount of a component in the sample. This method has been commonly used by micropaleontologists since the 1960s (Benninghoff, 1962; Stockmar, 1971, Firth, 1993). Benninghoff (1962) added a known number of Lycopodium spores to a sediment sample in order to calculate the absolute abundance of pollen per gram sediment. Firth (1993) added Lycopodium spores to sediment samples in order to calculate the absolute abundances of various organic constituents including dinoflagellate cysts. Slide preparation after the addition of the tracer, however, did not usually involve random settling. Using tracer particles for estimating nannofossil accumulation rates and absolute abundances is now easier because of the availability

of microbeads with uniform diameter within the size range of coccoliths. In this study, the SM is improved by introducing an aliquot of microbeads to the settling chamber to produce a uniform distribution of microbeads as well as nannofossils. The absolute abundance of nannofossils is calculated from the known value of microbeads added to a sample and the ratio of nannofossils counted to microbeads counted. This method produces an independent value of the absolute abundance that can be compared with the RST.

The RST uses the following equation to calculate N/Sg:

$$\frac{\left(\frac{NC}{(FV \times VFV)} \times VW\right)}{IWS} = \frac{\#N}{Sg} \qquad (1)$$

and the SM uses the following equation to calculate of N/Sg

$$\frac{NC}{NB} \times \frac{2.31 \times 10^{8}}{1ml} \times \frac{V}{IWS} = \frac{N}{Sg} \qquad (2)$$

where

NC = number of specimens of the nannofossil species counted on one slide,

NB = the number of beads counted on one slide,

2.20×10^{8} = number of microbeads in 1 ml of suspension (given by the manufacturer),

V = volume of microbead suspension added,

IWS = amount of sediment in grams.

FV = number of fields of view examined,

VFV = volume of field of view which is = area of field of view 0.000356 cm^2 x height of water above the cover slip (4.6 cm),

VW = volume of water in the beaker used for dilution (500 ml), and N/Sg = number of nannofossils per gram of sediment.

The sample processing technique is described below:

1. The sediment samples were dried in an oven for 24 hours.

2. 0.15 ml of microbead solution, containing about 3.30×10^7 ($\pm 6.9 \times 10^6$) microbeads was measured out using a micropipette. The number of microbeads per milliliter of solution was determined from the information given by the manufacturer of the microbeads (Polysciences, Inc.). 0.15 ml was chosen to produce a slide that had a sufficient number of microbeads for the calculation of nannofossil absolute abundances.

3. The microbead solution was put in a 43 ml vial and filled with ammonium acetate buffered tap water (pH 8.4). The vial was then put in an ultrasonic bath for 3 minutes. Buffered tap water was used throughout the procedure to avoid dissolution of the calcareous nannofossils, which occurred when distilled water was used. This is because distilled water is undersaturated with Ca. An ultrasonic bath was used to disaggregate the microbeads.

4. 0.02g of sediment was weighed out using a high precision weighing balance.

5. The sediment was then added to the vial containing the microbeads and the vial was put in an ultrasonic bath for 20 seconds to disaggregate the nannofossils.

6. The sediment-microbead solution was then poured into the settling chamber and at the same time, the water in the chamber was mixed in an up and down motion using a perforated plunger. Vertical mixing of the water was performed rather than circular stirring, to avoid the possibility of centrifugal separation of different nannofossil size fractions (Brookshire, 2003).

7. The solution was then left for 24 hours to allow the calcareous nannofossils and microbeads to settle on the cover slip.

8. After 24 hours, the water was siphoned out of the chamber from below the cover slip and the cover slip was left to air dry. The water was allowed to drip at the rate of one drop per second or less, using a three-way stopcock, to avoid any disturbance of the settled microfossils and microbeads.

9. The cover slip was then mounted on a slide using Norland Optical Adhesive.

2.3 QUALITY CONTROL ON SLIDE PREPARATION AND COUNTING

2.3.1 Collector's Curve

To determine how many fields of view (FOV) should be counted so that there is a reasonable representation of all the different taxa present in a sample, a collector's curve (also called a species effort curve or a species accumulation curve; Hayek and Buzas, 1997) was plotted. This curve plots the cumulative number of counted species against a randomly chosen number of FOV as successive FOV are added. The curves shown here (Fig. A3) represents the average of 50 individual curves in which the FOV

were added in random order. The collector's curves (Fig. A3) for five samples (samples 5, 6, 7, 8, and 9) show that as each succeeding field of view is observed there are fewer and fewer new species added. In sample 7, ten FOV were counted to compare with counting six in the other four samples; the plot shows that after the fifth FOV, only a few more species were added to the assemblage (Table B1). We concluded that six FOV were sufficient for estimating the total number of taxa present. The program used for this was EstimateS (Colwell, 2005).

For areas where the sediments have lower abundance of nannofossils, more FOV will have to be counted to get a good representation of the taxa present. During counting, the few broken and partially dissolved d specimens were included in the counts. Where dissolution prevented identification, the specimens were counted as unidentified species.

2.3.2 Chi-Squared (χ2) Test

After producing the slides, a chi-squared test was used to determine if the distribution of the nannofossils on the slides is indeed uniform with random variation. The null hypothesis tested was that the distribution of nannofossils on the slides is uniformly random (i.e., no bias from water currents, individual size differences, etc.). The equation for the χ2 measure is $\chi^2 = \sum_{k-1}^{n} \frac{(O_k - E_k)^2}{E_k}$ where χ2 = chi-squared, Ok = observed number of individuals in a field of view, n = number of fields of view, and Ek = number of expected individuals in a FOV assuming the null hypothesis is true. Ek was

calculated as the average of the number of specimens in each field of view for six FOV per slide. If $\chi 2$ is less than the critical value at the 0.05 probability level (11.07; degrees of freedom = n-1 = 5), then the difference between the observed and the expected distribution is not statistically significant and the two cannot be distinguished. Table B2 shows that the $\chi 2$ values obtained for the 19 samples studied are all lower than 11.07 except sample 11, which is 11.33. In only one case, then, using our proposed method, can the null hypothesis that nannofossil distribution on the cover slips is uniform be rejected.

2.3.3 Height of Water Above the Cover Slip

One of the assumptions about RST is that the concentration of particles on the cover slip is proportional to the height of the water column above the cover slip (H) and to the volume of water in the settling chamber (V). To test these assumptions two experiments were performed with two samples. In experiment 1, H was reduced from the original 4.6 cm to 3.7 cm for both samples while V remained the same (500 ml). This was done by increasing the height of the platform in the settling chamber (Fig. A2). In experiment 2, V was increased to 575 ml but H remained 4.6 cm. This was done by adding more water and then raising the height of the platform to maintain a depth of 4.6 cm. The two slides generated from the two experiments were then counted and compared with the original method (H = 4.6 cm and V = 500 ml) to see if there were any significant changes in the absolute abundances of the nannofossils. The results of these

experiments showed no significant difference among the three slides (Fig. A4; original slide, H = 4.6cm and V = 500 ml; Exp. 1, H = 4.6 cm and V = 575 ml and Exp. 2, H = 3.7 cm and V = 575 ml). This agrees with the results from Geisen et al. (1999) by which changing H from 5 cm to 2 cm produced no significant difference in the absolute abundance.

2.4 ERROR ANALYSIS

The uncertainties involved in the RST and SM were estimated using an equation given by Taylor (1997). The equation states that if several quantities x, y, and z are measured with uncertainties δx, δy, δz and the measured values are used to compute q = (x + y)-z, then the uncertainty in the computed value of q is the sum, δq ≈ δx + δy + δz, of all the original uncertainties. In other words, adding up the uncertainties in all the measured values used to compute the value of a certain quantity, q, gives the maximum uncertainty (or error) in that computed value. For products and quotients, if $q = \frac{x \times \ldots\ldots \times u}{v \times \ldots\ldots \times z}$ then the error in q can be estimated using this equation:

$\frac{\delta q}{|q|} \approx \frac{\delta x}{|x|} + \ldots\ldots + \frac{\delta z}{|z|}$ where δq is the uncertainty in q, $|q|$ is the best estimate of q and $\frac{\delta q}{|q|}$ is the fractional uncertainty in q. In this study, the uncertainties that were considered include those from all the measured quantities: number of microbeads per milliliter of solution, weight of the sediment sample, volume of water in the beaker, size variation in microbeads and height of water above the cover slip. All these uncertainties were

calculated and applied to the RST and SM equations to estimate the uncertainty in the calculated N/Sg.

2.5 RESULTS

Table B2 shows the calculated N/Sg using the equations for the RST and SM and the differences between their values. Figure A5 shows plots of nannofossil absolute abundances against depth with the associated error bars. For the five plots in Figure A5, the shape of the curves for the values obtained with the RST and SM are similar (correlation coefficient r = 0.68 to 0.93) although the difference between the two values is greater for the samples in the upper part of the section (81.38 – 82.08 rmcd) than for those in the lower part (Fig. A5). This is more obvious on the plots for *R. reticulatum*, *C. pelagicus*, and the total nannofossil abundances than for *D. barbadiensis* and *R. bisecta* (Fig. A5). It is not clear why this is so but further investigations of the samples down the hole will confirm if this pattern is apparent or real. The SM yielded higher N/Sg values (the ratio of SM to RST is 1.01 to 1.62; Table B2) except for samples 16 and 19. The number of microbeads counted was calculated using equation 1 and compared with the known number of microbeads put into the settling chamber ($3.30 \times 10^7 \pm 6.9 \times 10^6$) to check if the calculated number matches the known number of microbeads added. The values are comparable (2×10^7 to 4×10^7; Table B2) to the known number of microbeads added.

To further test the combined RST and SM, duplicate slides were made from five samples (samples 14, 15, 16, 17, and 18) using the same preparation technique to compare the abundances of the major taxa obtained from the original slides. The N/Sg of the four taxa studied in the duplicate slides is close to what was obtained from the original slide (Table B3). The number of *R.reticulatum* and total number of nannofossils obtained from the original and duplicate slides were plotted against depth for both the RST and SM (Fig. A6). The curves show a high similarity (r = 0.89 to 0.95) indicating the reproducibility of the methods. The calculated errors (Tables B4 and B5) for the RST and SM showed that the uncertainty in the N/Sg is about 13% of the total count for the RST and about 22% of the total count for SM. The higher error in the SM is mainly due to the error associated with the diameter of the microbeads.

2.6 DISCUSSION

The number of nannofossils per gram of sediment (N/Sg) for our middle Eocene samples can be reliably estimated with either of the two methods described herein given the small differences between their values. The absolute abundances of nannofossils show similar patterns of variation regardless of which method is used. For example, the RST shows that for sample 1 (Table B2), *R. reticulatum* is the most abundant, followed by *C. pelagicus*, *D.barbadiensis* and *R. bisecta* respectively. This order is the same when the SM was applied to the same sample. Therefore our methods make it possible to identify which species is the most abundant at any

particular horizon and also to see how the abundance of each species changed through time within our sample interval.

The values obtained by using our RST and SM are closer to each other than the values obtained by Geisen et al. (1999) using similar techniques. The results obtained by Geisen et al. (1999) showed that when using a light microscope, the calculated number of nannofossils based on the RST was consistently 1.82 times higher than the number of nannofossils obtained from the SM. Bollmann et al. (1999) also calculated N/Sg by using the RST and SM and their results showed that the RST gave values that were three times higher than the number of nannofossils from the SM. In this study, the SM yielded higher values, suggesting that differences in the preparation techniques and the microbeads used can affect the final result. Also, the difference in values between our two methods is not constant but varies from sample to sample. The shape of the settling chamber, the height of the cover slip from the base of the chamber, the height of water column above the cover slip, the different types of microbeads, and the step by step preparation methods used are factors that could affect the number of nannofossils and microbeads on the cover slip, causing the difference between the methods described in this study and those described in other studies.

2.7 CONCLUSIONS

1. The random settling technique (RST) and spiking method (SM) are two independent, comparable and reproducible ways of calculating nannofossil absolute abundances.

Both methods yielded similar patterns of absolute abundance variations when applied to samples from the middle Eocene of Blake Nose, western North Atlantic.

2. Collector's curves showed that for our samples at least 6 FOV (between 300 and 800 specimens) need to be counted per sample to ensure that most species are adequately represented in the counts. This could vary from place to place depending on the abundance of nannofossils in sediment.

3. The 2 test showed that distribution of the nannofossils on the slides is uniform within a 95% confidence level.

4. Experiments performed with different heights of water above the cover slip (H) and volume of water in the settling chamber (V) revealed that changing H, V or both H and V will not significantly alter the nannofossil absolute abundance.

5. The larger amount of error associated with the SM is mainly because of the uncertainties associated with the diameter of the microbeads (6.8%), which gave an error of ~ 21% for the number of microbeads, per milliliter of latex.

6. The duplicate slides showed that the results of the combined RST and SM are reproducible.

7. In contrast to Geisen et al. (1999), our area method (equation 1), which is based on the assumption that the number of specimens in the volume of water above the cover slip is proportional to the number of specimens in the total volume of water, yielded results that are comparable with the results from the SM.

3. RECONSTRUCTION OF LATE MIDDLE EOCENE PALEOENVIRONMENTAL VARIABILITY AT BLAKE NOSE, ODP SITE 1052

3.1. INTRODUCTION

Geochemical, paleontological, and sedimentological data indicate that the early Eocene was the warmest interval of the Cenozoic (e.g. Wolfe, 1980; Adams et al., 1991, Zachos et al., 1994). Temperatures during peak Eocene warmth at ~50 Ma were as high as 18°C at high latitudes and >30°C at low latitudes (e.g. Burgess et al., 2008; Sluijs et al., 2007; Pearson et al., 2007) suggesting little or no ice at the poles and a reduced equator-to-pole gradient compared to the modern. Following the Early Eocene peak, global temperatures declined, culminating in the expansion of ice-sheets in Antarctica by the earliest Oligocene (e.g. Miller et al., 1991; Zachos et al., 1996; 2001; Lear et al., 2000; Coxall et al., 2005).

Oxygen isotope records from high, mid and low latitudes indicate high amplitude variations at orbital and sub-orbital time scales during the Eocene cooling trend (e.g., Diester-Haass and Zhan, 1996; Bohaty and Zachos, 2003; Wade and Kroon, 2001; Wade and Kroon, 2002). In the Southern ocean, Diester-Haass and Zhan (1996) reported short-term fluctuations with periodicities of 100-400 ka in benthic foraminiferal stable isotope and abundance data from the Eocene-Oligocene (45 – 26 Ma) interval of ODP Site 689, Maud Rise, Weddell Sea. Bohaty and Zachos (2003) generated high resolution stable isotope records from the middle Eocene (49 – 34 Ma)

of Kerguelen Plateau and Maud Rise (ODP Sites 689, 690, 744, 748 and 738) and found a distinct negative $\delta^{18}O$ excursion (~1‰) at 41.5 Ma (the Middle Eocene Climatic Optimum). They attributed 0.4‰ of the excursion to ice volume build up in the late middle Eocene based on Mg/Ca data by Billups and Schrag (2003) and the rest to a transient warming in the surface and intermediate deep waters (1000 to 2000 m) of 4°C over 600 k.y.

In the subtropical North Atlantic (Blake Nose; Fig. A1), Wade and Kroon (2002) found evidence of significant variability in the oxygen isotope records from late middle Eocene mixed-layer dwelling planktonic foraminifera (Fig. A7) from ODP Site 1052. These data indicate $\delta^{18}O$ changes of up to 1.4‰ in about 2500 to 4000 yrs. They attributed the high amplitude $\delta^{18}O$ shifts to changes in sea surface temperatures (SSTs) based on the presumed absence of significant ice sheets and hence little contribution from changes in the overall seawater $\delta^{18}O$ values (the “ice volume effect”).

Such large temperature shifts present a significantly different view of the Eocene subtropics which were thought to be relatively stable compared to polar temperatures (e.g. Pearson, et al. 2007). However, the magnitude of the temperature variation inferred from the Site 1052 $\delta^{18}O$ is similar to that observed during the Pleistocene (Kroon et al., 2000) suggesting that the subtropical SSTs during relatively warm, and presumed ice-free climatic intervals could have been more variable than previously thought.

The relatively large changes in SSTs were based on the assumption that the only source of foraminiferal $\delta^{18}O$ variations was seawater temperature. However, recent evidence suggests that significant polar ice may have existed as far back as the late middle Eocene (St. John, 2008) raising the possibility that some portion of the magnitude of the subtropical North Atlantic foraminiferal $\delta^{18}O$ variations could have been due to changes in the seawater isotopic composition. Thus, the assumption that ice volume variations did not affect the foraminiferal $\delta^{18}O$ values changes at Blake Nose may have resulted in an overestimate of the magnitude of SST changes.

To evaluate the magnitude of SST change at Site 1052, and better understand the nature of sub-precessional scale environmental change during the late middle Eocene, we present a high resolution planktonic foraminiferal Mg/Ca record from ODP Site 1052 to compliment the $\delta^{18}O$ data. The Mg/Ca ratios provide an independent estimate of SST indicating significant changes in the seawater $\delta^{18}O$ composition of the western subtropical North Atlantic not previously recognized.

3.2 MATERIALS AND METHODS

3.2.1 Sampling

We collected 121 samples at 10 cm (about 2.5 to 4 ky) resolution over the interval 94.43 - 82.98 mcd (37.86 - 37.50 Ma) from ODP Site 1052 using the same samples and foraminiferal genus (*Globigerinatheka*) for Mg/Ca analysis as those used

by Wade and Kroon (2002) for stable isotope analysis. The genus *Globigerinatheka* is a mixed-layer dweller (Wade, 2004; Premoli-Silva et al., 2006).

3.2.2 Mg/Ca as a Paleothermometer

Mg/Ca ratios of modern planktonic foraminifera predominantly reflect the temperature of the water in which they calcified. The proportion of Mg in foraminiferal calcite increases with increasing temperature (Delaney et al., 1985; Nürnberg et al., 1996; Elderfield and Gansen, 2000; Lea et al., 2000; Dekens et al., 2002; Anand et al., 2003; Barker et al., 2005). The recent development of a multispecies Mg/Ca-temperature calibration for tropical and subtropical planktonic foraminifera (Anand et al., 2003), which is similar to previous laboratory and core-top calibrations for single species (e.g., Nurnberg, 1995; Lea et al., 2000; Dekens et al., 2002), enables the study of sediments containing subtropical foraminiferal species that were not used in earlier single-species calibrations.

Mg/Ca analyses paired with $\delta^{18}O$ values of foraminiferal calcite aid in distinguishing between the contributions of seawater temperature and the isotopic composition of the seawater to the $\delta^{18}O$ calcite values (e.g. Lear et al., 2000; Elderfield and Gansen, 2000). Temperature can be determined from Mg/Ca and when temperature is known, the isotopic composition of the seawater, and hence any ice volume or regional $\delta^{18}O_{sw}$ changes can be estimated.

We employ the equation by Anand et al. (2003) to estimate the SSTs at ODP Site 1052 by applying a middle Eocene seawater Mg/Ca ratio of 4.07 mol/mol (Wilkinson and Algeo, 1989): Mg/Ca = 0.38 exp (0.09 SST). This is equivalent to a 9.0 ± 0.3% change in Mg/Ca per 1°C change in temperature.

3.2.3 Analytical Details

To generate the Mg/Ca record, we picked between 20 to 30 tests of *Globigerinatheka mexicana* from the 250–355 µm size fraction for each of the 121 samples analyzed. When *G. mexicana* specimens were not sufficiently abundant, we augmented the samples with *Globigerinatheka semiinvoluta* and *Globigerinatheka* index specimens.

We crushed and cleaned the picked foraminiferal samples using the standard rigorous reductive/oxidative cleaning protocol to remove the oxide coating and any residual organic material (e.g., Boyle, 1981; Boyle and Keigwin, 1985/1986). After cleaning, Mg/Ca values were determined using the Finnigan Element high resolution ICP-MS at the Keck Elemental Geochemistry Laboratory, Department of Geological Sciences, University of Michigan.

3.3 FORAMINIFERAL PRESERVATION

3.3.1 Scanning Electron Microscope Evaluation

Preservation of foraminiferal tests can be influenced by the selective dissolution of Mg-rich portions of the test and by precipitation of inorganic secondary calcite from pore fluids during diagenesis (e.g. Brown and Elderfield, 1996; Rosenthal et al., 2000). Dissolution causes the Mg/Ca of a foraminiferal test to decrease and increases $\delta^{18}O$ values, potentially obscuring the original paleoenvironmental signal. The absolute effect of secondary calcite on the Mg/Ca and $\delta^{18}O$ of a foraminiferal test depends on the pore fluid composition and the burial conditions of the particular sedimentary interval.

We examined foraminiferal specimens with a scanning electron microscope (SEM, Fig. A8) at the Microscopy and Imaging Center (MIC) at Texas A & M University, targeting specimens specifically from intervals characterized by prominent shifts in $\delta^{18}O$ (arrows in Fig. A7). Specimens are recrystallized, but there is no evidence of infilling. Minor amounts of fine carbonate debris, mainly coccoliths, were attached to the test surfaces but was removed by ultrasonication during the cleaning procedure prior to Mg/Ca analysis. Furthermore, there was no evidence for significant variations in preservation corresponding to the targeted intervals of $\delta^{18}O$ change.

3.3.2 Sr/Ca Measurements

Sr/Ca data provides an additional gauge of preservation. Recrystallization from pore waters reduces Sr/Ca values in foraminiferal calcite (Lorens and Bender, 1980). Foraminiferal Sr/Ca analyses indicate consistently high values (~1.2) from the bottom of the interval to 84.88 mcd, after which the values jumped to ~1.3 for the rest of the study interval (Fig A9). This sharp increase is close to the sharp shift in $\delta^{18}O$ at 85.41 mcd, however, as stated above, there was no significant difference in the visual assessment of foraminiferal preservation across this interval of sharp increase. Based on these we conclude that diagenesis had no significant influence on the Mg and $\delta^{18}O$ contents of the foraminifera tests and we interpret values and variations in terms of paleoceanographic conditions.

3.4 RESULTS

The planktonic foraminiferal Mg/Ca values range from 3.79 to 6.89 mmol/mol over the study interval (Table B6). The first order trend is an increase from ~5.0 mmol/mol at 94.43 mcd to ~5.7 mmol/mol at ~91.67 mcd (37.78Ma), followed by a gradual decrease to ~4.0 mmol/mol at 82.98 mcd (Fig. A10). Superimposed on these long term trends are high frequency variations of ~0.6 mmol/mol.

Four samples (mcd depths 83.18, 83.68, 84.18, and 84.78) at the top of the interval had significantly higher Mg/Ca values (Fig. A10, Table B6) than those recorded throughout the studied section. These higher values may be anomalous and we suspect

they are the consequence of calcite loss (much smaller sample size) during the cleaning for Mg/Ca analyses. Because they are anomalously high and do not correspond to any features in the $\delta^{18}O$ (Wade and Kroon, 2002), we do not include these values in the discussion for paleoceanographic implications.

3.5 DISCUSSION

3.5.1 Mg/Ca Paleotemperatures

Sea surface temperatures estimated from the planktonic foraminiferal Mg/Ca values range from ~28 and 33°C (Fig. A11). The long term trend in the calculated temperature consists of an increase from ~31°C at 37.85 Ma to ~ 32°C at 37.82 and then a decrease to ~29°C at 37.58 Ma, a cooling of ~3°C over 240 ky. In addition to the overall gradual decrease in temperature, the high frequency variations in the Mg/Ca record also indicate short-term variations in SST superimposed on the long-term trend. These variations correspond to shifts of ~0.8-1.5°C at a ~3000-year time-scale.

The reconstructed paleotemperatures from this study are similar to values from other mid- and low-latitude sites over this time interval. TEX_{86} derived paleotemperatures from the middle Eocene (~37-38 Ma) of Tanzania (Pearson et al., 2001) range from 29-33°C, comparable to values obtained from this study (the value for ~37 Ma is shown in Fig. A11). Tripati et al. (2003) reconstructed early Paleogene tropical temperatures from ODP Site 865 in the equatorial Pacific using planktonic foraminiferal Mg/Ca ratios and obtained a value of ~ 30°C at ~40 Ma (Fig. A11). Sexton

et al. (2006), in an attempt to assess the extent of diagenetic alteration in "frosty" planktonic foraminifera, compared the Mg/Ca of planktonic foraminifera from the middle Eocene (~39 Ma) of ODP Sites 865 and 1052 to "glassy" foraminifera from Istra More 5 (Adriatic Sea). The Mg/Ca values (3.71 – 5.97 mmol/mol) they reported from ~39 Ma at ODP Site 1052 and the calculated temperatures (~28 – 33 °C) are similar to those from this study (Fig. A11).

3.5.2 Isotopic Composition of Sea Water ($\delta^{18}O_{sw}$)

Mg/Ca derived temperature estimates can be used to constrain variations in the $\delta^{18}O$ of seawater ($\delta^{18}O_{sw}$) enabling us to examine the possibility that ice volume or surface hydrography varied over the study interval. The $\delta^{18}O_{sw}$, expressed as ‰ deviation from the Standard Mean Ocean Water (SMOW) scale, is calculated using the following equation by Erez and Luz (1983): $T = 17.0 – 4.52 (\delta^{18}O_c – \delta^{18}O_{sw}) + 0.036 (\delta^{18}O_c – \delta^{18}O_{sw})$ where $\delta^{18}O_c$ is the isotopic composition of the foraminiferal calcite test (derived from the data set of Wade and Kroon, 2002), $\delta^{18}O_{sw}$ is the isotopic composition of the seawater and T is temperature derived from Mg/Ca ratios (this study).

The calculated $\delta^{18}O_{sw}$ indicates a long term decrease from ~3‰ at 37.83 Ma to ~2‰ at 37.6 Ma (Fig. A11). These values are much higher than the current $\delta^{18}O_{sw}$ at Blake Nose (~1‰, LeGrande and Schimdt, 2006) but are comparable to $\delta^{18}O_{sw}$ values (~4 to 2‰, Fig. A11) calculated from the Mg/Ca data of Sexton et al. (2006).

3.5.3 Causes of T and $\delta^{18}O_{sw}$ Variations

Several factors may have caused the hydrographic variations identified at Blake Nose. Here we discuss three factors that may have altered the temperature-salinity composition of surface waters in the region: ice volume, the Gulf Stream and hydrological cycling.

3.5.3.1 Ice Volume: Global continental ice volume is one of the primary factors that influences the overall isotopic composition of seawater ($\delta^{18}O_{sw}$). Increased ice volume on the continents will lead to higher $\delta^{18}O_{sw}$ values and vice versa. Our data indicate that SSTs gradually cooled throughout the study interval, however the corresponding $\delta^{18}O_{sw}$ actually decreased (Fig. A11). This relationship suggests that continental ice volume likely was not the controlling factor of the $\delta^{18}O_{sw}$ changes. St. John (2008) recently reported Arctic sea ice in the middle Eocene (~ 46 Ma) however the combined trends in Mg/Ca paleotemperature and $\delta^{18}O_{sw}$ over the short time interval of this study suggests that continental ice buildup was not significant between 37.85-37.50 Ma. Burgess et al. (2008) used benthic and planktonic foraminiferal oxygen isotope and Mg/Ca and TEX_{86} from the Southern Pacific Ocean (New Zealand) to study global ice volume in the middle Eocene (~41 Ma) and their results also suggest that the continents at ~41 Ma were largely ice-free.

3.5.3.1 Variations in the Gulf Stream: The magnitude of the short-term variations in temperature observed at Blake Nose (Fig. A11) could be due to changes in local/regional hydrography. The current Gulf Stream has a different temperature and

salinity composition than the surrounding water masses (Levitus, 1994a,b) and variations in its position during the Eocene could have resulted in several °C of SST change. Watkins and Self-Trail (2005) suggested that the Gulf Stream was present during the late Maastrichtian. Wade and Kroon (2002) attributed the high-frequency, high-amplitude $\delta^{18}O$ shifts to changes in the position of the proto-Gulf Stream. Pinet and Popenoe (1985) also suggested that the position of the proto-Gulf Stream varied in the past.

In addition to migration of the Gulf Stream track, changes in the distribution of Gulf Stream rings may have produced periodic hydrographic changes at Blake Nose. Gulf Stream rings are bodies of water, usually 100-200 km in diameter, which form from the cut-off of Gulf Stream meanders. The meanders grow and separate from the Gulf Stream and they migrate northward of the stream to form anticyclonic (warm-core) eddies and southward to form cyclonic (cold-core) eddies (Richardson, 1983). They have a life span of a few days to several weeks. Rings also move westward when they are not touching the Gulf Stream and eastward when they are attached to it (Fuglister, 1972; Richardson, 1983). Since these rings have a different temperature and salinity signature from the surrounding water, their migration to surrounding areas could cause variation in SST and $\delta^{18}O_{sw}$ similar to those identified at Blake Nose.

Upwelling of deep cold waters could also cause the hydrographic variations at Blake Nose area (Wade et al., 2000). Several climate model simulations (Bice et al., 2000 and Sloan and Huber, 2000) have predicted Ekman driven upwelling along the

eastern North Atlantic margin during the Eocene. Wade et al. (2000) also suggested upwelling as the cause of $\delta^{18}O$ variations in the middle Eocene of Blake Nose. These Gulf Stream variations could explain some of the short term variations but likely were not the cause of the long term changes.

3.5.3.3 Changes in the Hydrologic Cycle: Surface water $\delta^{18}O$ can be influenced by factors such as evaporation, precipitation, atmospheric vapor transport and Rayleigh distillation. High rates of evaporation or evaporation–precipitation (E-P) results in relatively high local/regional surface water $\delta^{18}O_{sw}$. Thus regions characterized by high rates of evaporation, such as the subtropics, have higher $\delta^{18}O_{sw}$ values than regions characterized by high rates of precipitation, such as the ITCZ region or the poles.

Studies from the Arctic, IODP Expedition 302 coring expedition (e.g. Brinkhuis et al., 2006; Pagani et al., 2006; Sluijs et al., 2007) suggest that the early Paleogene "greenhouse" interval was characterized by an intensified hydrologic cycle. This means that enhanced rates of evaporation, presumably from the subtropics, led to enhanced rates of precipitation at the poles. Brinkhuis et al. (2006) suggested episodes of increased freshening of Arctic surface waters during the early Paleogene (~50 Ma) based on the presence of the fresh water fern *Azolla*. Pagani et al. (2006) found enriched δD (deuterium isotope) the Arctic precipitation during the early Paleogene due to decreased rainout during moisture transport from lower latitudes to the arctic and increased moisture delivery to the arctic. Sluijs et al. (2007) attributed increased sediment accumulation rates during the PETM in the Arctic Ocean to enhanced

siliciclastic input by rivers in response to an intensification of the hydrological cycle. The middle Eocene was a transitional time from the greenhouse world to a modern climate. The gradual decrease in $\delta^{18}O_{sw}$ over the study interval (Fig. A11) may be evidence of overall decreasing rates of evaporation in the subtropics as global climate transitioned from greenhouse to icehouse status.

3.6 CONCLUSIONS

Middle Eocene planktonic foraminifera Mg/Ca values from ODP Site 1052 show a gradual long term decrease from 6.89 mmol/mol at ~37.8 Ma to 3.79 mmol/mol at ~37.5 Ma. This translates to a decrease in SSTs from ~33 to 28°C. The $\delta^{18}O_{sw}$ values calculated from the Mg/Ca paleotemperature also decreased from ~3‰ at 37.83 Ma to ~2‰ at 37.6 Ma. Superimposed on these long term trends are short term (3000 ky) variations in both SSTs and the $\delta^{18}O_{sw}$. The combined trends of the SST and $\delta^{18}O_{sw}$ suggest that continental ice did not have a major influence on the climate during the study interval. Variations in the Gulf Stream may explain the short-term hydrographical changes at Blake Nose. The long-term hydrographical changes at Blake Nose, however, may have been due to weakening of the hydrological cycling as the climate transitioned from a greenhouse to an icehouse.

4. CALCAREOUS NANNOFOSSIL RESPONSE TO PALEOCEANOGRAPHIC VARIABILITY IN THE MIDDLE EOCENE OF BLAKE NOSE, ODP SITE 1052

4.1 INTRODUCTION

The middle Eocene was characterized by gradual cooling of global temperatures from the warm Early Eocene to the cool Early Oligocene. High resolution $\delta^{18}O$ studies at low, mid and high latitudes indicate that the middle Eocene cooling was punctuated by orbital as well as transient high-amplitude variations (e.g., Diester-Haass and Zhan, 1996; Wade and Kroon, 2002; Bohaty and Zachos, 2003).

Wade et al. (2001) and Wade and Kroon (2002) generated high resolution planktonic foraminiferal stable isotope records from the middle Eocene of Blake Nose, ODP Sites 1051 and 1052, western North Atlantic (Fig. A1), in the interval between ~38.0-38.5 Ma and 37.3-39.6 Ma, respectively. They recognized significant variability in the oxygen isotope records (up to 1.4‰ in about 2500 to 4000 yrs, Fig. A7) from middle Eocene mixed-layer dwelling planktonic foraminifera which they attributed to large shifts in temperature of about 4-6°C. These variations are comparable to what is found in same region during the Pleistocene (Wade and Kroon, 2002). Udeze et al., (in prep) observed a long term decrease in paleotemperature (~3°C over 240 ky) at Blake Nose, Site 1052, using Mg/Ca ratios of the same planktonic foraminiferal genus as Wade and Kroon (2002).

Previous studies of the environmental preferences of nannoplankton have been based on the latitudinal differentiation of calcareous nannoplankton assemblages in the modern ocean and on the assumption that the distribution patterns are primarily related to the temperature of surface waters (McIntyre and Bé, 1967; McIntyre et al., 1970; Okada and Honjo, 1973). By studying the paleobiogeographic patterns of calcareous nannoplankton relative abundances and their changes through time, others inferred changes in sea surface temperatures which they related to climatic change (Haq and Lohmann, 1976; Haq et al, 1977; Wei and Wise, 1990; Wei and Wise, 1992). However, relative abundance data can be misleading when used to reconstruct paleoceanographic conditions. A high relative abundance of one species in an assemblage may reflect an increase in total flux of that species rather than a high standing crop at any moment in time (e.g. Williams and Bralower, 1995). In addition, past paleobiogeographic studies did not directly compare nannofossil absolute abundances (specimens/gram of sediment) with geochemical proxies (stable isotopes and Mg/Ca) from the same samples. Therefore, the paleoecological interpretations of fossil nannoplankton are limited by the indirect nature of comparison to the paleoclimatic records.

Here we present high resolution absolute nannofossil abundance data from a set of samples with previously published oxygen isotope data (Wade and Kroon's, 2002) and Mg/Ca data (Udeze et al., in prep) in order to more precisely determine nannofossil

paleoecological preferences and the timing of response of nannofossil assemblages to paleoenvironmental change.

4.2 MATERIALS AND METHODS

Calcareous nannofossils (Mita, 2001) and planktonic (Bellier,et al., 2001; Wade 2004) and benthic foraminifera (Friedrich and Hemleben, 2007) are abundant and well preserved at Blake Nose (Fig. A1). In addition, shipboard paleomagnetic analyses (Norris et al., 1998) yielded high-quality magnetostratigraphic data. The well-defined bio- and magnetostratigraphy indicated that no unconformities were found between ~41.6 Ma and ~35 Ma (Norris et al., 1998). The continuous expanded records show Milankovitch-related cyclicity that was used for astronomical calibration of the Eocene time scale (Pälike et al., 2001, age model used in this paper).

The age model by Pälike et al., (2001) is based on orbital tuning of XRF Ca/Fe ratio data that displays cyclicity. They used the XRF counts of iron and calcium, a proxies of the relative contribution from calcium carbonate and terrestrial material, to construct a new composite depth record. This new composite depth record provided the basis to extend the astronomically calibrated geological time scale into the middle Eocene and resulted in revised estimates for the age and duration of magnetochrons C16 through C18.

We collected a total of 139 samples at 10 cm (about 2.5 to 4 k.y.) resolution over the interval 81.38 - 94.43 mcd (37.85-37.45 Ma) from ODP Site 1052, (a set of

samples from the intervals studied by Wade and Kroon, 2002). This allowed sufficient resolution to resolve the response of nannofossils to paleoceanographic changes.

A combination of the random settling technique (RST) and spiking method (SM) described by Udeze et al. (2005a) and Udeze et al. (in press) was used for sample processing and slide preparation for determining nannofossil absolute abundances. The RST involves using a known weight of sample mixed and homogenized with a known volume of water. The water-nannofossil mix is poured into a settling chamber with a cover slip at the bottom where the nannofossils are left to settle. The SM involves adding microbeads as a spike in order to provide information on absolute abundances of coccoliths. Combining the two methods produces two independent and comparable nannofossil absolute abundance estimates (Udeze et al., in press).

4.3 RESULTS AND DISCUSSION

4.3.1 Comparison of 1052 Nannofossil Assemblage with Other Eocene Nannofossil Assemblages

The following taxa found within this study interval (CP14b, NP 17) were also reported by Mita (2001) from Sites 1052 and 1051: *Braarudosphaera bigelowii, Calcidiscus protoannulus, Coccolithus pelagicus, Cribrocentrum reticulatum* (now called *Reticulofenestra reticulata*), *Discoaster barbadiensis, Discoaster saipanensis, Reticulofenestra bisecta, Reticulofenestra* spp., and *Sphenolithus moriformis*. Some

species identified in this study were not identified by Mita (2001) at Site 1052. These include *Bramletteius serraculoides*, c.f. *B. serraculoides*, and *Sphenolithus editus*.

The nannofossil assemblages identified in this study are similar to three of the seven assemblages delineated by Haq and Lohman (1976) in the Eocene of the North Atlantic. The three assemblages are: The *Reticulofenestra* Assemblage consisting primarily of small *Reticulofenestra* and *Braarudosphaera* spp.; the *Discoaster* Assemblage consisting primarily of *Discoaster* spp. with small numbers of *Coccolithus pelagicus* and *Reticulofenestra bisecta*, and the *Reticulofenestra umbilica* - *Reticulofenestra bisecta* - *Coccolithus pelagicus* Assemblage consisting of approximately equal proportions of these taxa. The common species that make up these three assemblages are also common within this study interval.

The assemblage identified in this study is similar to the taxa that make up the warm and temperate-water assemblages of Wei and Wise (1990) identified from the Eocene of the South Atlantic. They include *Coccolithus formosus*, *Coccolithus pelagicus*, *Discoaster* spp., *Reticulofenestra* spp., and *Sphenolithus* spp.

The Blake Nose assemblage defined from Site 1052 also has some taxa in common with the assemblage at Maud Rise, Weddell Sea (Pospichal and Wise, 1990). These include *Coccolithus formosus*, *Coccolithus pelagicus*, *Discoaster* spp., *Reticulofenestra* spp., *Sphenolithus* spp. and *Zygrhablithus bijugatus*. *Discoaster* spp. and *Sphenolithus* spp. are rare or absent at Maud Rise whereas *Chiasmolithus* spp. are abundant. In contrast, Blake Nose has rare *Chiasmolithus* spp. and abundant *Discoaster*

spp. and *Sphenolithus* spp. This could be due to the high latitude location of Maud rise and as such the environment and assemblage are quite different from Blake Nose.

The new assemblage data from Blake Nose are comparable to the taxa considered warm and temperate by Villa et al. (2008). They include *Coccolithus formosus*, *Coccolithis pelagicus*, *Discoaster* spp., *Reticulofenestra bisecta*, *Reticulofenestra umbilicus* and *Sphenolithus moriformis*. The "cool" taxa of Villa et al. (2008) include *Chiasmolithus* spp. and *Reticulofenestra daviesi* which are rare or absent at Blake Nose.

Lupi and Wise (2006) analyzed low latitude middle Eocene calcareous nannofossils from Demerara Rise, ODP Site 1260A. They identified assemblages that are generally dominated by *Braarudosphaera*, *Coccolithus*, *Discoaster*, *Helicosphaera*, *Sphenolithus*, *Reticulofenestra*, *Thoracosphaera*, and *Zygrhablithus bijugatus*. Most of the taxa they identified are also present in the Blake Nose assemblage.

4.3.2 Downcore Variations in Abundance Patterns

Approximately 48 taxa were identified in this study (Appendix C and D). The assemblage is quite diverse with lower Shannon index (H`) values at the bottom of the study interval and higher values at the top (Fig A13). These taxa have been grouped into major, minor and rare taxa based on their abundance in any given sample. The major taxa are those that make up >2% of the specimens in any particular sample. Together they contribute ~75% of the total nannofossils in the study interval. The

minor species make up 0.5-2% of the individuals in any given sample while the rare species make up < 0.5%.

4.3.2.1 Major Taxa: Major taxa (Appendix E, Plate 1) in order of decreasing abundance are: small *Reticulofenestra* (0-6 µm), *Pemma* spp., *Coccolithus pelagicus*, *Reticulofenestra bisecta*, *Reticulofenestra reticulata*, *Discoaster barbadiensis*, *Zygrhablithus bijugatus* and *Discoaster saipanensis*. These taxa show long-term (~100 ky) variations in their abundances and superimposed on this long-term pattern are short-term variations of ~ 3ky (Figure A12).

The abundance of total nannofossils reached maxima at ~37.82, ~37.6 and ~37.47 Ma and a minimum at ~37.7 Ma. Small *Reticulofenestra* spp. (0-6µm) is the most abundant taxon and it shows a similar abundance pattern to *C. pelagicus* which is the third most abundant taxon. Together they consist of about 20-50% of the whole assemblage. They both show maxima at ~37.8 Ma and ~37.6 Ma (Fig. A12) and a minimum at ~ 37.7 Ma, similar to the pattern of total nannofossils. Superimposed on this long-term trend is a sharp, brief decrease at ~ 37.76 Ma.

Pemma spp. and *Reticulofenestra bisecta* are the second and fourth most abundant taxa. They reached their maximum abundances at ~ 37.8 Ma and ~ 37.64 Ma, and a minimum at ~ 37.7 Ma. Superimposed on their long-term trends are a sudden decrease at ~ 37.77 Ma and an increase at 37.64 Ma. *Discoaster barbadiensis* reached a maximum at ~ 37.78 Ma and ~37. 58 Ma and a minimum at ~ 37.75 Ma. For *Discoaster saipanensis*, the obvious events are a maximum at ~37.58 Ma and two sharp increases

at 37.63 Ma and 37.57 Ma. Two maxima at ~ 37.8 and ~37.6 Ma with a broad minimum in between characterize the absolute abundance pattern of *Zygrhablithus bijugatus*.

Reticulofenestra reticulata shows a distinct pattern compared to the other major species. The abundance remained constant (~ 20 million per gram of sediment) throughout the lower portion of the interval and then suddenly increased to about 300 million per gram of sediment at 37.55 Ma and remained at that level for the rest of the interval. According to Berggren et al. (1995) this species has its first occurrence in Chron C19r (CP14a, 42 Ma) and last occurrence in Chron C15r (CP15, 35 Ma). It is possible that the abundance pattern displayed by *R. reticulata* in the study interval is due to its evolutionary trend.

4.3.2.2 Minor Taxa: Significant minor taxa (Appendix E, Plate 2) in the assemblage are *Braarudosphaera spp*., *Calcidiscus protoannulus*, *Sphenolithus moriformis*, *Discoaster tanii*, *Coccolithus formosus*, c.f. *Bramletteius serraculoides*, and *Cyclicargolithus floridanus*. The abundance patterns of these species are more variable than those of the major species and do not show the patterns seen in the major species (Fig. A13). *C. formosus*, *D. tanii* and *S. moriformis* do show a somewhat gradual increase from the bottom of the interval to the top. The abundance spikes seen at 37.77 and 37.65 Ma in the major species also appear in the abundances of *S. moriformis* and *D. tanii* (Fig. A 13). *Calcidiscus protoannulus* and *Cyclicargolithus floridanus* were present throughout most of the interval but their abundances do not show any discernible pattern.

4.3.2.3 Rare Taxa: Rare taxa (Appendix E, Plate 3) in the assemblage include *Bramletteius serraculoides*, *Coronocyclus nitescens*, *Pedinocyclus larvalis*, *Discoaster nodifer*, *Helicosphaera compacta*, *Micrantholithus* spp., *Reticulofenestra* spp. (>10 µm) and *Sphenolithus radians*. Like most of the minor species, these rare species do not show any discernible pattern in their abundance. Appendix C shows the raw counts of all identified species and Appendix D shows the calculated absolute abundance data with uncertainty for each species calculated by using the error analysis methods described in section 2.3.

In summary, the major taxa did show some similarities in their abundance such as a maxima at ~37.6 Ma and a minima at ~37.7 Ma. The minor and rare species displayed a more variable abundance pattern and did not show some of the similarities seen in the major species.

4.3.3 Comparison of Selected Taxa Absolute Abundance to Geochemical Records

Sea surface temperatures (SST) derived from the Mg/Ca data range between ~29 and 33°C (Fig.A11). The calculated temperature showed a decrease from ~ 32°C at 37.82 Ma (91.87 mcd) to 29°C at 37.58 Ma (85.08 mcd), a cooling of ~3°C over 240 ky. The calculated SST was used to estimate $\delta^{18}O_{sw}$ (Fig. A11) from the foraminiferal $\delta^{18}O$ data (Wade and Kroon, 2002), which showed a long term decrease from ~2.8‰ at 37.83 Ma to 1.5‰ at 37.6 Ma. $\delta^{18}O_{sw}$ can be used as a proxy for salinity (Craig and Gordon, 1965) with which it is positively correlated. In addition to the overall gradual

trend, the paleotemperature and $\delta^{18}O_{sw}$ values show the presence of short-term variations (0.8-1.5°C and 0.3-0.8‰ in ~3000 years respectively; Fig. A11).

4.3.3.1 *Discoaster* spp. and *Sphenolithus* spp: *Discoaster* and *Sphenolithus* have been considered warm-water taxa throughout their geological range based on paleobiogeographic reconstructions and their consistent high abundance at low latitudes and during known warm intervals (e.g., Haq and Lohmann, 1976; Lohmann and Carlson, 1981; Bralower, 2002; Gibbs et al., 2006; Villa et al., 2008; Dunkley Jones, 2008). Therefore, they are believed to vary directly with temperature (e.g. Backman et al., 1986; Backman and Pestiaux, 1987). However, *Discoaster* spp. and *Sphenolithus* spp. increased in both absolute abundance and relative abundance as temperature decreased at Site 1052 (Fig. A14) which suggests that other environmental factors affected their abundance.

The abundances of *Discoaster* and *Sphenolithus* have also been related to nutrient levels and previous studies suggest that these taxa occupy oligotrophic environments (Haq and Lohmann, 1976; Chepstow-Lusty et al., 1992; Aubry, 1992a,b; Kelly et al., 1996; Kahn and Aubry, 2004; Villa et al., 2008). To see if nutrient levels controlled *Discoaster* spp. and *Sphenolithus* spp. abundances, we compared their abundances to $\delta^{13}C$ (Wade, 2004; Wade et al., unpublished data) data (Fig. A14). Their abundances did not show any robust correlation ($r = -0.03$, d.f. = 119, $r_{\alpha=.05} = 0.187$, N.S.) with $\delta^{13}C$ suggesting that a combination of environmental factors could be influencing their abundance.

4.3.3.2 *Coccolithus pelagicus* and Small *Reticulofenestra* spp: The present-day temperature range of *Coccolithus pelagicus* is 0 to 10°C (Baumann et al. 2000) hence *C. pelagicus* has been used traditionally as a cold water indicator. However, Wei and Wise (1990) found as many *C. pelagicus* in the middle Eocene of tropical Site 366 as in the mid- and high-latitude sites of the South Atlantic Ocean. They suggested that this species must have gone through a change of temperature preference, tending to prefer warmer temperatures during the Eocene and cooler environments in more recent times. The abundance patterns of *C. pelagicus* and small *Reticulofenestra* spp. in this study increased and decreased in a cyclic manner and do not follow the Mg/Ca paleotemperature (Fig. A14, r = -0.2, d.f. = 119, $r_{\alpha=.05}$ = 0.174, N.S.). It is possible that a combination of environmental parameters, rather than any single environmental parameter, influenced their abundance.

4.3.3.3 *Chiasmolithus*: *Chiasmolithus* is considered a specialist preferring eutrophic, cold waters (Bralower, 2002; Gibbs et al., 2006). *Chiasmolithus* was rare in the study area. In order to investigate if *Chiasmolithus* had a relation to any environmental parameter, we scanned 51 samples and counted the total number of *Chiasmolithus* specimens identified. The genus consists mainly of *C. grandis* with some *C. expansas* and *C. solitus*. The total number of counted *Chiasmolithus* is plotted against SST and C isotope data (Fig. A15, r = 0.02 and -0.02 respectively, d.f. = 49, $r_{\alpha=.05}$ = 0.28 N.S.) and there is no obvious relationship between the counted *Chiasmolithus* specimens and the geochemical proxies of SST and productivity.

4.3.4 Multivariate Statistical Analyses

4.3.4.1 Correspondence Analyses (CA) and Cluster Analyses: To investigate if the species showed any groupings or associations, we did correspondence analyses and cluster analyses on the nannofossil data. Both analyses were done on 35 species (excluding the species that have 5 occurrences or less) and also on the 12 species used in the canonical correspondence analysis discussed in the next section. The cluster analyses were done using the relative Euclidean distance measure and the Wards group linkage method.

The results of the cluster analyses (Fig. A16) did not show robust groupings of the species, suggesting that there are no distinct species associations in the data. The CA for the larger data set (Fig. A17) displays a species distribution along axes 1, 2 and 3, however the distribution seems to be mainly controlled by abundance with the less common and less evenly distributed species occurring at the ends of the axes. Axis 2 did not show as much scatter in the distribution of the species as Axis 1 and 3. These suggest that there are probably no robust associations in the data that can be identified with CA and cluster analyses.

4.3.4.2 Canonical Correspondence Analysis (CCA): In order to further investigate the response of nannoplankton to environmental factors, we performed CCA (ter Braak 1986, 1994, 1995; Palmer, 1993). CCA constrains an ordination of one matrix by a multiple linear regression on variables in a second matrix. In environmental studies, CCA is used to pair a matrix of sample units × species with a matrix of sample

units × environmental variables (McCune and Grace, 2002). CCA was chosen because it can perform ordination on the species assemblage data and it can also relate the ordination of the species assemblage data to the measured environmental variables (SST and productivity). This will permit the species gradients to be related to the measured environmental variables (McCune and Grace, 2002).

CCA has been applied by other workers to investigate nannoplankton species-environment relationships (Boeckle and Baumann, 2004; Hoffmann et al., 2008). Boeckel and Baumann (2004) used CCA to investigate the relationship between Recent coccolith assemblages from the South Atlantic Ocean and environmental factors such as temperature, salinity and nutrient level. They were able to identify four different coccolith assemblages based on their associations and environmental preferences. The environmental parameters used for the CCA in this study are oxygen isotope data (Wade and Kroon, 2002), carbon isotope data (Wade, 2004; Wade, unpublished data) and Mg/Ca data (Udeze et al., in Prep).

The CCA was done on a culled data set using only 12 species. Species with low abundances (less than 5 individuals) and species with inconsistent occurrences were not included in order to focus on abundance patterns of the major taxa. Results of the CCA are shown in Figure A18. In this study, CCA axis 1, axis 2 and axis 3 show the Mg/Ca, $\delta^{13}C$ and $\delta^{18}O$ gradients respectively. The coefficient of correlation between CCA axis 1 and the Mg/Ca; CCA axis 2 and $\delta^{13}C$; and CCA axis 3 and $\delta^{18}O$ are -0.89, 0.82 and 0.62 respectively which are significant at 5% significant level. Species axis 1, axis 2

and axis 3 show the taxa whose abundances correspond to CCA axes 1, 2 and 3, respectively. The results indicate that the species most sensitive to temperature (inferred from Mg/Ca data) are *Reticulofenestra bisecta* and *Pemma* spp., responding to warmer temperatures, and *Coccolithus formosus* and the *Discoaster* responding to cooler temperatures. CCA axis 2 shows that *Discoaster barbadiensis*, *Coccolithus formosus* and *Coccolithus pelagicus* respond to lower surface productivity (inferred from $\delta^{13}C$ values) while c.f. *Bramletteius serraculoides*, *Discoaster tanii* and small *Reticulofenestra* respond to higher surface productivity. CCA axis 3 shows that *Sphenolithus moriformis* and *Discoaster* spp. probably respond to increased $\delta^{18}O$ values while *Braarudosphaera* and c.f. *Bramletteius serraculoides* respond to possible lower $\delta^{18}O$ values.

The CCA results do not agree with previously suggested environmental preferences for the nannofossil taxa used for the analysis. CCA Axis 1 (Fig. A18), for example, suggests that *Discoaster* spp. responded to cooler temperatures and *R. bisecta* responded to warmer temperatures. This is the opposite of the interpretations given to these taxa based on paloebiogeography and comparison with paleotemperature proxies (e.g., Haq and Lohmann, 1976; Lohmann and Carlson, 1981; Bralower, 2002; Gibbs et al., 2006; Villa et al., 2008; Dunkley Jones et al., 2008). Several factors, discussed below, could account for the inconsistencies and lack of correlation between nannofossil taxa and environmental factors.

4.3.5 Environmental Implications of Combined Nannofossil Abundance and Foraminifera Geochemical Data

Most of the individual taxa did not show a strong, expected correlation with a single geochemical proxy. Recent studies have recognized poor correlation between nannofossil absolute abundance and reconstructed environmental parameters (Haidar and Thierstein, 2001; Renaud and Klaas, 2001; Gibbs et al. 2004) and attributed this to dominance of biotic controls (competition, grazing, viral infections, etc.) over the abiotic controls or environmental controls (e.g. temperature, salinity etc.). If biotic factors are dominating abiotic factors, then the effect of abiotic factors may not be strong enough to cause any changes in the nannofossil assemblage which could be correlated to the environmental parameters used in this study.

Multiple environmental parameters acting equally and simultaneously could prevent the nannoplankton from responding to any one particular environmental factor, thereby influencing the nannofossil absolute abundances. Also different environmental parameters could have been dominant at different times during the study interval. If one environmental parameter is dominant, it could reduce the effect of the other environmental parameters. This would produce a mixed signal in the nannofossil abundance data and cause lack of strong correlation with any one particular environmental parameter.

The difference in depth habitat between the planktonic foraminifera used for the geochemical proxies and the nannoplankton may explain much of the lack of

correlation. Oxygen and carbon isotopes obtained from planktonic foraminifera tests reflect their calcification depth. Oxygen isotope values of the mixed layer dwellers are most depleted while the carbon isotopic values of near-surface dwelling planktonic foraminifera are more enriched. However, little or nothing is known about the isotopic signatures of individual nannofossil taxa or of their depth habitats. The geochemical paleoenvironmental proxies used here were all derived from mixed-layer foraminifera which may have different isotopic signatures from the nannofossils, thereby limiting the comparison of nannofossil absolute abundance with planktonic foraminifera-derived geochemical proxies.

Factors with no reconstructable record such as turbidity and micronutrients (Gibbs et al. 2004) and the evolutionary trends of the taxa (e.g. *Reticulofenestra reticulata* in this study) could also influence the nannofossil absolute abundance and cause lack of correlation between the taxa and environmental factors.

4.4 CONCLUSIONS

High resolution quantitative nannofossil assemblage analysis of ODP Site 1052 has revealed a diverse nannofossil assemblage. The absolute abundance patterns of the major and minor species showed short-term (as short as 3 ky) variations that are superimposed on longer term variations. When compared with the geochemical proxies none of the taxa showed a robust correlation with any single environmental parameter. However, results of the CCA showed significant correlation between the

nannofossil absolute abundances and environmental factors, although the relationships between the nannofossils and environmental conditions are different from those suggested by previous studies.

The lack of correlation between the nannofossil abundance data and geochemical proxies could be due to dominance of biotic control over abiotic control, different depth habitats of the planktonic foraminifera used for the geochemical proxies (*Globigerinatheka*, mixed layer dwellers) and calcareous nannoplankton (photic zone), and different environmental controls operating at different magnitudes during the study interval, thus making it difficult to see any strong correlation between the nannofossil absolute abundance and any single environmental variable.

The results of this study suggest that the response of calcareous nannoplankton is not as simple and straight forward as has been suggested by previous studies. This study has shown that deviations from the suggested environmental preferences of nannoplankton could arise when there are multiple environmental parameters acting equally at the same time. The proximity of Blake Nose to the Gulf Stream makes it susceptible to the influence of different environmental parameters. The implication of this to paleoceanography is that the environmental preferences of calcareous nannoplankton are dependent on a combination of all the environmental parameters operating at the study location during a particular time. Locations and/or time intervals that are influenced by multiple environmental parameters, such as Blake Nose, will be more likely to produce nannofossil abundance data that does not show any robust

correlation to any single environmental parameters. Locations and/or time intervals that are influenced by one major parameter (e.g. high latitude locations and time intervals such as the PETM) will probably show nannofossil taxa that respond to the major environmental parameter prevailing at that time (e.g. *Discoasters* responding to warmer temperature).

Future study that should help clarify the weak correlation between nannofossil absolute abundance and environmental factors includes studying longer time spans that will incorporate time intervals with different climatic events (e.g. PETM) at the same high resolution so that comparison can be made on how the nannofossils respond from a time interval dominated by one strong parameter (e.g. temperature during the PETM) to an interval where multiple environmental parameters are acting equally, studying other sites for comparison of the response of nannoplankton at different locations and if possible, study of paleodepth habitats of nannofossil species via geochemical data. Understanding the mechanism of all the environmental parameters acting at a particular location during a given time interval is of utmost important when assessing the response of calcareous nannoplankton to environmental parameters.

5. DESCRIPTION OF CYCLICITY TRENDS IDENTIFIED IN SPECIFIC TAXA AND THEIR POSSIBLE PALEOCLIMATIC SIGNIFICANCE

5.1. INTRODUCTION

Oxygen isotope, sedimentological parameters and faunal abundances have shown that the Cenozoic climate varied at periodicities corresponding to orbital parameters (Norris and Röhl, 1999; Pälike et al., 2001; Wade et al., 2001; Gibbs et al., 2006). Since nannoplankton respond to environmental variations (e.g. sea surface temperature) we expect that their abundances should show variations corresponding to orbital cycle parameters. Backman et. al, (1986) and Backman and Pestiaux (1987) recognized that fluctuations in the absolute abundance of Pliocene *Discoasters* show periodicities that correspond to orbital parameter cycles. Orbital forcing on *Discoaster* abundance was also recognized in Pliocene sediments from the North Atlantic by Chepstow-Lusty et al. (1989). Apart from *Discoasters*, Milankovitch scale cyclicity has also been recognized in the abundance of *Coccolithus pelagicus*, *Reticulofenestra pseudoumbilica*, *Florisphaera profunda* and *Sphenolithus* (Beaufort and Aubry, 1990; Gibbs et al., 2004). The high sampling resolution (2500 – 3000 years) and good to excellent preservation of middle Eocene nannofossils from Blake Nose present the opportunity for spectral analyses of Eocene nannofossil abundances allowing comparison of planktonic community responses in a much warmer world than the aforementioned Pliocene examples.

5.2 METHODS

Analyseries program was used for the time series analysis. The raw nannofossil data was analyzed using the Blackman-Tukey method without any data modification.

5.3 RESULTS AND DISCUSSION

Coccolithus pelagicus shows three spectral peaks at 256 ky, 42 ky and 22 ky (Fig. A19). The peaks at 22 ky and 42 ky probably reflect the precession and obliquity cycles, respectively. The peak at 256 ky could be a variation of the eccentricity cycle, however the time span of the data set is too short (~400 ky) to make any conclusion about eccentricity signals. Small *Reticulofenestra* shows three peaks at 333ky, 35ky and 20ky (Fig. A19). *Pemma* spp showed one peak at 28ky. The common *Discoaster* species that make up total *Discoaster* used in the spectral analyses are *D. barbadiensis* and *D. saipanensis*. Combined *D. barbadiensis* and *D. saipanensis* showed a clear precession peak at 24ky and a possible variation of obliquity at 41 ky (Fig. A19).

Since some of the nannofossil abundance data showed orbital related cyclicity, it is expected that the environmental parameters influencing their abundance should also show orbitally related cyclicity. However, the geochemical data used in this study did not show any clear orbital cyclicity in their values. The nannofossil abundances, as discussed in the previous section, seem to be influenced by multiple environmental factors rather than one, making it possible for orbital cyclicity to influence their abundances and not in the individual proxies for environmental parameters. The

conclusion from the previous section was that that hydrological cycling is one of the major factors controlling the hydrographical variations at Blake Nose. However, the nannofossils could be responding to oceanographic processes and this could cause the lack of cyclicity in the geochemical data while the nannofossils show orbital cycling. The fact that the foraminifera used to derive the geochemical taxa have a different depth habitat than the nannofossils could also cause the lack of correlation in orbital cyclicity.

5.4 SUMMARY

Spectral analysis showed that the absolute abundance of *C. pelagicus*, total *Discoaster*, *Pemma* spp. and small *Reticulofenestra* could be influenced by orbital forcing. However, none of the environmental parameters showed any influence of orbital cycling suggesting that the nannoplankton could have been influenced by oceanographic processes while the geochemical proxies are influenced by hydrological cycling.

6. INTEGRATED BIO-MAGNETO STRATIGRAPHY FOR THE (SUB) TROPICAL MIDDLE EOCENE

6.1 INTRODUCTION

Biostratigraphy is one of the primary tools used in constructing age models. The biostratigraphy of ODP Leg 171B, Site 1051 and 1052 (Blake Nose, Fig. A1) was first performed by the Shipboard Scientific Party and subsequently by Mita (2001). However, the resolution used for these initial biostratigraphic studies was low, about 1 to 5 samples per core section (i.e. 1 to 5 samples per 150 cm core section). In this study, we present a high resolution (every 10 cm) biostratigraphy of the middle Eocene of Sites 1051 and 1052. The goal is to produce more precise datum depths and ages than those from Mita (2001).

6.2 METHODS

A total of 328 Samples (188 from 1051A and 140 from 1052A) collected at 10 cm resolution were analyzed for nannofossil biostratigraphic purposes. Sampling from 1051 and 1052 will provide a better correlation between the two sites. Nannofossil events were recalculated and tied to the shipboard paleomagnetic data and Cande and Kent (1995) global polarity timescale to produce a refined biochronology. The ages were recalculated by using linear interpolation to tie the revised depth of the datum to the Cande and Kent (1995) timescale. Figure A20 and the age-depth model for Sites

1051 and 1052 using nannofossil, planktonic foraminifera and paleomagnetic data (Table A7).

6.3 RESULTS AND CONCLUSIONS

Two biostratigraphic datums were identified in Hole 1051A: The last occurrence of *C. solitus* and the first occurrence of *R. reticulata*. One datum was identified in Hole 1051A: The last occurrence of *C. solitus* (Table B8; Figure A21). Comparison of this study with that of Mita (2001) shows that there are depth differences (Table B8; Fig. A21) between where the events were identified in this study and that of Mita (2001). Mita (2001) assigned ages to the events he identified based on the "global scale" biostratigraphy by Bergreen et al. (1995). These ages are often based on one region and do not account for differences in age of events that could occur due to latitudinal and regional differences. The ages given for Mita (2001) in this study (Table B8) were recalculated using the depths of the datum identified by Mita (2001) and the magnetochronology of Cande and Kent (1995). Table B9 shows the recalculated ages of all the events published by Mita (2001).

The last occurrence of *C. solitus* was identified in both holes providing the opportunity to compare the occurrence of that event in both holes. Figure A 21 shows that in 1051A, the event was found at 40.4 Ma in Hole 1051A and at 42.38 Ma in 1052A. This means that there is a ~2 Ma difference between the last occurrences of *C. solitus* in both holes. *Chiasmolithus* in general are rare in these samples and have

“spotty” occurrence which could have affected the depth picked for the datum. This and other factors such as reworking could cause the large difference in age between the last occurrences of *C. solitus* in the two sites.

7. CONCLUSIONS

The random settling technique (RST) and spiking method (SM) are two independent, comparable and reproducible ways of calculating nannofossil absolute abundances. Both methods yielded similar patterns of absolute abundance variations when applied to samples from the middle Eocene of Blake Nose, western North Atlantic.

Middle Eocene planktonic foraminifera Mg/Ca values from ODP Site 1052 showed a gradual long term decrease from 6.89 mmol/mol at ~37.8 Ma to 3.79 mmol/mol at ~37.5 Ma. This translates to a decrease in SSTs from ~33 to 28°C. The $\delta^{18}O_{sw}$ values calculated from the Mg/Ca paleotemperature also decreased from ~3‰ at 37.83 Ma to ~2‰ at 37.6 Ma. Superimposed on these long term trends are short term (3000 ky) variations in both SSTs and the $\delta^{18}O_{sw}$. The combined trends of the SST and $\delta^{18}O_{sw}$ suggest that continental ice did not have a major influence on the climate during the study interval. Variations in the Gulf Stream may explain the short-term hydrographical changes at Blake Nose. The long-term hydrographical changes at Blake Nose may have been due to weakening of the hydrological cycling as the climate transitioned from a greenhouse to an icehouse.

The absolute abundance patterns of the major species showed short-term (as short as 3 ky) variations that are superimposed on longer term variations. When compared with the geochemical proxies none of the species showed a robust

correlation with any single environmental parameter. Results of the multivariate statistical analysis also show lack of correlation between the nannofossil absolute abundances and environmental factors. This could be due to dominance of biotic control over abiotic control, different depth habitats of the planktonic foraminera used for the geochemical proxies (*Globigerinatheka*, mixed layer dwellers) and calcareous nannoplankton, and different environmental controls operating at different magnitudes during the study interval, thus making it difficult to see any strong correlation between the nannofossil absolute abundance and any single environmental variable. Spectral analysis showed that the absolute abundances of *C. pelagicus*, total *Discoaster*, *Pemma* spp. and small *Reticulofenestra* may be controlled by orbital forcing.

The results suggest that the environmental preferences of calcareous nannoplankton are dependent on a combination of all the environmental parameters operating at the study location during a particular time. Care should be taken to first understand the environmental parameters operating in a location at a particular time before accurate interpretation of the response of calcareous nannoplankton, and microorganisms in general, to environmental parameters can be made.

Future study that should help clarify the weak correlation between nannofossil absolute abundances and environmental factors includes studying longer time spans at the same high resolution, studying other sites for comparison, and if possible, study of paleodepth habitats of nannofossil species via geochemical data.

REFERENCES

Adams, C. G., D. E. Lee, and B. R. Rosen (1991), Conflicting isotopic and biotic evidence for tropical sea-surface temperatures during the Tertiary, *Palaeogeography, Palaeoclimatology, Palaeoecology*, *77*, 289–313.

Anand, P., H. Elderfield, and M. H. Conte (2003), Calibration of Mg/Ca thermometry in planktonic foraminifera from a sediment trap time series, *Paleoceanography*, *18*(2), doi:10.1029/2002PA000846.

Aubry, M. P. (1992a), Late Paleogene nannoplankton evolution: A tale of climatic deterioration, in *Eocene – Oligocene Climatic and Biotic Evolution*, edited by D.R. Prothero and W. A., Berggren, *Princeton Univ. Press, Princeton, NJ*, 272– 309.

Aubry, M. P. (1992b), Paleogene Calcareous nannofossils from the Kerguelen Plateau, Leg 120, *Proc. ODP. Sci*. *Results*, *6*, 471–491.

Backman, J., and P. Pestiaux (1987), Pliocene *Discoaster* abundance variations, deep sea drilling project Site 606: Biochronology and paleoenvironmental implications, *Init. Repts. DSDP, 94,* Pt. 2*,* 903-910.

Backman, J., and N. J. Shackleton (1983), Quantitative biochronology of Pliocene and Early Pleistocene calcareous nannofossils from the Atlantic, Indian and Pacific Oceans, *Marine Micropaleontology*, *8*, 141-170.

Backman, J., P. Pestiaux, H. Zimmerman, and O. Hermelin (1986), Palaeoclimatic and palaeoceanographic development in the Pliocene North Atlantic; *Discoaster*

accumulation and coarse fraction data, *Spec. pap., Geol. Soc. Lond*. *21*, 231–242.

Barker, S., I. Cacho, H. Benway, and K. Tachikawa (2005), Planktonic foraminiferal Mg/Ca as a proxy for past oceanic temperatures: A methodological overview and data compilation for the last glacial maximum, *Quat. Sci. Rev*. *24*, 821–834.

Baumann, K. H., A. H. Andruleit, and C. Samtleben (2000), Coccolithophores in the Nordic Seas: Comparison of living communities with surface sediment assemblages, *Deep Sea Res. II*, *47*, 1743–1772.

Baumann, K. H., A. H. Andruleit, and S. Xin (1999), Comparison of different preparation techniques for quantitative nannofossil studies, *Journal of Nannoplankton Research*, *20*, 75-80.

Beaufort, L. (1991), Adaptation of the random techniques for quantitative studies of calcareous nannofossils, *Micropaleontology*, *37*, 415-418.

Beaufort, L., and M. P. Aubry (1990), Fluctuations in the composition of Late Miocene calcareous nannofossil assemblages as a response to orbital forcing, *Paleoceanography*, *5*, 845– 865.

Bellier, J. P., M. R. Moullade, and B. T. Huber (2001), Mid-Cretaceous planktonic foraminifers from Blake Nose: Revised biostratigraphic framework., *Proc. ODP, Sci. Results, 171B* (online).

Benninghoff, W. S. (1962), Calculation of pollen and spores density in sediment by addition of exotic pollen in known quantities, *Pollen et Spores*, *4*, 332-333.

Berggren, W. A., D. V. Kent, C. C. Swisher III, and M. P. Aubry (1995), A revised Cenozoic geochronology and chronostratigraphy, in *Geochronology, Time Scales and Global Stratigraphic Correlation,* edited by W. A., Berggren, D. V., Kent , M. P., Aubry, and J. Hardenbol, *Spec. Publ.-SEPM (Soc. Sediment. Geol.)*, *54*, 129–212.

Bice, K. L., C. R. Scotese, D. Seidov, and Barron, E. J. (2000), Quantifying the role of geographic change in Cenozoic ocean heat transport using uncoupled atmosphere and ocean models, *Palaeogeography, Palaeoclimatology, Palaeoecology*, *161*, 295-310.

Billups, K., and D. P. Schrag (2003), Application of benthic foraminiferal Mg/Ca ratios to questions of early Cenozoic climate change, *Earth and Planetary Science Letters*, *209*, 181-195.

Bohaty, S. M., and J. C. Zachos (2003), Significant Southern Ocean warming event in the late middle Eocene, *Geology*, *31*, 1017–1020.

Boeckle, B., and K. H. Baumann, (2004), Distribution of coccoliths in surface sediments of the south-eastern South Atlantic Ocean: Ecology, preservation and carbonate contribution, *Marine Micropaleontology*, *51*, 301-320.

Bohaty, S.M., and J.C. Zachos (2003), A significant Southern Ocean warming event in the late middle Eocene, *Geology, 31*, 1017–1020.

Bollman, J., B. Brabec, M. Cortes, and M. Geisen (1999), Determination of absolute coccolith abundances in deep-sea sediments by spiking with microbeads and spraying (SMS method), *Marine Micropalaeontology*, *38*, 29-38.

Boyle, E. A. and, L. D. Keigwin (1985/1986), A Comparison of paleochemical records from the North Atlantic and North Pacific Ocean, changes in deep ocean circulation and chemical inventories, *Earth Planet. Sci. Lett*., *76*, 135-150.

Boyle, E. A. (1981), Cadmium, zinc, copper and barium in foraminiferal test, *Earth and Planetary Science Letters*, *53*, 11-35.

Bralower, T. J. (2002), Evidence of surface water oligotrophy during the Paleocene–Eocene thermal maximum: Nannofossil assemblage data from Ocean Drilling Program Site 690, Maud Rise, Weddell Sea, *Paleoceanography, 17*(2), doi:10.1029/2001PA000662.

Bramlette, M. N. (1958), Significance of coccolithophorids in calcium carbonate deposition, *Bulletin of the Geological Society of America, 69*, 121-126.

Brinkhuis, H., S. Schouten, M. E. Collinson, A. Sluijs, J. S. Sinninghe Damsté, G. R., Dickens, M., Huber, T. M., Cronin, J. Onodera, K. Takahashi, J. P. Bujak, R. Stein, J. van der Burgh, J. S. Eldrett, I. C. Harding, A. F. Lotter, F. Sangiorgi, H. van Konijnenburg–van Cittert, J. W. de Leeuw, J. Matthiessen, J. Backman, K. Moran, IODP Expedition 302 Scientists (2006), Episodic fresh surface waters in the Eocene Arctic Ocean, *Nature*, *441*, 606–609.

Brookshire, B. (2003), Unpublished masters thesis, Texas A&M University.

Brown, S. J., and H. Elderfield (1996), Variations in Mg/Ca and Sr/Ca ratios of planktonic foraminifera caused by postdepositional dissolution: Evidence of shallow Mg-dependent dissolution, *Paleoceanography*, *11*, 543–551.

Burgess, C. E., P. N. Pearson, C. H. Lear, H. E. G. Morgans, L. Handley, R. D. Pancost, and S. Schouten (2008), Middle Eocene climate cyclicity in the Southern Pacific: Implications for global ice volume, *Geology*, *36*, 651- 654.

Cande, S. C., and D. V. Kent (1995), Revised calibration of the geomagnetic polarity timescale for the Late Cretaceous and Cenozoic, *Journal of Geophysical Research*, *100*, 6093–6095.

Chepstow-Lusty, A., N. J. Shackleton, and J. Backman (1992), Upper Pliocene *Discoaster* abundance variations from the Atlantic, Pacific, and Indian Oceans: The significance of productivity pressure at low latitudes, *Memorie di Scienze Geologiche*, *44*, 357–373.

Chepstow-Lusty, A., J. Backman, and N. J. Shackleton (1989), Comparison of upper Pliocene *Discoaster* abundance variations from North Atlantic Sites 552, 607, 658, 659 and 662: Further evidence for marine plankton responding to orbital forcing, *Proc. ODP. Sci. Results*, *108*, 121-141.

Colwell, R. K. (2005), EstimateS: Statistical estimation of species richness and shared species from samples, Version 7.5, User's Guide and application published at http://purl.oclc.org/estimates.

Coxall, H. K., P. A. Wilson, H. Pälike, C. H. Lear, and J. Beckman (2005), Rapid stepwise onset of Antarctic glaciations and deep calcite compensation in the Pacific Ocean, *Nature*, *433*, 53–57.

Craig, H., and L. I. Gordon (1965), Deuterium and oxygen-18 variations in the ocean and the marine atmosphere in *Proceedings of a Conference on Stable Isotopes in Oceanographic Studies and Paleotemperatures* edited by E. Tongiorgi, Spoleto, Italy, 9-130.

Dekens, P. S., D. W. Lea, D. K. Pak, and H. J. Spero (2002), Core top calibration of Mg/Ca in tropical foraminifera: refining paleotemperature estimation, *Geochemistry Geophysics Geosystems*, *3*(4), 10.1029/2001GC000200.

Delaney M. L., A. W. H. Be, and E. A. Boyle (1985), Li, Sr, Mg, Na in foraminiferal calcite shells from laboratory culture, sediment traps, and sediment cores, *Geochim. Cosmochim. Acta*, *49*, 1327- 1341.

Diester-Haass, L., and R. Zahn (1996) Eocene–Oligocene transition in the Southern Ocean: History of water mass circulation and biological productivity, *Geology, 24*, 163–166.

Dunkley Jones,T., P. Bown, P. Pearson, B. S. Wade, H. K. Coxall, and Lear, C. H. (2008), Major shifts in calcareous phytoplankton assemblages through the Eocene-Oligocene transition of Tanzania and their implications for low-latitude primary production, *Paleoceanography*, *23*, PA4204, doi:10.1029/2008PA001640.

Elderfield, H., and G. Gansen (2000), Past temperature and $\delta^{18}O$ of surface ocean waters inferred from foraminiferal Mg/Ca ratios, *Nature*, *405*, 422–445.

Erez, J., and Luz, B. (1983), Experimental paleotemperature equation for planktonic foraminifera, *Geochim. et Cosmochim Acta* , *47*, 1025‐1031.

Estes, R. and J. H. Hutchison (1980), Eocene lower vertebrates from Ellesmere Island, Canadian Arctic Archipelago, *Palaeogeography, Palaeoclimatology, Palaeoecology*, *30*, 325-347.

Firth, J. V. (1993), Palynofacies and thermal maturation analysis of sediments from the Nankai Trough, *Proceedings of the Ocean Drilling Program, Scientific-Results, 131,* 57-69.

Flores, J. A., and F. J. Sierro (1998), Revised technique for calculation of calcareous nannofossil accumulation rates, *Micropaleontology*, *43*, 321-324.

Friedrich, O., and C. Hemleben (2007), Early Mastrichtian benthic foraminiferal assemblages from the western North Atlantic (Blake Nose) and their relation to paleoenvironmental changes, *Marine Micropaleontology*, *62*, 31-44.

Fuglister, F. C. (1972), Cyclonic rings formed by the Gulf Stream 1965–1966, in *Studies in Phys. Oceanogr.: A tribute to George Wust on his 80th Birthday,* edited by A. Gordon, Gordon and Breach, New York , 137–168.

Geisen, M., J. Bollmann, J. O. Herrle, J. Mutterlose, and J. R. Young (1999), Calibration of the random settling technique for calculation of absolute abundances of calcareous nannoplanktons, *Micropaleontology*, *45*, 437-442.

Gibbs, S., N. J. Shackleton, and J. Young (2004), Orbitally forced climate signals in mid-Pliocene nannofossil assemblages, *Mar. Micropaleontol*., *51*, 39–56.

Gibbs, S. J., T. J. Bralower, P. R. Bown, J. C. Zachos, and L. M. Bybell (2006), Shelf and open-ocean calcareous phytoplankton assemblages across the Paleocene–

Eocene Thermal Maximum: Implications for global productivity gradients, *Geology, 34*, 233–236.

Haidar, A. T., and H. R. Thierstein (2001), Coccolithophore dynamics off Bermuda (N. Atlantic), *Deep-Sea Res., Part 2*, *48*, 1925–1956.

Haq, B. U., and G. P. Lohmann (1976), Early Cenozoic calcareous nannoplankton biogeography of the Atlantic Ocean., *Mar. Micropaleontol*., *1*, 119–194.

Haq, B. U., I. Premoli-Silva, and G. P. Lohmann (1977), Calcareous plankton paleobiogeographic evidence for major climatic fluctuations in the Early Cenozoic Atlantic Ocean, *J. Geophys. Res*., *82*, 3876–3961.

Hayek, L. A. C., and M. A., Buzas (1997), *Surveying Natural Populations*, 563 pp., New York, Columbia University Press.

Hoffmann, R., H. Schulz, J. Waniek, and M. Kucera (2008), Coccolithophorid and calcareous dinoflagellate species fluxes in the vicinity of the Azores Front (33°N 22°W) during 2003/2004: a sediment trap investigation, *The micropaleontological society's foraminifera and nannofossil groups' joint spring meeting 2008, Bioindicators of past and present environments*, Tubingen Germany.

Kahn, A., and M. P. Aubry (2004), Provincialism associated with the Paleocene/Eocene thermal maximum: Temporal constraint, *Mar. Micropaleontol*., *52*, 117–131.

Kelly, D. C., T. J. Bralower, J. Zachos, I. Premoli-Silva, and E. Thomas (1996), Rapid diversification of planktonic foraminifera in the tropical Pacific (ODP Site 865) during the late Paleocene thermal maximum, *Geology*, *24*, 423–426.

Kroon, D., J. J. G. Reijmer, and R. Rendle (2000), Middle- to late-Quaternary variations in the oxygen isotope signature of *Globigerinoides ruber* at Site 1006 in the western subtropical Atlantic, *Proceedings of the Ocean Drilling Program, Scientific Results,* 166, 13–22.

Kulhanek, D. K., and D. K. Watkins (2002), Paleocene calcareous nannofossil biostratigraphy and magnetobiochronology from ODP Leg 171B Blake Nose, *Journal of Nannoplankton Research*, *24*, 127– 128.

Lea, D. W., D. K. Pak, and H. J. Spero (2000), Climate impact of late quaternary equatorial Pacific sea surface temperature variations, *Science*, *289*, 1719–1724.

Lear, C. H., H. Elderfield, and P. A. Wilson (2000), Cenozoic deep-sea temperatures and global ice volumes from Mg/Ca in benthic foraminiferal calcite, *Science*, *287*, 269-272.

LeGrande, A. N., and G. A. Schmidt (2006), Global gridded data set of the oxygen isotopic composition in seawate,. *Geophys. Res. Lett*., *33*, doi:10.1029/2006GL026011.

Levitus, S., and T. P. Boyer (1994a), Temperature, NOAA atlas NESDIS, *World Ocean atlas 1994*, *4*, Washington, D.C., U.S. Government Printing Office.

Levitus, S., R. Burgett, and T. P. Boyer (1994b), Salinity, NOAA Atlas NESDIS, *World Ocean atlas 1994, 3*: Washington, D.C., U.S. Government Printing Office.

Lohmann, G. P. and J. J., Carlson (1981), Oceanographic significance of Pacific late Miocene calcareous nannoplankton, *Marine Micropaleontology*, *6*, 53–579.

Lorens, R. B. and M. L. Bender (1980), The impact of solution chemistry on *Mytilus edulis* calcite and aragonite, *Geochim. Cosmochim. Acta*, *44*, 1265-1278.

Lupi, C., and S. W. Wise, Jr. (2006), Calcareous nannofossil biostratigraphic framework for middle Eocene sediments from ODP Hole 1260A, Demerara Rise, in *Equatorial Cretaceous and Palaeogene Stratigraphy and Paleoceanography, Part II* edited by J., Erbacher, T., Danelian, and H.Nishi, Demerara Rise (Leg 207): *Rev. Micropaleontol*., *49*, 245–253.

McCune, B., and J. B. Grace (2002), *Analysis of ecological communities*, MjM Software Design, Gleneden Beach, OR.

McIntyre, A., and A. W. H. Be´, (1967), Modern coccolithophoridae of the Atlantic Ocean I. Placoliths and cyrtoliths, *Deep-Sea Research, 14*, 561– 579.

McIntyre, A., A. Be´, M. Roche (1970), Modern Pacific coccolithophorida: A paleontological thermometer, *Transactions of the New York Academy of Sciences II*, *32*, 720 – 731.

McPhaden, M. J. (1999), Genesis and evolution of the 1997–98 El Niño, *Science, 283*, 950 – 954.

Miller, K. G., S. D. Wright, and R. G. Fairbanks (1991), Unlocking the ice-house: Oligocene-Miocene oxygen isotopes, eustacy, and margin erosion, *Journal of Geophysical Research*, *96*, 6829-6848, Washington, D.C.

Mita, I. (2001), Data report: Early to late Eocene calcareous nannofossil assemblages of Sites 1051 and 1052, Blake Nose, Northwestern Atlantic Ocean, *Proceedings of the Ocean Drilling Program, Scientific Results, 171B*,1–28.

Norris, R. D., and P. A. Wilson (1998), Low-latitude sea-surface temperatures for the mid-Cretaceous and the evolution of planktonic foraminifera, *Geology*, *26*, 823–826.

Norris, R. D. et al. (1998), *Proceedings of the Ocean Drilling Program, Initial Results, 171b*, 749, College Station, Texas, Ocean Drilling Program.

Norris, R. D., and U. Röhl (1999), Carbon cycling and chronology of climate warming during the Paleocene/Eocene transition, *Nature*, *401*, 775–778.

Nürnberg, D., (1995), Magnesium in tests of *Neogloboquadrina pachyderma* (sinistral) from high northern and southern latitudes, *Journal of Foraminiferal Research*, *25*, 350–368.

Nürnberg, D., J., Bijma, and C., Hemleben (1996), Assessing the reliability of magnesium in foraminiferal calcite as a proxy for water mass temperatures, *Geochimica et Cosmochimica Acta*, *60*, 803–814.

Okada, H. and S. Honjo (1973), The distribution of oceanic coccolithophorids in the Pacific, *Deep-Sea Research*, *20*, 355–374.

Pagani, M., N. Pendentchouk, M. Huber, A. Sluijs, S. Schouten, H. Brinkhuis, J. S. Sinninghe–Damste, G. R. Dickens, IODP Expedition 302 Scientists (2006), The Arctic's hydrological response to global warming during the Paleocene–Eocene thermal maximum, *Nature*, *442*, 671–675.

Pagani, M., D. Lemarchand, A. Spivack and J. Gaillarde (2005), A critical evaluation of the boron isotope-pH proxy: the accuracy of ancient ocean pH estimates, *Geochim. Cosmochim. Acta*, *69*, 953–961.

Pälike, H., N. J. Shackleton, and U. Röhl (2001), Astronomical forcing in late Eocene marine sediments, *Earth and Planetary Science Letters*, *193*, 589–602.

Palmer, M. W. (1993), Putting things in even better order: The advantages of canonical correspondence analysis, *Ecology, 74*, 2215-2230.

Pearson, P. N., P. W. Ditchfi eld, J., Singano, K. G., Harcourt-Brown, C. J. Nicholas, R. K. Olsson, N. J. Shackleton, and M. A., Hall (2001), Warm tropical sea surface temperatures in the late Cretaceous and Eocene epochs, *Nature*, *413*, 481–487, doi: 10.1038/35097000.

Pearson, P. N., and M. R. Palmer (2000), Atmospheric carbon dioxide concentrations over the past 60 million years, *Nature, 406*, 695-699.

Pearson, P. N., B. E. van Dongen, C. J. Nicholas, R. D. Pancost, S., Schouten, J. M. Singano, and B. S. Wade (2007), Stable warm tropical climate through the Eocene epoch. *Geology*, *35,* 211-214.

Pinet, P. R., and P., Popenoe (1985), A scenario of Mesozoic–Cenozoic ocean circulation over the Blake Plateau and its environs, *Geological Society of America Bulletin*, *96*, 618–626.

Pospichal, J. J., and S. W. Wise Jr. (1990), Paleocene to middle Eocene calcareous nannofossils of ODP Sites 689 and 690, Maud Rise, Weddell Sea, *Proc. ODP. Sci. Results*, *113*, 613–638.

Premoli-Silva, I., B. S., Wade, and P. N. Pearson (2006),Taxonomy, biostratigraphy, and phylogeny of *Globigerinatheka* and *Orbulinoides*, in *Cushman Foundation for Foraminiferal Research Special publication*, *41*, 169-212.

Renaud, S. and Klaas, C. (2001), Seasonal variations in the morphology of the coccolithophore *Calcidiscus leptoporus* off Bermuda (N. Atlantic), *Journal of Plankton Research*, *23*, 779-795.

Richardson, P. L. (1983), Gulf Stream Rings, in *Eddies in Marine Science*, edited by A. R. Robinson, Springer–Verlag, Berlin, 19–45.

Röhl, U., T. Westerhold, S. Monechi, E. Thomas, J. C. Zachos, and B. Donner (2005), The third and final early Eocene thermal maximum: characteristics, timing, and mechanisms of the "X" event, *Geological Society of America Annual Meeting – Abstracts*, **37(**7), 264.

Rosenthal, Y., G. P., Lohmann, K. C., Lohmann, and R. M. Sherrell (2000), Incorporation and preservation of Mg in *Globigerinoides sacculifer*: Implications for

reconstructing the temperature and O-18/O-16 of seawater, *Paleoceanography*, *15*(3), 135–145.

Roth, P. H. (1986), Mesozoic palaeoceanography of the North Atlantic and the Tethys Oceans, in *SEPM Special Publication, 32,* edited by C. P., Summerhayes and N. J. Shackelton, 517–546.

Sanfilippo, A., and C. D. Blome (2001), Biostratigraphic implications of mid-latitude Paleocene–Eocene radiolarian faunas from Hole 1051A, ODP Leg 171B, Blake Nose, western North Atlantic, in *Western North Atlantic Palaeogene and Cretaceous Paleoceanograph* edited by D., Kroon, R. D. Norris, and A, Klaus, *Geological Society of London*, *Special Publications*, *183*, 185–224.

Self-Trail, J. (2001), Biostratigraphic subdivision and correlation of upper Maastrichtian sediments from the Atlantic Coastal Plain and Blake Nose, Western Atlantic, in *Western North Atlantic Palaeogene and Cretaceous Paleoceanography* edited by D., Kroon, R. D., Norris, and A. Klaus, *Geological Society of London, Special Publications*, *183*, 93–110.

Sexton, P., P. Wilson, P. Pearson (2006), Microstructural and geochemical perspectives on planktic foraminiferal preservation: “glassy” versus “frosty”, *Geochem. Geophys. Geosystem* , 7, Q12P19. doi:10.1029/2006GC001291.

Sloan, L. C, and Huber, M., (2001), Eocene Oceanic Responses to Orbital Forcing on Precessional Time Scales, *Paleoceanography*, *16*(1), 101-111.

Sluijs, A., H. Brinkhuis, S. Schouten, J. C. Zachos, C. M. John, S. Bohaty, J. S. Sinninghe Damsté, E. M. Crouch, G. R. Dickens (2007), Environmental precursors to rapid carbon injection at the Paleocene Eocene boundary, *Nature*, *450*, 1218-1221.

Sluijs, A., U. Röhl, S. Schouten, H. J. Brumsack, F. Sangiorgi, J. S. Sinninghe Damsté, and H. Brinkhuis (2008), Arctic late Paleocene–early Eocene paleoenvironments with special emphasis on the Paleocene-Eocene thermal maximum (Lomonosov Ridge, Integrated Ocean Drilling Program Expedition 302), *Paleoceanography*, *23*, PA1S11, doi:10.1029/2007PA001495

St. John K. (2008), Cenozoic ice-rafting history of the central Arctic Ocean: Terrigenous sands on the Lomonosov Ridge, *Paleoceanography*, *23*, doi:10.1029/2007PA001483.

Stockmarr, J. (1971), Tablets with spores used in absolute pollen analysis, *Pollen et Spores*, *13*, 615-621.

Street, C., and P. R., Bown (2000), Palaeobiogeography of Early Cretaceous (Berriasian–Barremian) calcareous nannoplankton, *Mar. Micropaleontol., 39*, 265–291.

Su, X., (1996), Development of late Tertiary and Quaternary coccolith assemblages in the northeast Atlantic, *Geomar Rep*. *48*, 1-120.

Taylor, J. R. (1997), *An introduction to error analysis*, 327 pp., Sausalito, California, University Science Books.

Ter Braak, C. (1995), Ordination, in *Data Analysis in Community and Landscape Ecology* edited by R., Jongman, C., ter Braak, and O. van Tongeren, Netherlands: Pudoc Wageningen, 91-173.

Ter Braak, C. J. F. (1986), Canonical correspondence analysis: A new eigenvector technique for multivariate direct gradient analysis, *Ecology, 67*, 1167-1179.

Ter Braak, C. J. F. (1994), Canonical community ordination. Part I: Basic theory and linear methods, *Ecoscience, 1*, 127-140.

Tripati, A., M. L. Delaney, J. C. Zachos, L. D. Anderson, D. C. Kelly and H. Elderfield (2003), Tropical Sea-Surface Temperature Reconstruction for the Early Paleogene Using Mg/Ca Ratios of Planktonic Foraminifera, *Paleoceanography*, *18*(4), 1101, doi:10.1029/2003PA000937.

Udeze, C. U., J. V. Firth, and T. D. Olszewski (2005a), A new sample preparation technique for calculating calcareous nannofossil absolute abundances and uncertainties for paleoceanographic studies, *Geological Society of America 2005 Abstracts with Programs,* Salt Lake City annual meeting.

Udeze, C. U., J. V. Firth, and T. D. Olszewski (2005b), Sample Preparation for Quantitative Analyses of Calcareous Nannofossils*, North American Micropaleontology Society Section 2005 Abstracts with Program*, Geologic Problem Solving with Microfossils.

Udeze, C. U., J. V. Firth, and T. D. Olszewski, in press, Calculating calcareous nannofossil absolute abundances and uncertainties for paleoceanographic studies, *SEPM Special Publication*.

Udeze et al. In prep., Reconstruction of late middle Eocene paleoenvironmental variability at Blake Nose, ODP Site 1052.

Villa, G. , C. Fioroni, L. Pea, S. Bohaty, and D. Persico (2008), Middle Eocene–late Oligocene climate variability: Calcareous nannofossil response at Kerguelen Plateau, Site 748, *Marine Micropaleontology*, *69*, P. 173-192.

Wade, B. and S. Kroon (2002), Middle Eocene regional climate instability: Evidence from the western North Atlantic, *Geology*, *30*, 1011-1014.

Wade, B. S. (2004), Planktonic foraminiferal biostratigraphy and mechanisms in the extinction of *Morozovella* in the late Middle Eocene, *Marine Micropaleontology*, *51*, 23-38.

Wade, B. S., D. Kroon, and R. D. Norris (2000), Upwelling in the late Middle Eocene at Blake Nose?: *GFF (Geological Society of Sweden)*, *122*, 174–175.

Wade, B. S., D. Kroon, and R. D. Norris (2001), Orbitally forced climate change in the late middle Eocene at Blake Nose (Leg 171B): Evidence from stable isotopes in foraminifera, in *Western North Atlantic Palaeogene and Cretaceous palaeoceanography*, edited by D., Kroon, R. D., Norris, and A., Klaus, *Geological Society [London] Special Publication, 183*, 273–291.

Watkins, D. K., and J. M. Self-Trail (2005), Calcareous nannofossil evidence for the existence of the Gulf Stream during the late Maastrichtian, *Paleoceanography 20*, PA3006 doi: 10.1029/2004PA001121.

Wei, W. and S. W. Wise Jr. (1990), Biogeographic gradients of middle Eocene – Oligocene calcareous nannoplankton in the South Atlantic Ocean, *Palaeogeogr. Palaeoclimatol. Palaeoecol*., *79*, 29– 61.

Wei, W. and S. W. Wise Jr. (1992), Eocene–Oligocene calcareous nannofossil magnetobiochronology of the Southern Ocean, *Newsl. Stratigr., 26*, 119–132.

Wilkinson, B. H., and T. J. Algeo (1989), Sedimentary carbonate record of calcium-magnesium cycling, *Am. J. Sci*., *289*, 1158–1194.

Williams, J. R. and T. J. Bralower (1995), Nannofossil assemblages, fine fraction stable isotopes, and the paleoceanography of the Valanginian-Barremian (Early Cretaceous) North Sea Basin, *Paleoceanography*, *10*(4), 815-839.

Wolfe, J. A. 1980, Tertiary climates and floristic relationships at high latitudes in the northern hemisphere, *Palaeogeography, Palaeoclimatology, Paleoecology*, 30, 313-323.

Zachos, J., M. Pagani, L. Sloan, E. Thomas, and K. Billups (2001), Trends, rhythms, and aberrations in global climate 65 Ma to present, *Science*, *292*, 686-693.

Zachos, J. C., T. M. Quinn, and K. Salamy (1996), High resolution (104 yr) deep-sea foraminiferal stable isotope records of the Eocene–Oligocene climate transition. *Paleoceanography*, *11*(2), 251–266.

Zachos, J. C., L. D. Stott and K. C. Lohmann (1994), Evolution of early Cenozoic marine temperatures, *Paleoceanography*, *9*(3), 353–387.

APPENDIX A. FIGURES

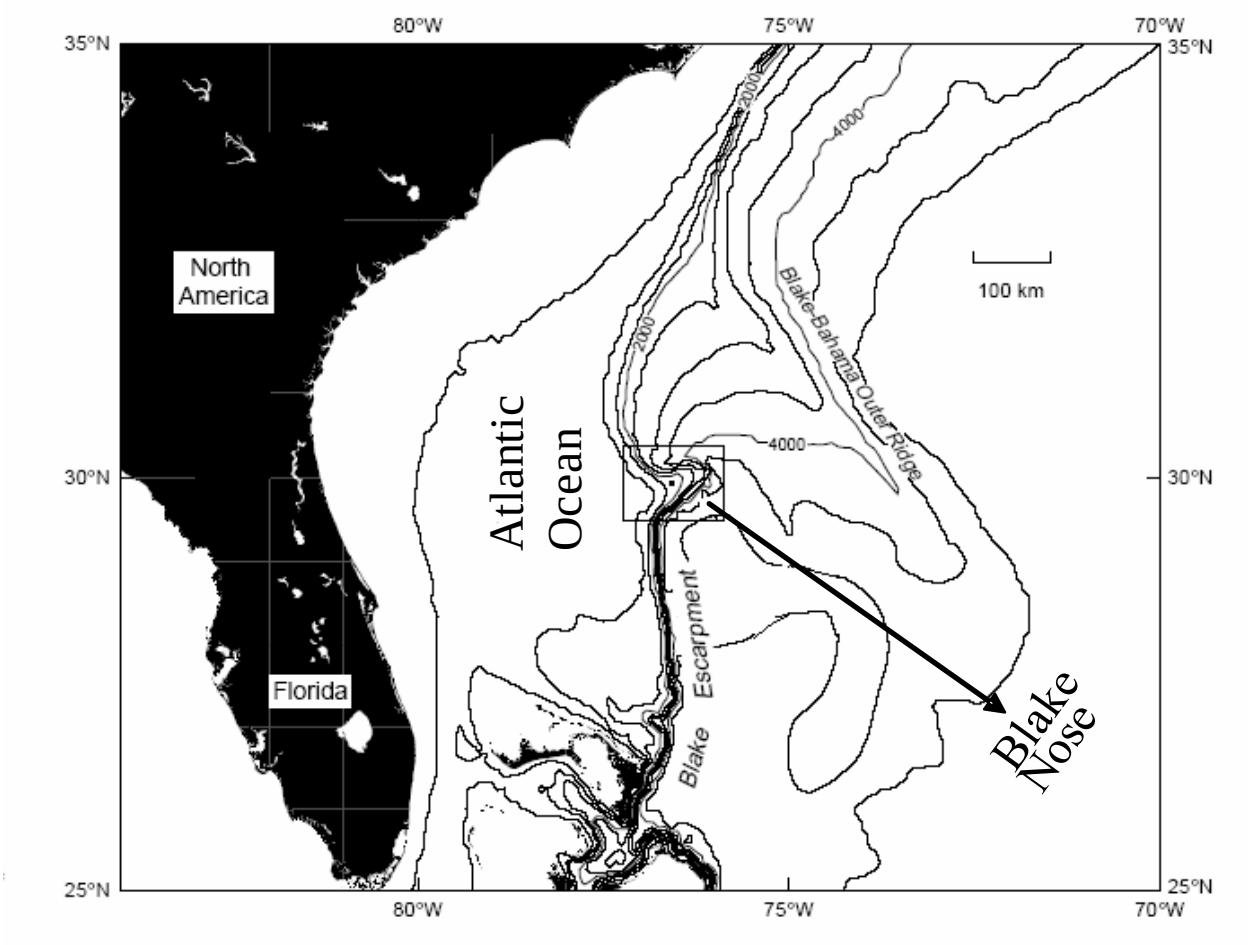

Figure A1. Location of Blake Nose, ODP Leg 171B, modified after Norris et al., (1998).

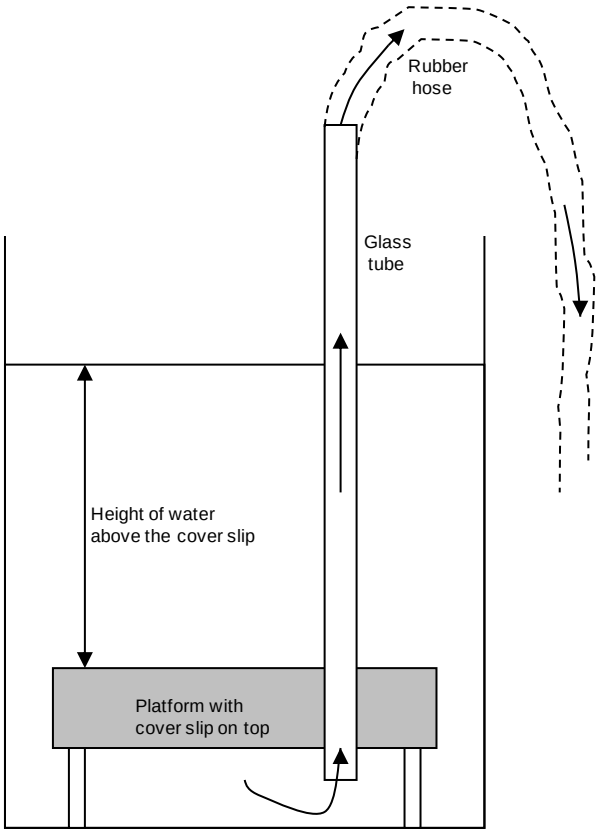

Figure A2. The settling chamber.

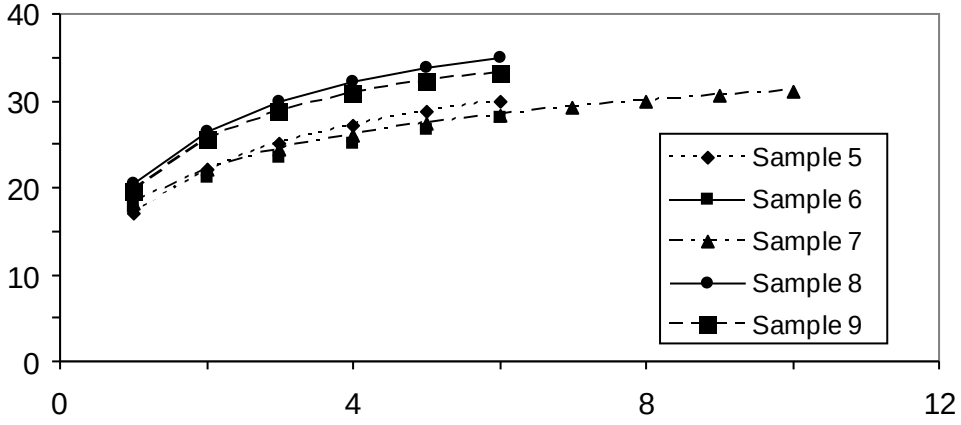

Figure A3. Plots of expected cumulative number of species against number of fields of view.

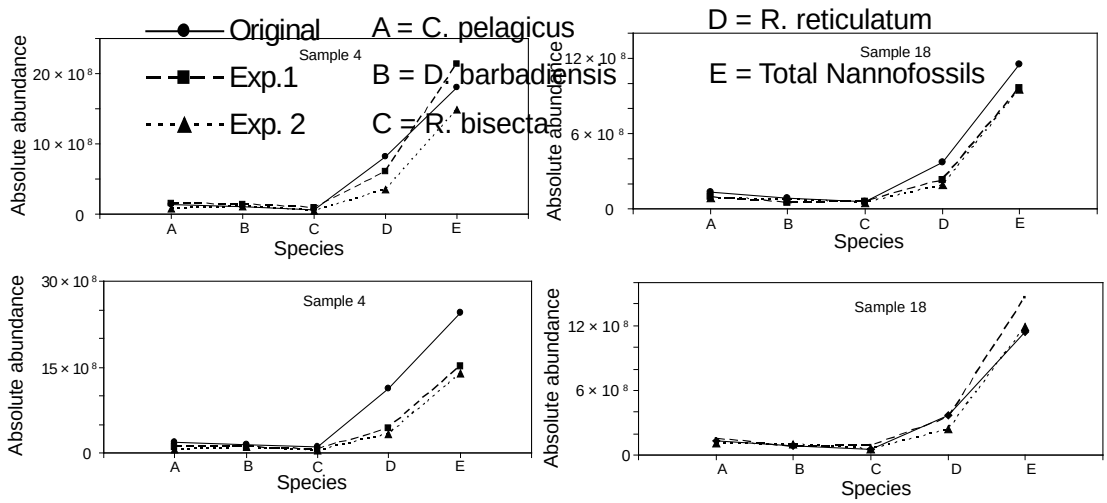

Figure A4. Absolute abundances of *C. pelagicus*, *D. barbadiensis*, *R. bisecta*, *R. reticulatum* and Total nannofossil abundance obtained by varying height of water above the cover slip (H) and water volume (V) in samples 4 and 8. Original slide: H = 4.6cm and V = 500ml, Exp. 1: H = 3.7 and V = 500ml and Exp. 2: H= 4.6 and V = 575 ml.

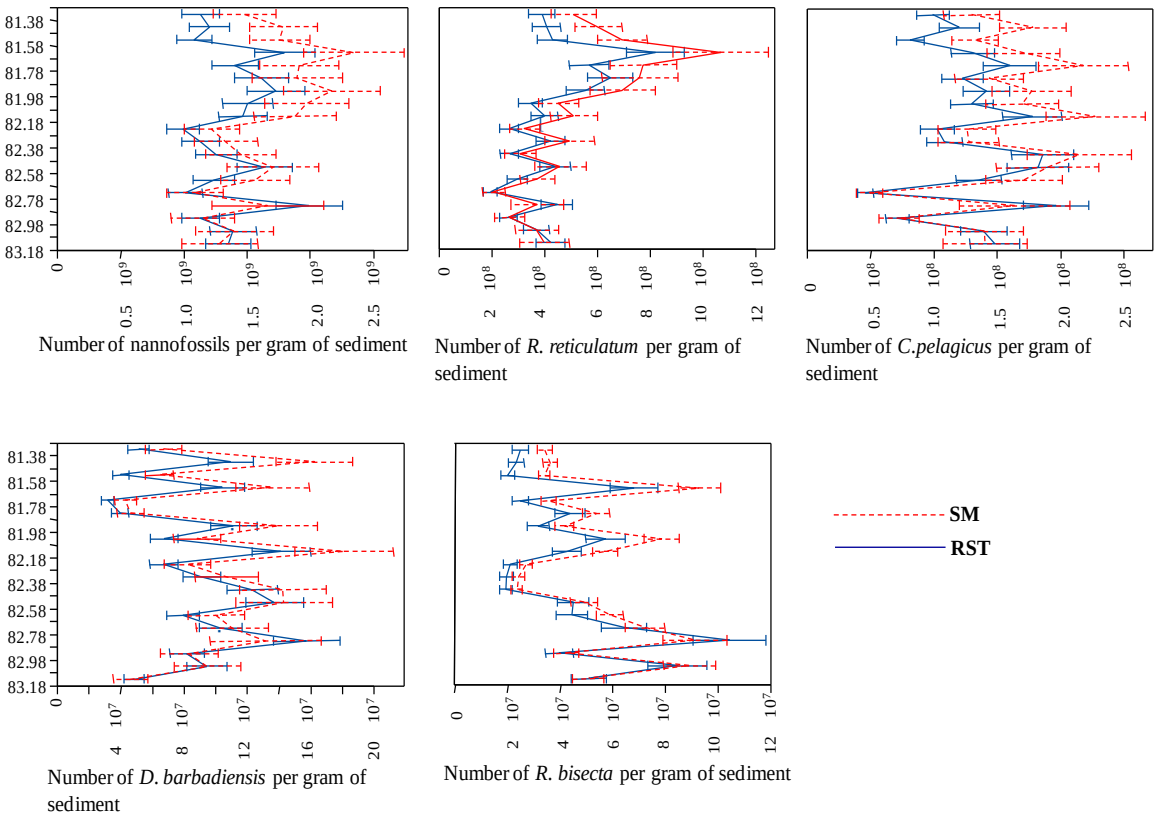

Figure A5. Plots of nannofossil absolute abundances per gram of sediment against depth. Red stands for values obtained with the SM and blues is for values with the RST.

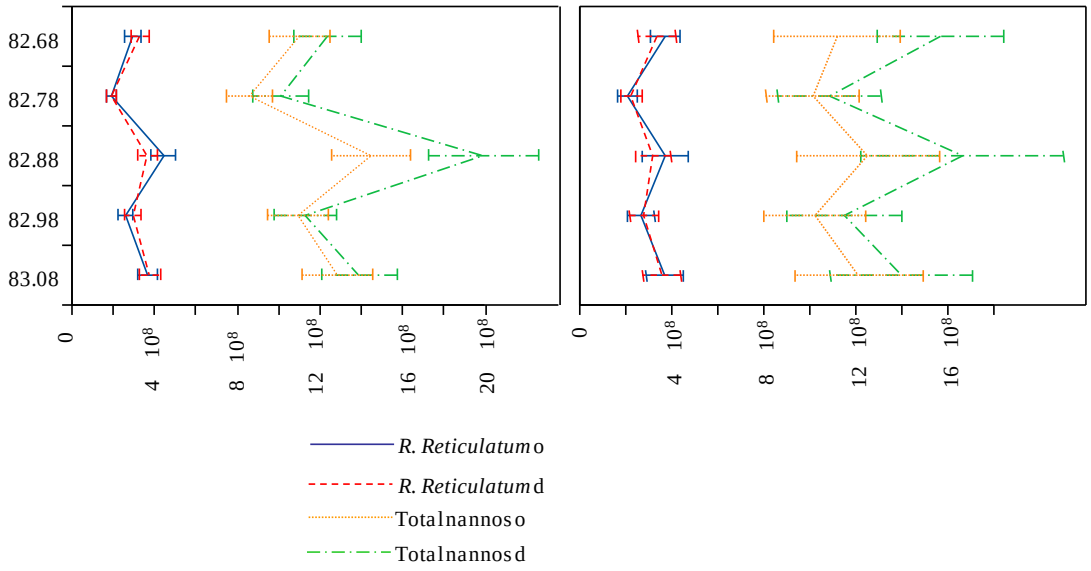

Figure A6. Plots of the absolute abundances of R. reticulatum and total number of nannofossils for the duplicate (d) and original (o) using RST and SM.

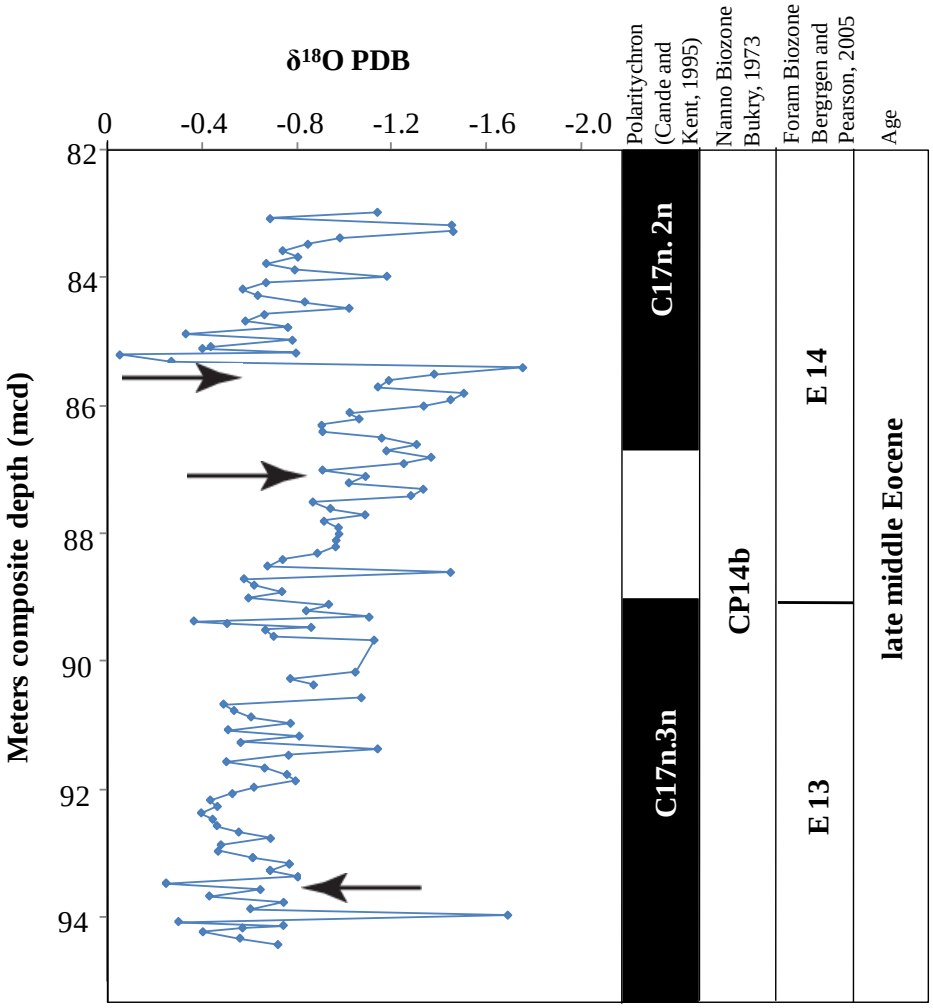

Figure A7. Oxygen isotope data from Site 1052, Wade and Kroon 2002. Arrows refers to intervals where samples were taken for SEM images.

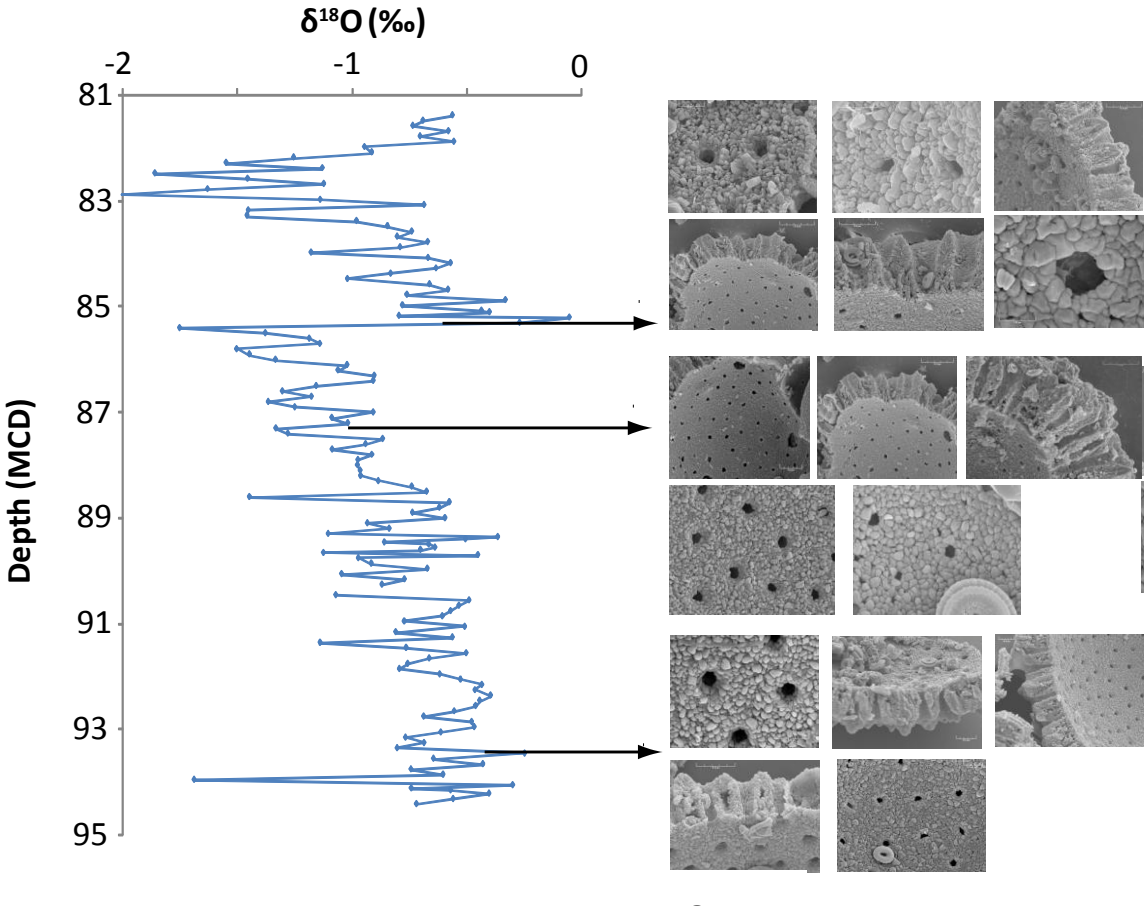

Figure A8. SEM of internal test walls of *Globigerinatheka* at different angles and magnifications. The specimens were taken from three different intervals showing different magnitudes of $\delta^{18}O$ variations to determine if there were any changes in preservation. A: 85.41 mcd; B: 87.21 mcd and C: 93.47 mcd.

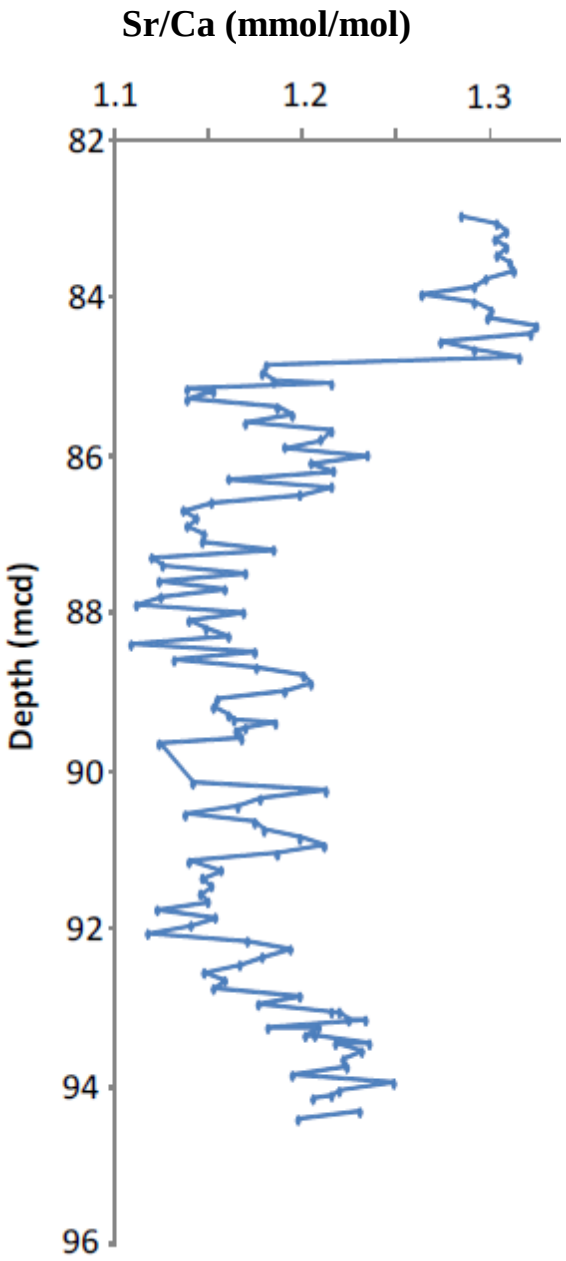

Figure A9. Sr/Ca from ODP Site 1052.

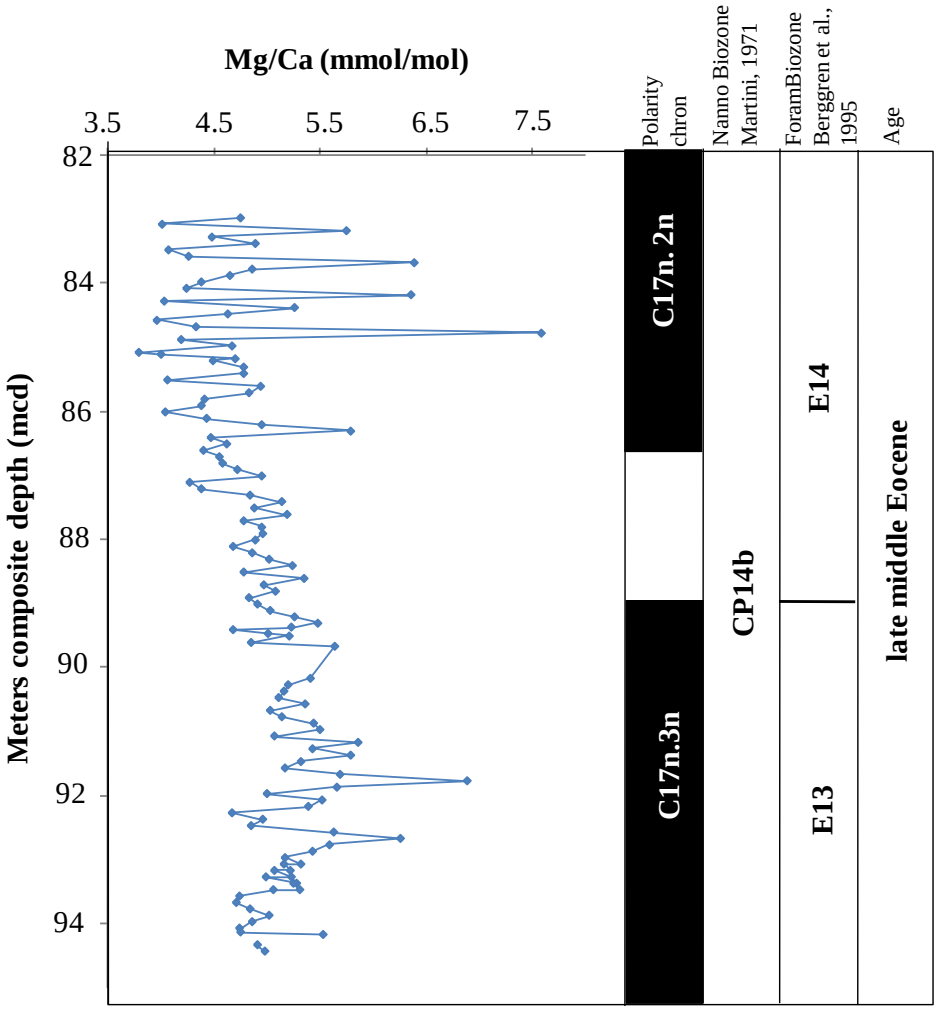

Figure A10. Site 1052 Mg/Ca ratios. The sample gaps in the data are samples with insufficient carbonate for the Mg/Ca analyses.

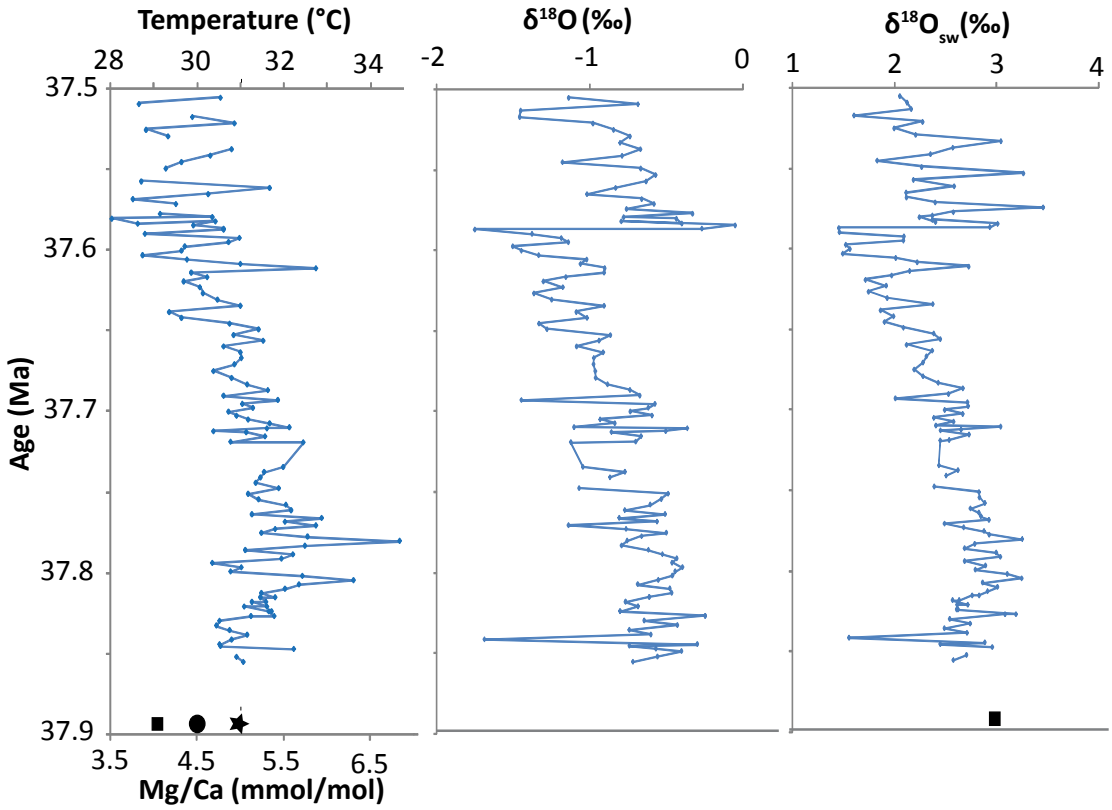

Figure A11. Mg/Ca, Temperature, $\delta^{18}O$ and $\delta^{18}O_{sw}$ against Age. The black square in the first panel is the paleotemperature estimate of Pearson et al., 2001 for 37 Ma, the circle is the paleotemperature estimate of Tripati et al., 2003 for ~40 Ma and the star is the paleotemperatures estimate of Sexton et al., 2003 for ~39 Ma. Black closed square in the third panel represents average value of $\delta^{18}O_{sw}$ calculated from the Mg/Ca of Sexton et al. (2006).

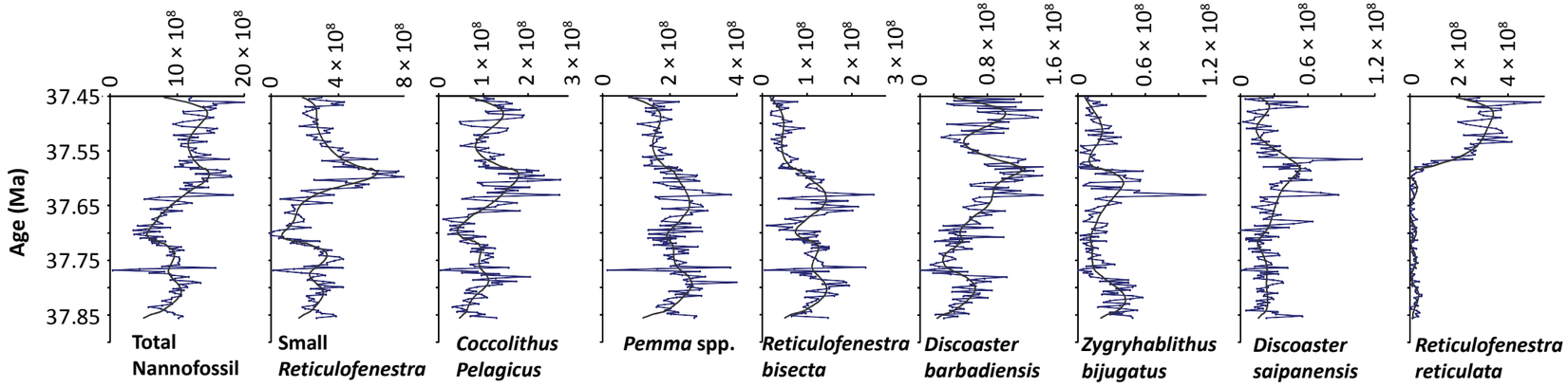

Figure A12. Abundance patterns of total nannofossil and major taxa.

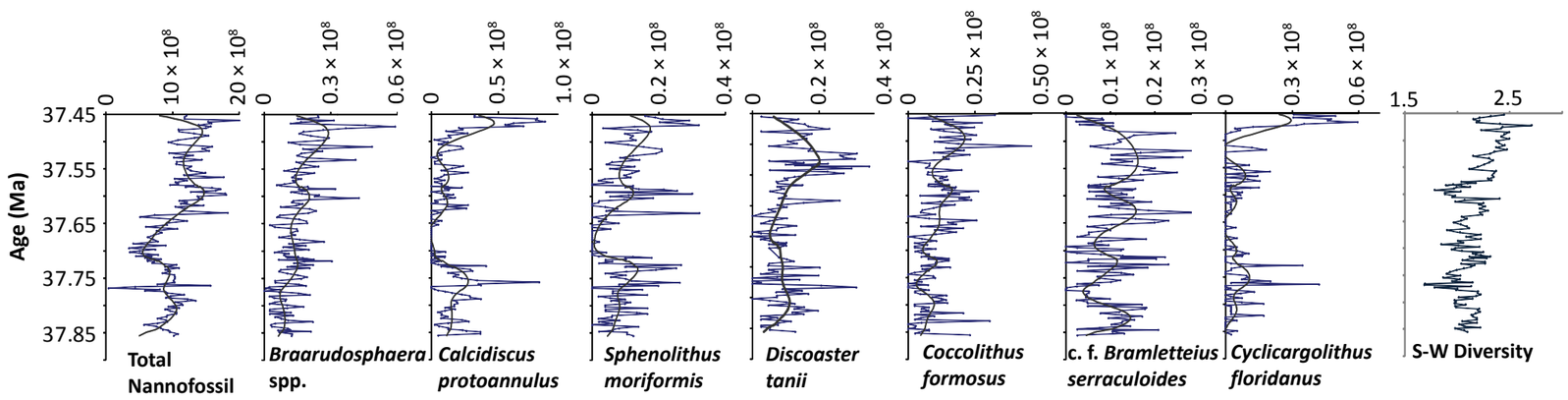

Figure A13. Abundance patterns of total nannofossil and minor taxa and S-W diversity plot.

a. **Absolute abundance (× 10^8)**

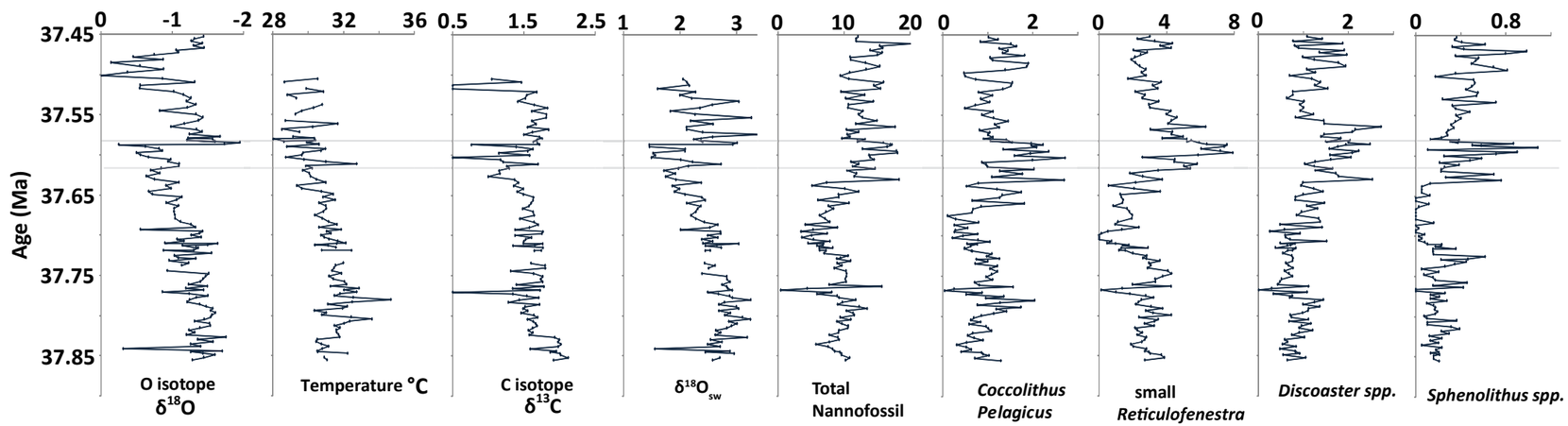

b. **Relative abundance (%)**

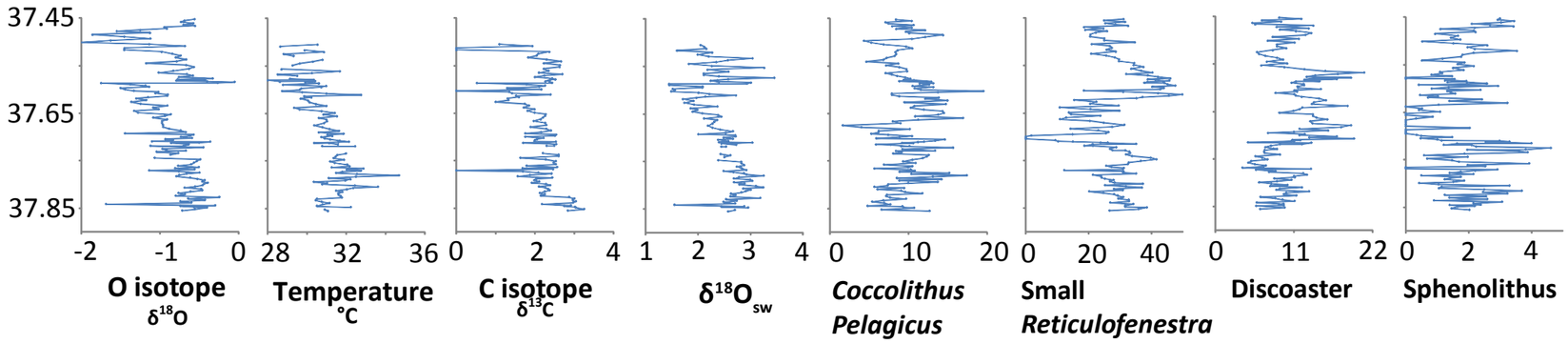

Figure A14. Comparison of Nannofossil absolute (a) and relative (b) abundance to geochemical data.

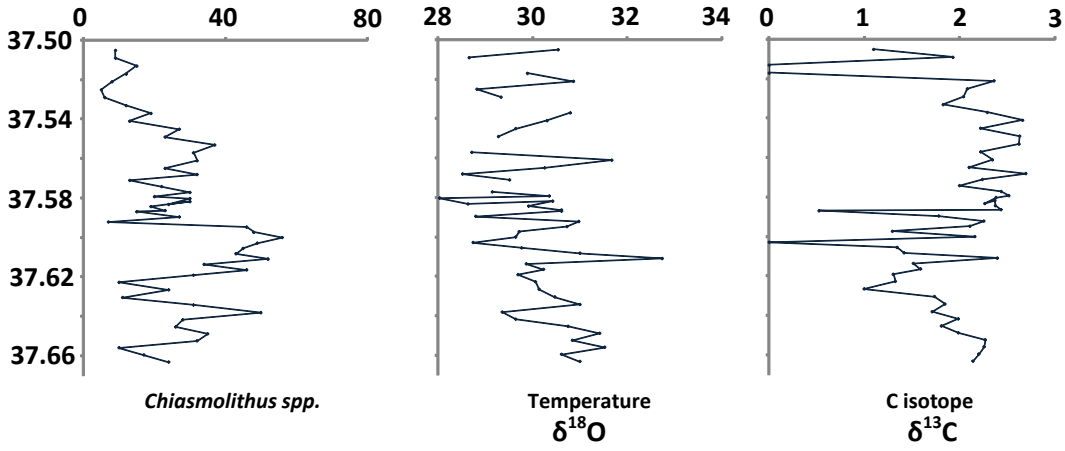

Figure A15.Plots of *Chiasmolithus* count and geochemical data.

a. Larger data set (35 Species)

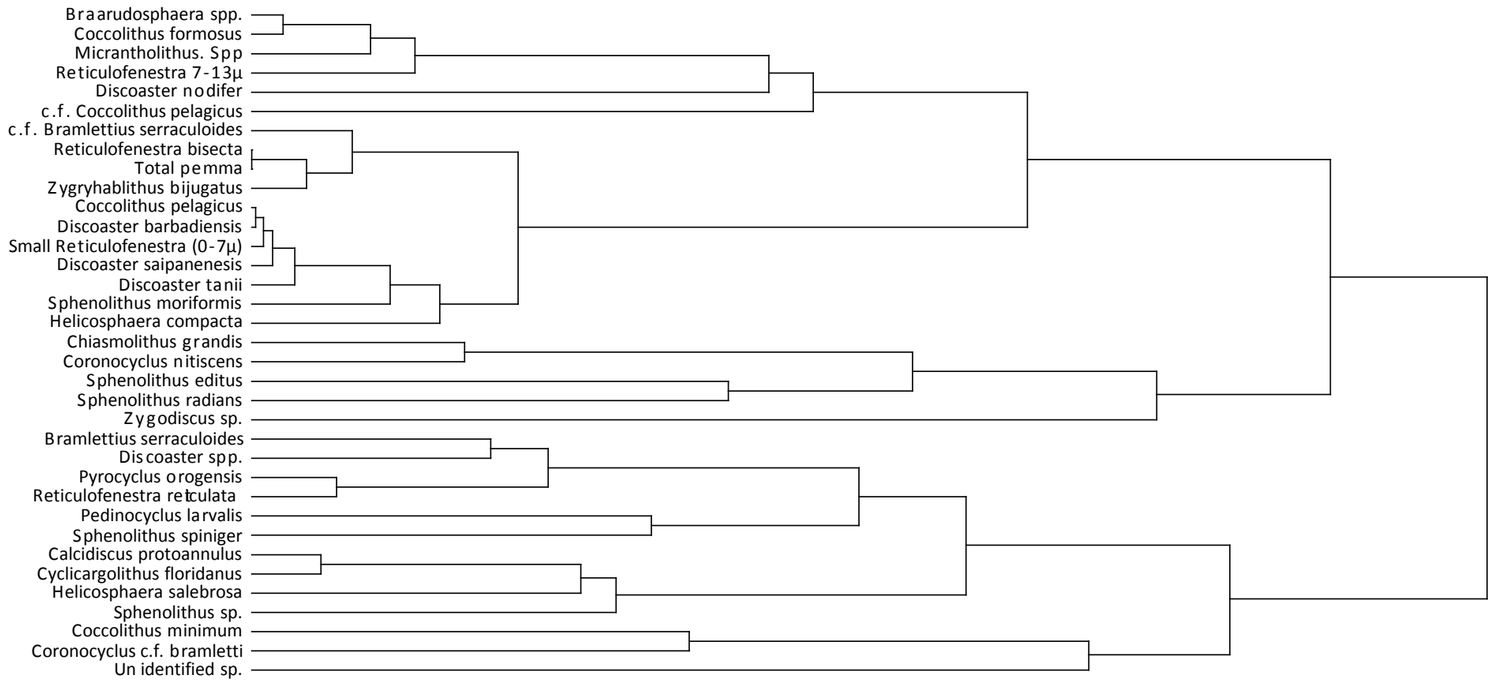

b. Smaller data set (12 Species)

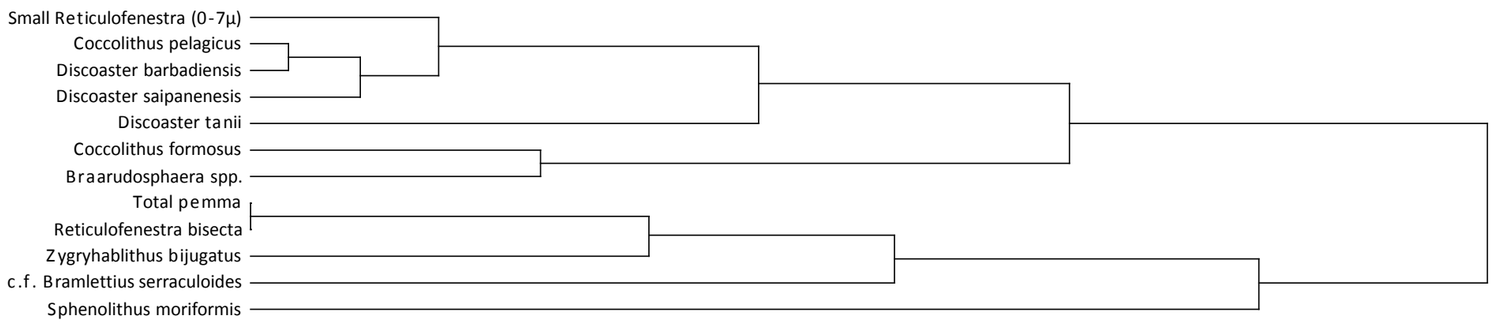

Figure A16. Results of the cluster analyses for a large (35 species, a) and small (12 species, data set).

a. Large data set (35 species).

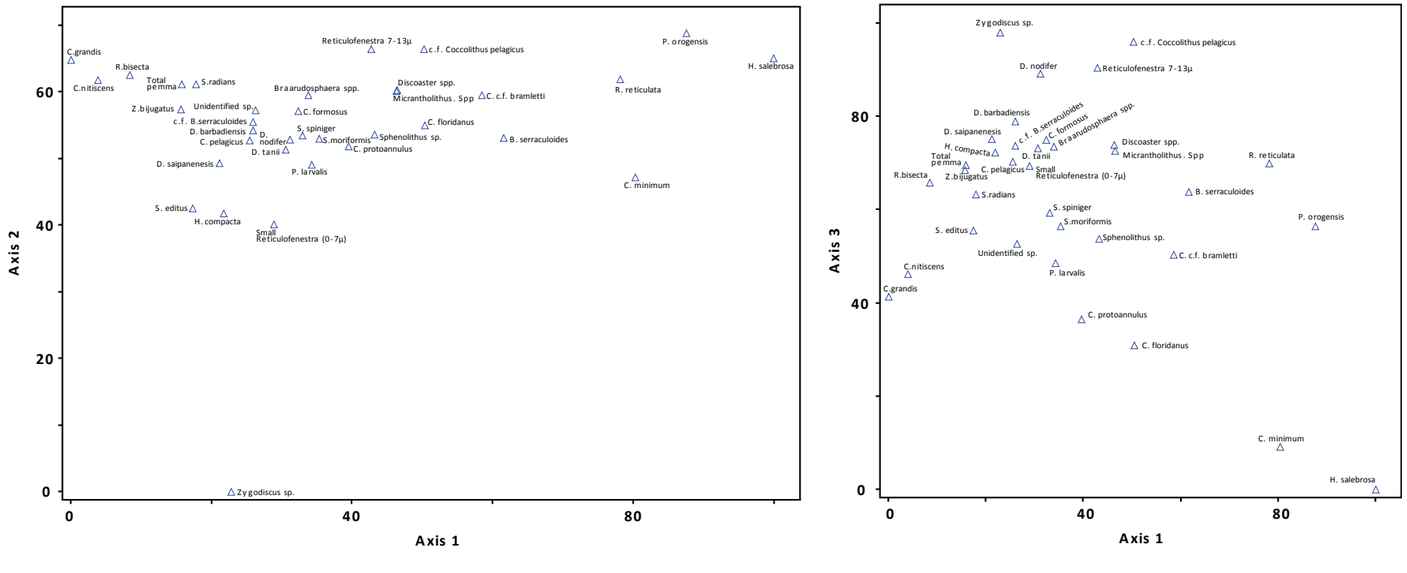

b. Small data set (12 species).

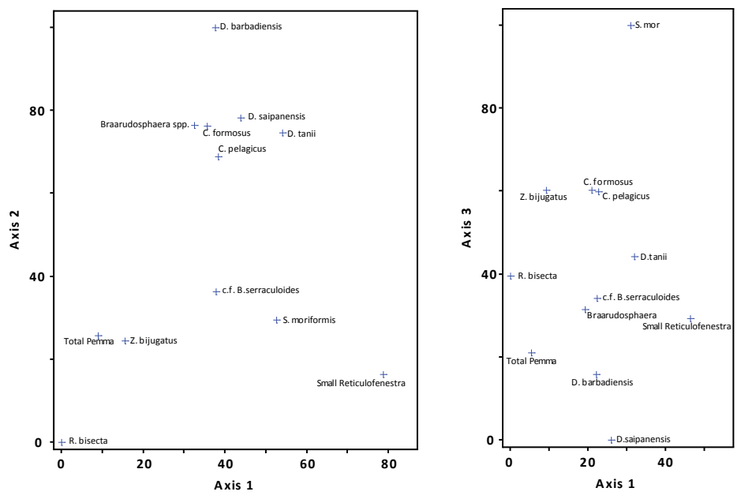

Figure A17. Results of the correspondence analyses (CA) for a large (35 species) and small (12 species) data set. Total inertia is 0.3602 and 0.0669 respectively. For the 12 species data set, CA axes 1,2, and 3 make up 29.2, 16.4 and 12.0% of the total intertia. For the 35 species data set, CA axes 1, 2 and 3 make up 20.3%, 10.8% and 6.7% of the total inertia respectively.

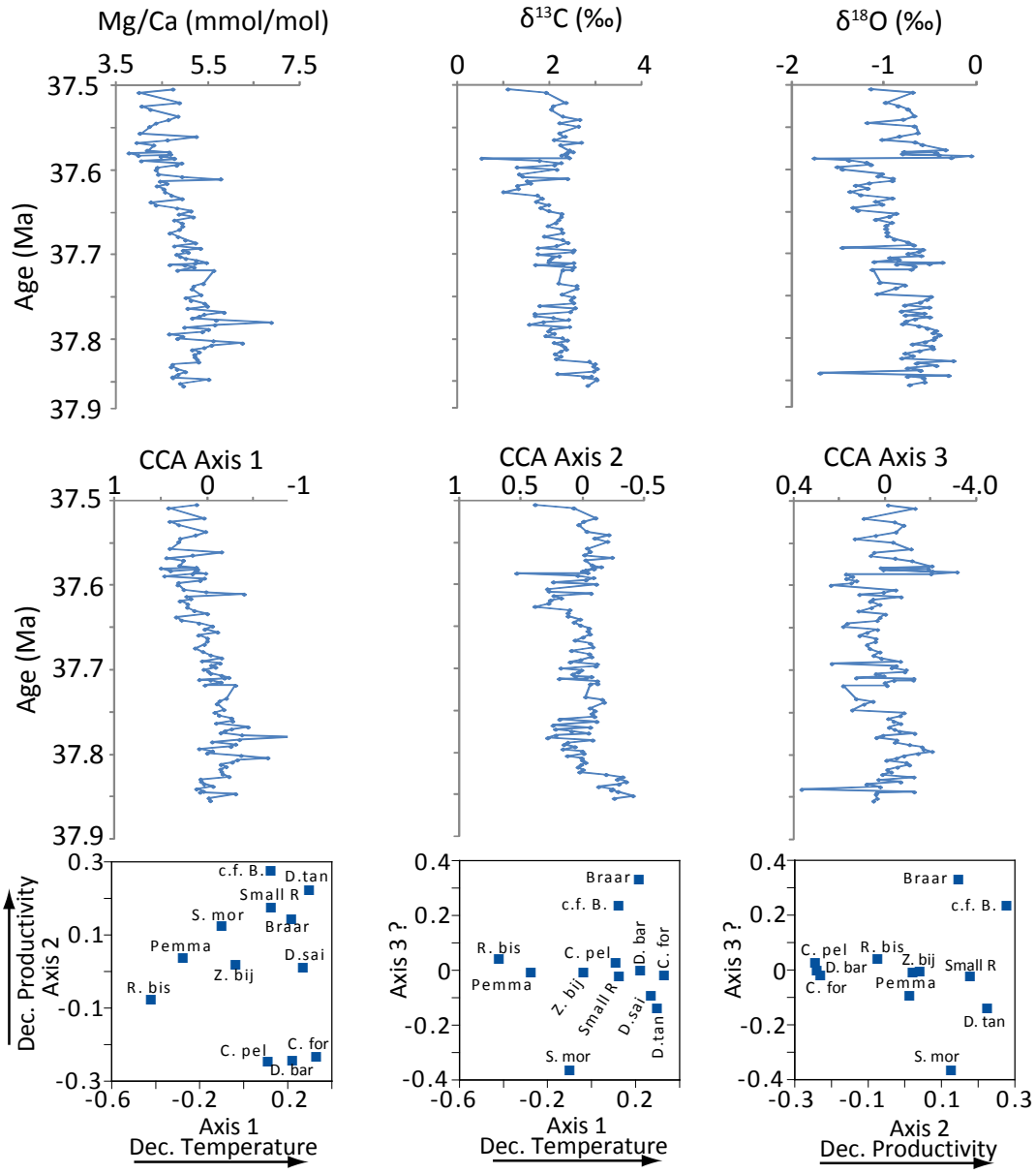

Figure A18. Results of CCA. Total species inertia = 0.00428. CCA axes 1, 2 and 3 make up 5.1%, 1.1% and 0.2% of total species inertia respectively. Full meaning of taxa abbreviations are as follows: Braa = *Braarudosphaera* spp.; C.for = *Coccolithus formosus*; c. f. Bra = c. f. *Bramletteius serraculoides*; C. pel = *Coccolithus pelagicus*; D. bar = *Discoaster barbadiensis*; D. sai = *Discoaster saipanensis*; D. tan = *Discoaster tanii*; Pemma = *Pemma* spp.; R. bis = *Reticulofenestra bisecta*; S. mor = *Sphenolithus moriformis*; Small R = small *Reticulofenestra*; Z. bij = *Zygrhablithus bijugatus*.

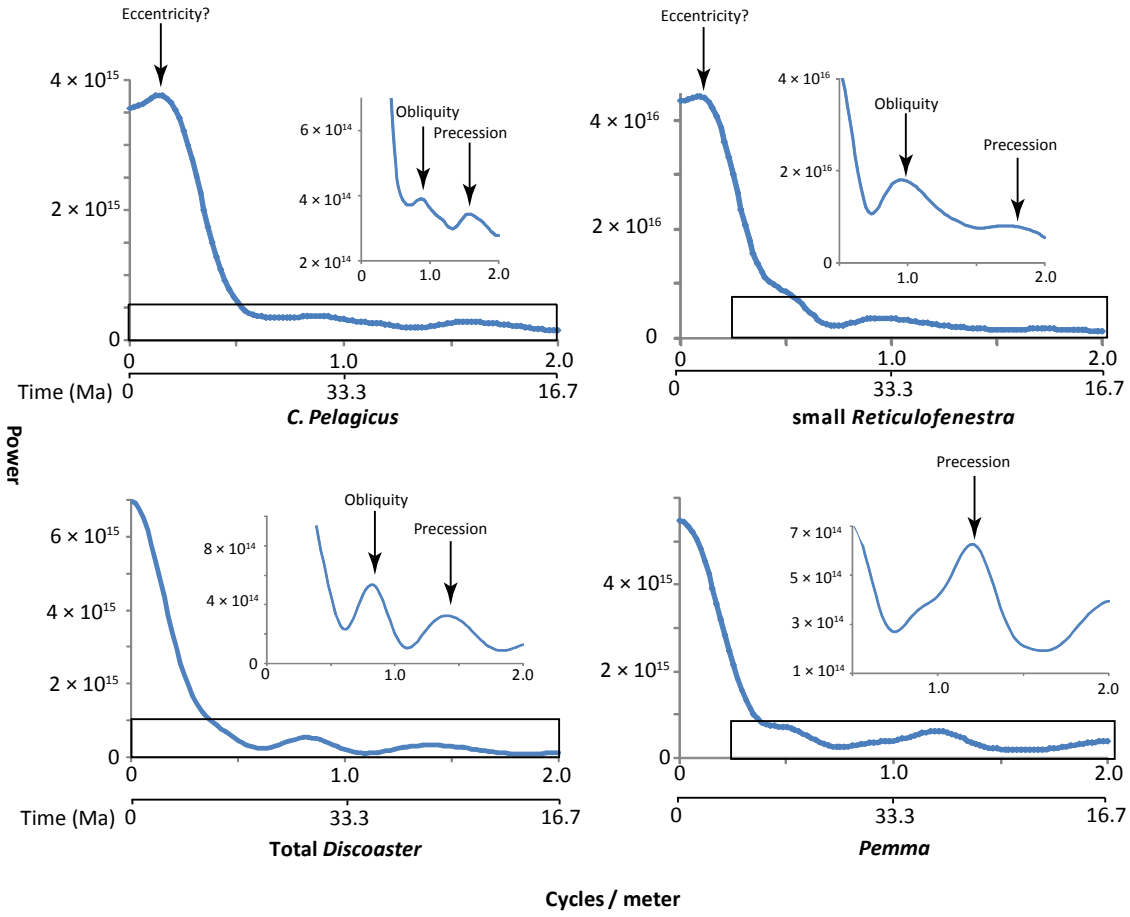

Figure A19. Spectral analysis of selected nannofossil taxa. The small insert in each figure is an exaggerated view of the area in the black box. The time scale was calculated using sedimentation rate of 3.0 cm/ky.

a) 1051A

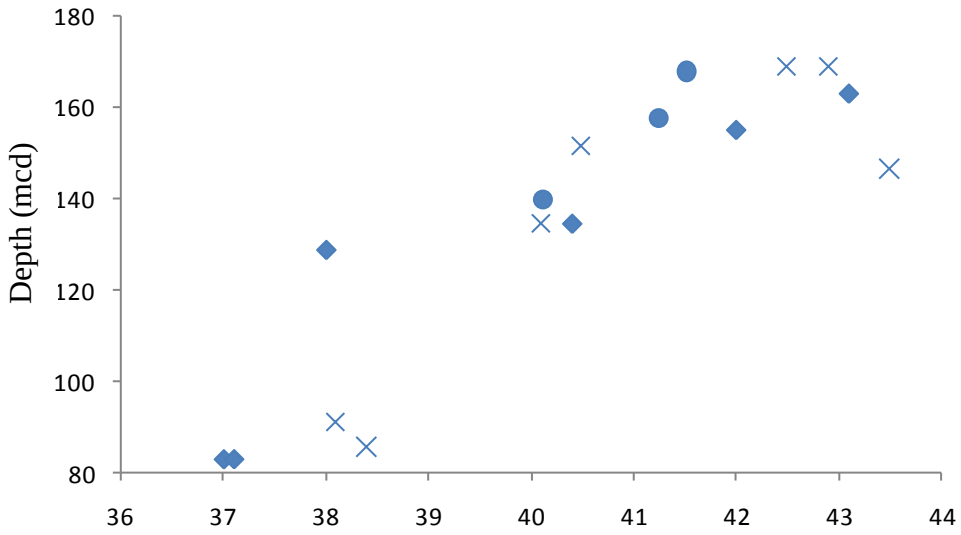

a. 1052 A

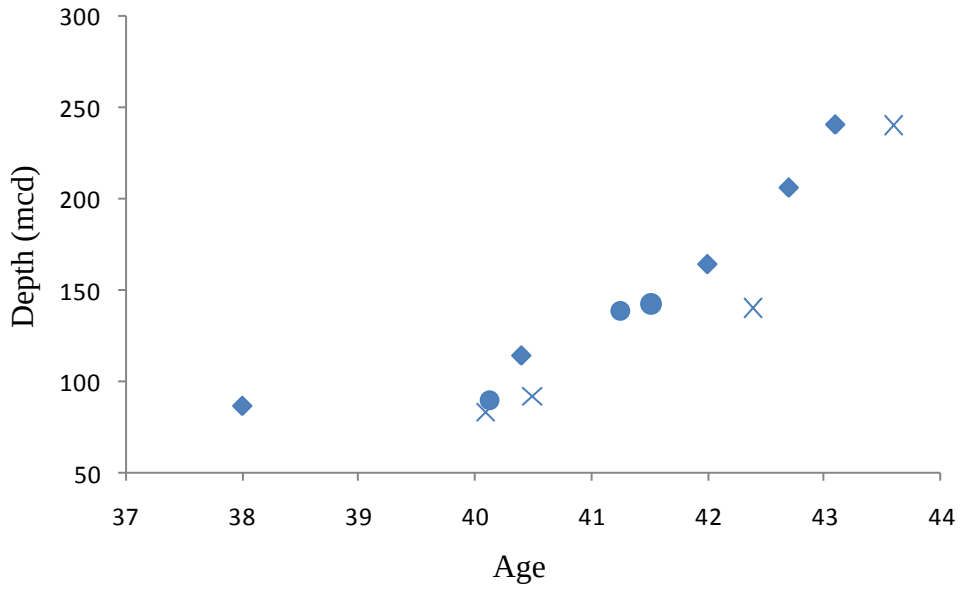

Figure A20. Age-depth model for Sites 1051 and 1052 using nannofossil (closed diamonds), planktonic foraminifera (cross) and paleomagnetic data (closed circles) from table B7.

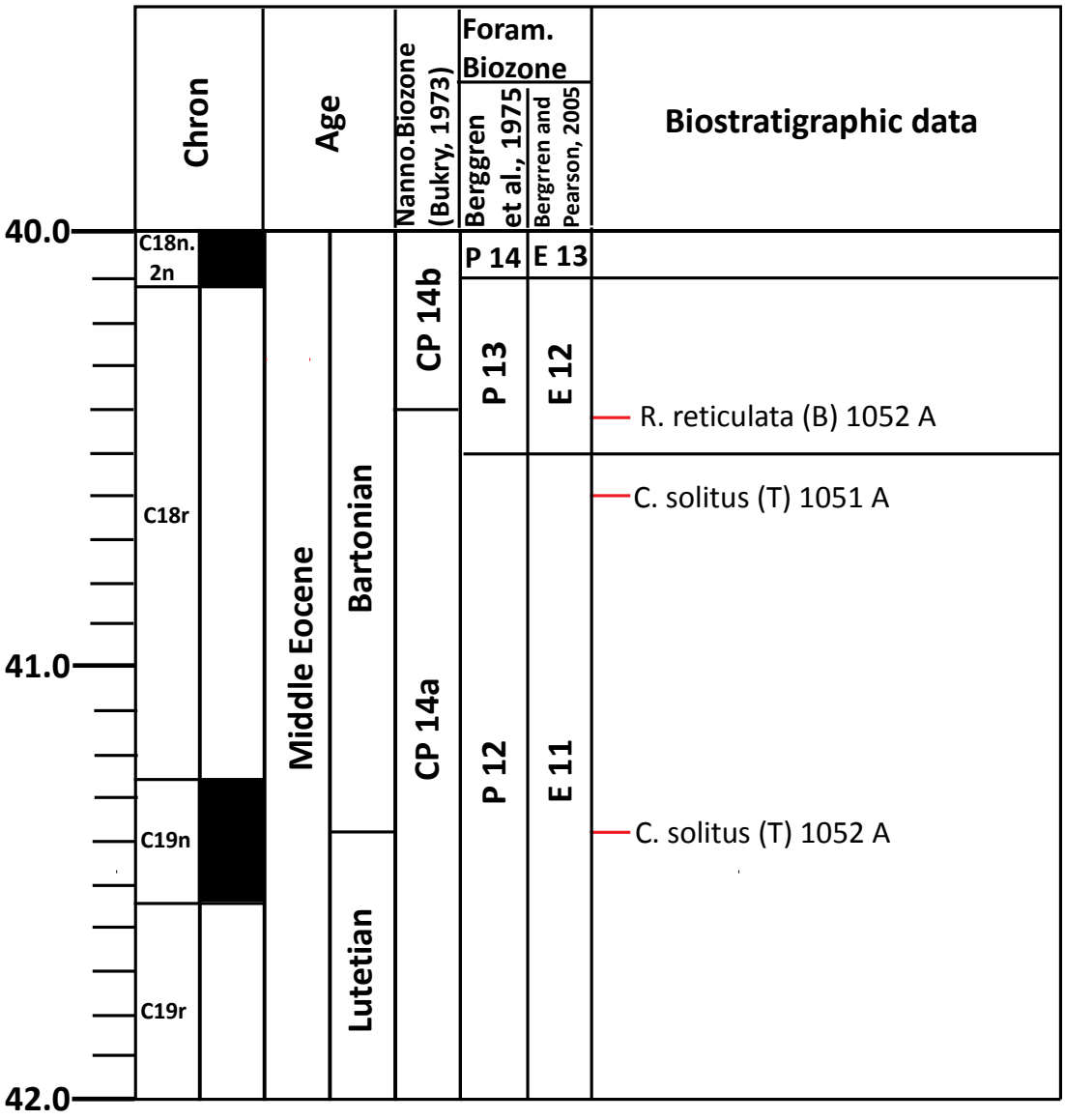

Figure A21. New and revised calcareous nannofossil biostratigraphic data for the middle Eocene (Ocean Drilling Program Site 1051 and 1052) against the magnetochronology of Cande and Kent (1995).

APPENDIX B. TABLES

Table B1. Data for the collectors curve showing the number of new species added for each sample as more fields of view were counted.

Sample number / Fields of view	5	6	7	8	9
1	17	17.67	18.1	20.5	19.5
2	22.07	21.13	22	26.4	25.47
3	25	23.35	24.34	29.95	28.7
4	27.07	25.13	25.99	32.27	30.8
5	28.67	26.67	27.25	33.83	32.17
6	30	28	28.29	35	33
7			29.16		
8			29.89		
9			30.5		
10			31		

Table B2. Results showing the calculated N/Sg using the RST and SM and results of the χ^2 test.

Sample Number	Depth	Beads	C.Pelagicus	D.barbadiensis	R. bisecta	C. floridanus	Total number of nannofossils	FOV	Weight of sediment in g	RST Number of C.pelagicus/g.× 10^8	RST Number of D.barbadiensis/g. × × 10^8	RST Number of R. bisecta/g. × 10^8	RST Number of R. reticulatum /g.× 10^8	RST Number of nannos /g. × 10^8	SM Number of C.pelagicus /g. × 10^8	SM Number of D.barbadiensis /g. × × 10^8	SM Number of R. bisecta /g. × 10^7	SM Number of C.floridanus /g. × 10^8	SM Number of nannos /g. × 10^9	Number of microbeads × 10^7	SM / RST	χ^2 value
1	81.38	496	56	29	14	220	641	6	0.0288	0.99	5.10	0.25	3.90	11.32	1.30	0.67	0.32	5.1	14.8	0.25	1.31	2.81
2	81.48	437	57	52	11	193	573	6	0.0242	1.20	11.00	0.23	4.10	12.00	1.80	1.61	0.34	6	17.9	0.22	1.49	5.35
3	81.58	400	41	20	10	215	544	6	0.0256	0.81	4.00	0.20	4.30	10.82	1.30	0.65	0.32	6.9	17.6	0.2	1.63	1.73
4	81.68	498	54	43	28	338	742	6	0.021	1.30	10.00	0.68	8.20	18.10	1.70	1.4	0.88	11	23.5	0.25	1.30	5.72
5	81.78	476	71	14	11	252	623	6	0.0226	1.60	3.20	0.25	5.70	14.06	2.20	0.43	0.34	7.7	19.1	0.24	1.36	6.81
6	81.88	554	59	19	21	312	778	6	0.0245	1.20	3.90	0.44	6.50	16.20	1.40	0.46	0.51	7.6	18.9	0.28	1.17	6.23
7	81.98	863	94	74	21	368	1150	10	0.0203	1.40	11.00	0.32	5.50	17.30	1.80	1.41	0.4	6.9	21.7	0.26	1.25	8.06
8	82.08	496	50	26	22	133	580	6	0.0196	1.30	6.80	0.57	3.50	15.01	1.70	0.88	0.75	4.5	19.7	0.25	1.31	3.25
9	82.18	507	88	70	21	197	727	6	0.0252	1.80	14.00	0.42	4.00	14.70	2.30	1.82	0.54	5.1	18.8	0.26	1.28	1.19
10	82.28	529	49	32	10	126	475	6	0.0243	1.00	6.70	0.21	2.60	9.91	1.30	0.82	0.26	3.2	12.2	0.27	1.23	5.93
11	82.38	552	50	42	9	194	523	6	0.0235	1.10	9.10	0.19	4.20	11.20	1.30	1.11	0.23	4.9	13.3	0.28	1.19	11.33
12	82.48	561	77	51	8	110	520	6	0.0211	1.90	12.00	0.19	2.70	12.60	2.10	1.4	0.22	3.1	14.5	0.29	1.15	3.46
13	82.58	623	73	55	18	176	656	6	0.0204	1.80	14.00	0.45	4.40	16.41	1.90	1.4	0.47	4.6	17.1	0.32	1.04	3.22
14	82.68	514	58	34	19	126	531	6	0.0218	1.40	7.90	0.44	2.90	12.40	1.70	1.01	0.56	3.7	15.7	0.26	1.27	3.61
15	82.78	606	20	45	28	84	442	6	0.0222	0.46	10.00	0.64	1.90	10.10	0.49	1.1	0.69	2.1	10.9	0.31	1.08	1.59
16	82.88	778	81	65	43	184	822	6	0.021	2.00	16.00	1.00	4.50	19.97	1.60	1.31	0.87	3.7	16.6	0.4	0.83	3.86
17	82.98	639	27	31	15	99	429	6	0.0193	0.71	8.20	0.40	2.60	11.32	0.72	0.83	0.4	2.7	11.5	0.33	1.02	2.93
18	83.08	646	56	38	34	148	560	6	0.0205	1.40	9.40	0.84	3.70	13.90	1.40	0.95	0.85	3.7	14	0.33	1.01	7.94
19	83.18	685	64	21	22	182	585	6	0.022	1.50	4.90	0.51	4.20	13.50	1.40	0.46	0.48	4	12.8	0.35	0.95	2.26

Table B3. Comparison of the absolute abundances of the major species between the original slides and the duplicates for RST and SM.

	RANDOM SETTLING TECHNIQUE					
	Slide number	Number of nannofossils counted	C. pelagicus × 10^8	D. barbadiensis × 10^8	R. bisecta × 10^7	R. reticulatim × 10^8
Original	14	531	1.4	7.9	4.4	2.9
	15	442	0.46	10	6.4	1.9
	16	822	2	16	10	4.5
	17	429	0.71	8.2	4	2.6
	18	560	1.4	9.4	8.4	3.7
Duplicate	14	471	0.75	4.4	3.5	3.3
	15	376	0.6	6	4.4	1.9
	16	596	1.3	11	6.5	3.7
	17	415	1.2	10	4.2	3
	18	517	1.6	6.2	4.7	3.8
	SPIKING METHOD					
	Slide number	Number of nannofossils counted	C. pelagicus × 10^8	D. barbadiensis × 10^7	R. bisecta × 10^7	R. reticulatum × 10^8
Original	14	531	1.7	10	5.6	3.7
	15	442	0.49	11	6.9	2.1
	16	822	1.6	13	8.7	3.7
	17	429	0.72	8.3	4	2.7
	18	560	1.4	9.5	8.5	3.7
Duplicate	14	471	0.76	4.5	3.6	3.3
	15	376	0.7	7	5.1	2.2
	16	596	1.1	9.7	5.7	3.2
	17	415	1.1	9.3	3.9	2.8
	18	517	1.5	5.9	4.5	3.6

Table B4. Results of the error analyses for the RST.

Sample number	Weight of sediment added IWS	Error in weight of sediment added	Volume of FOV	Error in VFV	Volume of water used for dilution	Error in volume of water used for dilution	Fractional uncertainty in IWS	Fractional uncertainty in VFV	Fractional uncertainty in VW	Sum of fractional Uncertainties	# of C.pel. /g. sed × 10^8	# of D.bar. /g. sed × 10^8	# of R. bis. /g. sed × 10^8	# of R. ret. /g. sed × 10^8	# of nannos /g. sed × 10^8	Uncertainty in # of C.pel. /g.sed × 10^8	Uncertainty in # of D.bar. /g.sed × 10^8	Uncertainty in # of R.bis. /g.sed × 10^8	Uncertainty in # of R. ret. /g.sed × 10^8	Uncertainty in # of nannos /g.sed × 10^8
1	0.0288	0.0001	0.0016	0.0002	500	2.6	0.0035	0.1221	0.0052	0.1308	0.99	0.51	0.25	3.89	11.30	0.13	0.07	0.03	0.51	1.48
2	0.0242	0.0001	0.0016	0.0002	500	2.6	0.0041	0.1221	0.0052	0.1315	1.20	1.09	0.23	4.06	12.00	0.16	0.14	0.03	0.53	1.58
3	0.0256	0.0001	0.0016	0.0002	500	2.6	0.0039	0.1221	0.0052	0.1312	0.82	0.40	0.20	4.27	10.80	0.11	0.05	0.03	0.56	1.42
4	0.021	0.0001	0.0016	0.0002	500	2.6	0.0048	0.1221	0.0052	0.1321	1.31	1.04	0.68	8.19	18.00	0.17	0.14	0.09	1.08	2.38
5	0.0226	0.0001	0.0016	0.0002	500	2.6	0.0044	0.1221	0.0052	0.1318	1.60	0.32	0.25	5.67	14.00	0.21	0.04	0.03	0.75	1.84
6	0.0245	0.0001	0.0016	0.0002	500	2.6	0.0041	0.1221	0.0052	0.1314	1.23	0.40	0.44	6.48	16.20	0.16	0.05	0.06	0.85	2.13
7	0.0203	0.0001	0.0016	0.0002	500	2.6	0.0049	0.1221	0.0052	0.1323	1.41	1.11	0.32	5.53	17.30	0.19	0.15	0.04	0.73	2.29
8	0.0196	0.0001	0.0016	0.0002	500	2.6	0.0051	0.1221	0.0052	0.1324	1.30	0.68	0.57	3.00	15.00	0.17	0.09	0.08	0.40	1.99
9	0.0252	0.0001	0.0016	0.0002	500	2.6	0.0040	0.1221	0.0052	0.1313	1.78	1.41	0.42	3.98	14.70	0.23	0.19	0.06	0.52	1.93
10	0.0243	0.0001	0.0016	0.0002	500	2.6	0.0041	0.1221	0.0052	0.1314	1.03	0.67	0.21	2.64	99.50	0.14	0.09	0.03	0.35	13.08
11	0.0235	0.0001	0.0016	0.0002	500	2.6	0.0043	0.1221	0.0052	0.1316	1.08	0.91	0.20	4.20	11.30	0.14	0.12	0.03	0.55	1.49
12	0.0211	0.0001	0.0016	0.0002	500	2.6	0.0047	0.1221	0.0052	0.1321	1.86	1.23	0.19	2.65	12.60	0.25	0.16	0.03	0.35	1.66
13	0.0204	0.0001	0.0016	0.0002	500	2.6	0.0049	0.1221	0.0052	0.1322	1.82	1.37	0.45	4.39	16.40	0.24	0.18	0.06	0.58	2.17
14	0.0218	0.0001	0.0016	0.0002	500	2.6	0.0046	0.1221	0.0052	0.1319	1.35	0.79	0.44	2.94	12.40	0.18	0.10	0.06	0.39	1.64
15	0.0222	0.0001	0.0016	0.0002	500	2.6	0.0045	0.1221	0.0052	0.1318	0.46	1.03	0.64	1.93	10.10	0.06	0.14	0.08	0.25	1.33
16	0.021	0.0001	0.0016	0.0002	500	2.6	0.0048	0.1221	0.0052	0.1321	2.00	1.58	1.04	4.46	19.90	0.26	0.21	0.14	0.59	2.63
17	0.0193	0.0001	0.0016	0.0002	500	2.6	0.0052	0.1221	0.0052	0.1325	0.71	0.82	0.40	2.61	11.30	0.09	0.11	0.05	0.35	1.50
18	0.0205	0.0001	0.0016	0.0002	500	2.6	0.0049	0.1221	0.0052	0.1322	1.39	0.94	0.84	3.67	13.90	0.18	0.12	0.11	0.49	1.84
19	0.022	0.0001	0.0016	0.0002	500	2.6	0.0045	0.1221	0.0052	0.1319	1.48	0.49	0.51	4.21	13.50	0.20	0.06	0.07	0.56	1.78

Table B5. Results of the error analyses for SM.

Sample number	Number of microbeads added (MB)	Error in number of microbeads added	Vol. of microbead solution added (V)	Error in vol. of microbead solution added	Weight of sediment added IWS	Error in weight of sediment added	Fractional uncertainty in MB	Fractional uncertainty in V	Fractional uncertainty in IWS	Sum of fractional Uncertainty	# of C.pel. /g. sed × 10^8	# of D.bar. /g. sed × 10^8	# of R. bis. /g. sed × 10^8	# of R. ret. /g. sed × 10^8	# of nannos /g. sed × 10^8	Uncertainty in # of C.pel. /g.sed × 10^8	Uncertainty in # of D.bar. /g.sed × 10^8	Uncertainty in # of R.bis. /g.sed × 10^8	Uncertainty in # of R. ret. /g.sed × 10^8	Uncertainty in # of nannos /g.sed × 10^8
1	2.20	0.46	0.15	0.0012	0.0288	0.0001	0.21	0.008	0.0035	0.2211	0.99	0.51	0.25	3.89	11.32	0.22	0.11	0.05	0.86	2.5
2	2.20	0.46	0.15	0.0012	0.0242	0.0001	0.21	0.008	0.0041	0.2217	1.20	1.09	0.23	4.06	12.04	0.27	0.24	0.05	0.9	2.67
3	2.20	0.46	0.15	0.0012	0.0256	0.0001	0.21	0.008	0.0039	0.2215	0.81	0.4	0.2	4.27	10.82	0.18	0.09	0.04	0.95	2.4
4	2.20	0.46	0.15	0.0012	0.021	0.0001	0.21	0.008	0.0048	0.2224	1.31	1.04	0.68	8.19	17.99	0.29	0.23	0.15	1.82	4
5	2.20	0.46	0.15	0.0012	0.0226	0.0001	0.21	0.008	0.0044	0.2220	1.60	0.32	0.25	5.67	14.03	0.35	0.07	0.06	1.26	3.11
6	2.20	0.46	0.15	0.0012	0.0245	0.0001	0.21	0.008	0.0041	0.2217	1.22	0.39	0.44	6.48	16.16	0.27	0.09	0.10	1.44	3.58
7	2.20	0.46	0.15	0.0012	0.0203	0.0001	0.21	0.008	0.0049	0.2225	1.41	1.11	0.32	5.34	17.30	0.31	0.25	0.07	1.23	3.85
8	2.20	0.46	0.15	0.0012	0.0196	0.0001	0.21	0.008	0.0051	0.2227	1.30	0.68	0.57	3.45	15.05	0.29	0.15	0.13	0.77	3.35
9	2.20	0.46	0.15	0.0012	0.0252	0.0001	0.21	0.008	0.0040	0.2216	1.78	1.41	0.42	3.98	14.68	0.39	0.31	0.09	0.88	3.25
10	2.20	0.46	0.15	0.0012	0.0243	0.0001	0.21	0.008	0.0041	0.2217	1.03	0.67	0.21	2.63	9.95	0.23	0.15	0.05	0.59	2.2
11	2.20	0.46	0.15	0.0012	0.0235	0.0001	0.21	0.008	0.0043	0.2219	1.08	0.91	0.19	4.2	11.33	0.24	0.2	0.04	0.93	2.51
12	2.20	0.46	0.15	0.0012	0.0211	0.0001	0.21	0.008	0.0047	0.2223	1.86	1.23	0.19	2.65	12.55	0.41	0.27	0.04	0.59	2.79
13	2.20	0.46	0.15	0.0012	0.0204	0.0001	0.21	0.008	0.0049	0.2225	1.82	1.37	0.45	4.39	16.37	0.41	0.31	0.10	0.98	3.64
14	2.20	0.46	0.15	0.0012	0.0218	0.0001	0.21	0.008	0.0046	0.2222	1.35	0.79	0.44	2.94	12.40	0.3	0.18	0.10	0.65	2.75
15	2.20	0.46	0.15	0.0012	0.0222	0.0001	0.21	0.008	0.0045	0.2221	0.46	1.03	0.64	1.93	10.13	0.1	0.23	0.14	0.43	2.25
16	2.20	0.46	0.15	0.0012	0.021	0.0001	0.21	0.008	0.0048	0.2224	1.96	1.58	1.04	4.46	19.91	0.44	0.35	0.23	0.99	4.23
17	2.20	0.46	0.15	0.0012	0.0193	0.0001	0.21	0.008	0.0052	0.2228	0.71	0.82	0.4	2.61	11.32	0.16	0.18	0.09	0.58	2.52
18	2.20	0.46	0.15	0.0012	0.0205	0.0001	0.21	0.008	0.0049	0.2225	1.39	0.94	0.84	3.67	13.90	0.31	0.21	0.19	0.82	3.09
19	2.20	0.46	0.15	0.0012	0.022	0.0001	0.21	0.008	0.0045	0.2222	1.48	0.49	0.51	4.21	13.54	0.33	0.11	0.11	0.94	3

Table B6. Geochemical data from Site 1052.

Depth(MCD)	Age	Mg/Ca (mmol/mol)	Sr/Ca (mmol/mol)	isotope	Calculated Paleotemperature	$\delta^{18}O_{sw}$
82.98	37.5052	4.75	1.335	-1.139	30.5	2.051158
83.08	37.5092	4.01	1.354	-0.687	28.7	2.121151
83.18	37.5132	**5.75**	1.359	-1.452		2.16218
83.28	37.5172	4.48	1.353	-1.458	29.9	1.60082
83.38	37.5212	4.89	1.359	-0.981	30.9	2.274091
83.48	37.5252	4.07	1.354	-0.846	28.8	1.99589
83.58	37.5292	4.26	1.361	-0.74	29.3	2.205251
83.68	37.5332	**6.39**	1.363	-0.804		3.041373
83.78	37.5372	4.86	1.348	-0.671	30.8	2.570349
83.88	37.5412	4.65	1.342	-0.791	30.3	2.351487
83.98	37.5452	4.38	1.314	-1.179	29.6	1.82897
84.08	37.5492	4.24	1.342	-0.67	29.3	2.264611
84.18	37.5532	**6.36**	1.351	-0.572		3.263109
84.28	37.5572	4.03	1.349	-0.635	28.7	2.184458
84.38	37.5612	5.26	1.375	-0.833	31.7	2.584396
84.48	37.5651	4.63	1.372	-1.02	30.3	2.112818
84.58	37.5682	3.96	1.324	-0.663	28.5	2.11661
84.68	37.5712	4.33	1.342	-0.583	29.5	2.399068
84.78	37.5743	**7.59**	1.366	-0.762		3.455951
84.88	37.5773	4.19	1.231	-0.332	29.1	2.575768
84.98	37.5794	4.67	1.229	-0.781	30.4	2.37111
85.08	37.5804	3.79	1.235	-0.437	28.0	2.24254
85.11	37.5834	4.00	1.266	-0.402	28.6	2.400474
85.18	37.5820	4.70	1.189	-0.796	30.4	2.370461
85.21	37.5845	4.49	1.203	-0.054	29.9	3.009837
85.31	37.5865	4.78	1.189	-0.271	30.6	2.933246
85.41	37.5871	4.78	1.237	-1.751	30.6	1.453246
85.51	37.5897	4.06	1.245	-1.378	28.8	1.458305
85.61	37.5923	4.94	1.220	-1.187	31.0	2.090792
85.71	37.5949	4.83	1.266	-1.141	30.7	2.086514
85.81	37.5975	4.41	1.260	-1.503	29.7	1.520357
85.91	37.6002	4.38	1.241	-1.447	29.6	1.56097
86.01	37.6030	4.04	1.285	-1.334	28.7	1.491089
86.11	37.6057	4.43	1.255	-1.022	29.8	2.011552
86.21	37.6084	4.95	1.267	-1.062	31.0	2.220302
86.31	37.6111	5.79	1.211	-0.904	32.7	2.725431
86.41	37.6138	4.47	1.266	-0.908	29.9	2.145791
86.51	37.6166	4.62	1.249	-1.157	30.2	1.970967
86.61	37.6193	4.40	1.202	-1.304	29.7	1.714241
86.71	37.6229	4.55	1.187	-1.177	30.1	1.916684
86.81	37.6267	4.58	1.194	-1.365	30.1	1.743446

Note: The bold Mg/Ca values are higher than normal values that were not used in the paleoenvironmental interpretation.

Table B6. continued

Depth(MCD)	Age	Mg/Ca (mmol/mol)	Sr/Ca (mmol/mol)	isotope	Calculated Paleotemperature	$\delta^{18}O_{sw}$
86.91	37.6306	4.72	1.189	-1.25	30.5	1.925972
87.01	37.6344	4.95	1.198	-0.908	31.0	2.374302
87.11	37.6383	4.27	1.197	-1.089	29.4	1.861551
87.21	37.6419	4.38	1.235	-1.019	29.6	1.98897
87.31	37.6455	4.84	1.170	-1.332	30.8	1.900136
87.41	37.6490	5.14	1.176	-1.28	31.4	2.086157
87.51	37.6526	4.88	1.220	-0.867	30.8	2.383521
87.61	37.6561	5.19	1.174	-0.941	31.5	2.446663
87.71	37.6597	4.78	1.209	-1.087	30.6	2.117246
87.81	37.6633	4.95	1.175	-0.914	31.0	2.368302
87.91	37.6668	4.96	1.162	-0.975	31.0	2.311802
88.01	37.6707	4.89	1.219	-0.977	30.9	2.278091
88.11	37.6750	4.68	1.190	-0.965	30.4	2.191904
88.21	37.6792	4.86	1.199	-0.963	30.8	2.278349
88.31	37.6832	5.02	1.211	-0.886	31.2	2.427598
88.41	37.6867	5.24	1.159	-0.74	31.6	2.668945
88.51	37.6902	4.78	1.225	-0.676	30.6	2.528246
88.61	37.6929	5.35	1.182	-1.447	31.9	2.007998
88.71	37.6953	4.97	1.226	-0.577	31.0	2.714293
88.81	37.6977	5.08	1.251	-0.62	31.3	2.720046
88.91	37.7001	4.83	1.255	-0.737	30.7	2.490514
89.01	37.7026	4.91	1.241	-0.596	30.9	2.668202
89.11	37.7050	5.03	1.205	-0.934	31.2	2.384029
89.21	37.7074	5.26	1.203	-0.839	31.7	2.578396
89.31	37.7098	5.48	1.211	-1.104	32.1	2.404113
89.37	37.7105	5.23	1.214	-0.366	31.6	3.038707
89.41	37.7123	4.68	1.236	-0.506	30.4	2.650904
89.47	37.7128	5.01	1.220	-0.86	31.1	2.449156
89.51	37.7154	5.21	1.215	-0.667	31.6	2.729203
89.61	37.7188	4.85	1.218	-0.702	30.8	2.534748
89.67	37.7191	5.64	1.174	-1.125	32.5	2.446635
90.17	37.7345	5.41	1.192	-1.046	32.0	2.433685
90.27	37.7375	5.20	1.263	-0.772	31.5	2.619937
90.37	37.7409	5.16	1.228	-0.87	31.5	2.504787
90.47	37.7443	5.11	1.216		31.4	
90.57	37.7477	5.36	1.188	-1.071	31.9	2.388133
90.67	37.7511	5.03	1.225	-0.491	31.2	2.827029
90.77	37.7545	5.14	1.230	-0.535	31.4	2.831157
90.87	37.7579	5.44	1.249	-0.607	32.1	2.884917
90.97	37.7613	5.50	1.262	-0.773	32.2	2.743163
91.07	37.7638	5.07	1.237	-0.51	31.3	2.825662
91.17	37.7661	5.86	1.190	-0.81	32.9	2.845848

Table B6. continued

Depth(MCD)	Age	Mg/Ca (mmol/mol)	Sr/Ca (mmol/mol)	isotope	Calculated Paleotemperature	$\delta^{18}O_{sw}$
91.27	37.7684	5.43	1.207	-0.563	32.0	2.924848
91.37	37.7707	5.79	1.197	-1.14	32.7	2.489431
91.47	37.7730	5.32	1.202	-0.765	31.8	2.677541
91.57	37.7753	5.17	1.196	-0.503	31.5	2.876088
91.67	37.7776	5.69	1.200	-0.664	32.5	2.927084
91.77	37.7803	6.89	1.173	-0.758	34.7	3.251138
91.87	37.7833	5.66	1.204	-0.794	32.5	2.785437
91.97	37.7860	5.00	1.191	-0.619	31.1	2.685705
92.07	37.7887	5.52	1.168	-0.528	32.2	2.996181
92.17	37.7913	5.39	1.221	-0.435	31.9	3.036489
92.27	37.7940	4.67	1.244	-0.465	30.4	2.68711
92.37	37.7967	4.96	1.229	-0.397	31.0	2.889802
92.47	37.7993	4.85	1.217	-0.445	30.8	2.791748
92.57	37.8020	5.63	1.198	-0.463	32.4	3.104723
92.67	37.8047	6.26	1.209	-0.555	33.6	3.24551
92.77	37.8073	5.59	1.203	-0.689	32.4	2.862997
92.87	37.8100	5.43	1.249	-0.48	32.0	3.007848
92.97	37.8127	5.17	1.227	-0.468	31.5	2.911088
93.07	37.8153	5.32	1.266	-0.614	31.8	2.828541
93.07	37.8153	5.16	1.270	-0.614	31.5	2.760787
93.17	37.8182	5.22	1.275	-0.768	31.6	2.632459
93.17	37.8182	5.07	1.284	-0.768	31.3	2.567662
93.27	37.8211	5.23	1.232	-0.687	31.6	2.717707
93.27	37.8211	4.99	1.259	-0.687	31.1	2.613244
93.37	37.8240	5.28	1.252	-0.804	31.7	2.621813
93.37	37.8240	5.25	1.257	-0.804	31.7	2.609175
93.47	37.8270	5.31	1.286	-0.249	31.8	3.189372
93.47	37.8270	5.06	1.268	-0.249	31.2	3.082268
93.57	37.8299	4.74	1.282	-0.646	30.5	2.53944
93.67	37.8328	4.71	1.272	-0.431	30.4	2.740222
93.77	37.8357	4.84	1.274	-0.744	30.8	2.488136
93.87	37.8386	5.02	1.245	-0.604	31.2	2.709598
93.97	37.8416	4.86	1.299	-1.688	30.8	1.553349
94.07	37.8445	4.74	1.270	-0.301	30.5	2.88444
94.13	37.8455	4.75	1.266	-0.743	30.5	2.447158
94.17	37.8474	5.53	1.256	-0.571	32.2	2.957178
94.23	37.8489			-0.404		
94.33	37.8523	4.91	1.281	-0.56	30.9	2.704202
94.43	37.8555	4.98	1.248	-0.72	31.1	2.575773

Table B7. Age-Depth data for Sites 1051 and 1052.

1051	Datum	Species/chron	Age	Depth(mcd)
	T	*G. beckmanni*	40.1	82.93
	B	*D. bisectus*	38	87.21
	B	*G. beckmanni*	40.5	91.43
	T	*C. solitus*	40.4	114.68
	B	*T. pomeroli*	42.4	140.09
	B	*C. reticulatum*	42	164.51
	B	*R. umbilica*	42.7	206.225
	T	*M. aragonensis*	43.6	240.24
	T	*N. fulgens*	43.1	240.62
	T	C18r	40.13	89.37
	T	C19n	41.257	138.67
	B	C19r	41.521	142.27
1052				
	B	*C. oamaruensis*	37	83.015
	T	*C. grandis*	37.1	83.035
	B	*D. bisecta*	38	128.76
	T	*C. solitus*	40.4	134.48
	B	*C. reticulatum*	42	154.97
	T	*N. fulgens*	43.1	162.91
	T	*M. spinulosa*	38.1	90.96
	B	*P. semiinvoluta*	38.4	85.59
	T	*O. beckmanni*	40.1	134.5
	B	*O. beckmanni*	40.5	151.54
	B	*T. pomeroli*	42.5	168.79
	B	*G. index*	42.9	168.79
	B	*M. lehneri*	43.5	146.51
	T	C18r	40.13	139.63
	T	C19n	41.257	157.63
	B	C19r	41.521	167.83

Table B8. New and revised calcareous nannofossil data from ODP Sites 1051 and 1052.

Event	Hole	This Study			Mita (2001)			Age (Ma) (CK 95)	
		Core and interval	Depth (mbsf)	Depth (mcd)	Core and interval	Depth (mbsf)	Depth (mcd)	This Study	Mita (2001)
Chiasmolithus solitus (T)	1051A	12H-3-40cm	104.2	115.13	12H-3-67 cm	104.47	115.40	40.60	40.61
Reticulofenestra reticulata (B)	1052A	17X-2-150 cm	139.3	144.62	19X-3-43 cm	158.73	164.35	40.42	41.34
Chiasmolithus solitus (T)	1052A	19X-1-100 cm	156.3	161.92	19X-3-43 cm	158.73	164.35	41.23	41.34

Table B9. Recalculated ages for biostratigraphic events published by Mita 2001.

1051A								
Datum	species	Age	Zone/ Subzone	core section int.	depth (mbsf)	Chron	Recalc. age	Error depth (mbsf)
B	*D.bisectus*	38		10H-6,90-91	90.2	C18r	41.45	91
T	*C.solitus*	40.4	CP14a	12H-3,67-69	103.15	C18r	41.68	104.47
B	*C.reticulatum*	42		17X-4,45-47	153.25	C19r	41.91	156.48
B	*R.umbilicus*	43.7	CP14a	24X-3,66-68	219.46	C20n	43.31	221.19
T	*N.fulgens*	43.1		25X-4,53-55	229.3	C20n	43.54	230.43
T	*C.gigas*	44.5	CP13c	27X-CC,36-38	252.85	C20r	44.08	254.47
B	*C.gigas*	46.1	CP13b	36X-4,56-58	336.16	C20r	45.95	340.89
B	*N.fulgens*	47.3	CP13a	37X-CC,13-16	347.06	C21n	46.30	350.67
B	*R.inflata*	48.5	CP12b	40X-CC,38-40	377.18	C21n	47.66	379.77
T	*T.orthostylus*	50.6		42X-1,81-83	380.58	C22n	?	390.71
B	*D.sublodoensis*	49.7	CP12a	44X-1,75-77	409.85	C22r	50.77	412.95
B	*D.lodoensis*	52.9	CP10	47X-2,72-74	440.12	C24n	52.54	443.18
T	*T.contortus*	53.6		48X-CC,52-54	456.72	C24n	52.89	457.3
B	*T.orthostylus*	53.6	CP9b	48X-CC,52-54	457.3	C24n	52.90	457.11
T	*T.bramlettei*	53.9		49X-2,50-52	457.85	C24n	52.92	459.08
B	*T.contortus*	54.4		51X-CC,39-41	476.56	C24n	53.32	481.69
B	*T.bramlettei*	55.2	CP9a	55X-CC,19-22	510.82	C24r	55.25	518.55
T	*F.tympaniformis*	55.3		56X-3,65-66	510.82	C24r	55.25	518.55
1052A								
T	*C. grandis*	37.1	t CP14b	9H-6, 87-89	77.06	C17n	37.66	78.55
B	*D. bisecta*	38	?	17X-1, 68-70	136.68	C18r	40.32	138.67
T	*C. solitus*	40.4	t CP14a	19X-3, 43-44	157.49	C19n	41.40	158.73
B	*C. reticulatum*	42	?	19X-3, 43-44	157.49	C19n	41.40	158.73
T	*N. fulgens*	43.1		19X-4, 63-65	158.73	C19n	41.43	160.44
B	*R. umbilicus*	43.7	b CP14a	19X-4, 63-65	161.95	C19n	41.49	160.44
B*	*N. fulgens*	47.3		19X-4, 63-65	161.95	C19n	41.49	160.44
B*	*R. inflata*	48.5	b CP12b	20X-1, 40-41	163.41	C19n	41.52	162.72

APPENDIX C. NANNOFOSSIL RAW COUNTS

Depth	microeads	Blackities spinosus	Braarudosphaera spp.	Bramlettius serraculoides	c.f. Bramlettius cerraculoides	c.f. C. pelagicus	Calcidiscus protoannulus	Cepekiella lumina	Chiasmolithus grandis	Coccolithus formosus	Coccolithus minimus	Coccolithus pelagicus	Coronocyclus cf. bramletti	Coronocyclus nitiscens	Coronocyclus spp.	Cyclicargolithus floridanus	Discoaster barbadiensis	Discoaster nodifer	Discoaster saipanensis	Discoaster spp.	Discoaster tanii	Ericsonia sp.	Helicosphaera salebrosa	Helicosphaeracompacta	Lanternithus procerus	Markailus inversus	Micrantholithus spp.	Neococcolithes protenus	Pedinocyclus larvalis	Pontosphaera plana	Pontosphaera sp.	Pyrocyclus orogensis	Pyrocyclus sp.	Reticulofenestra bisecta	Reticulofenestra reticulata	Reticulofenestra sp. (0-7µ)	Reticulofenestra sp. (7-13 µ)	Sphenolithus editus	Sphenolithus moriformis	Sphenolithus obtusus	Sphenolithus radians	Sphenolithus sp.	Sphenolithus spiniger	Total pemma	Unidentified sp.	Zygodiscus sp.	Zygrhablithus bijugatus	Total
81.38	496	0	13	1	0	0	18	0	0	18	2	56	0	0	0	17	29	3	16	5	7	2	1	0	0	0	24	0	0	0	0	2	0	14	157	207	6	1	11	0	3	1	4	43	1	0	5	668
81.48	437	0	11	3	0	0	15	0	0	5	0	57	1	0	0	23	52	2	2	3	7	0	5	1	1	0	16	0	0	0	0	0	0	11	104	136	5	1	11	0	0	4	0	68	0	0	4	548
81.58	400	0	7.4	2	4	0	39	0	0	0	2	41	0	0	0	15	20	0	8	3	7	0	0	1	0	0	2.2	0	1	1	0	1	0	10	134	183	5	0	13	0	1	4	2	69	0	0	5	580
81.68	498	1	11	0	3	0	28	0	1	6	0	54	0	0	1	17	43	0	18	4	2	0	4	1	0	0	4.8	0	2	0	0	3	0	28	191	183	9	0	13	0	0	4	5	81	0	0	7	725
81.78	476	0	7.2	1	1	0	37	0	0	4	3	71	3	0	0	20	14	0	10	4	7	0	1	1	0	0	2.8	0	2	0	0	2	0	11	185	190	4	0	11	0	1	2	0	66	0	0	6	667
81.88	554	0	5.6	1	5	0	29	0	0	13	0	59	0	0	0	28	19	0	17	1	5	0	2	0	0	0	3.2	1	7	0	0	5	0	21	175	242	2	1	16	0	0	0	3	71	1	0	12	745
81.98	863	0	30	0	2	3	36	1	0	9	0	94	0	0	0	23	74	0	39	1	10	0	0	0	0	0	10	0	2	0	1	2	0	21	154	167	34	0	26	0	1	2	2	119	0	0	41	904
82.08	496	0	22	5	4	0	26	0	0	6	0	50	2	0	0	12	26	0	12	9	4	2	2	0	1	1	5.2	2	2	0	0	3	0	22	140	146	7	0	6	0	2	2	3	48	0	0	20	593
82.18	507	0	18	2	4	2	10	0	0	12	0	88	0	0	0	6	70	3	8	4	10	0	0	2	0	0	7.2	0	2	0	0	3	0	21	181	137	16	0	2	0	2	2	2	99	0	0	14	727
82.28	529	0	12	1	4	4	11	0	0	4	0	49	0	0	0	2	32	0	3	2	9	0	0	0	0	0	3.6	0	2	0	0	0	0	10	134	131	3	0	8	1	0	1	1	60	0	0	20	508
82.38	552	0	8	2	5	1	5	0	0	6	0	50	0	0	0	3	42	0	6	1	7	0	0	0	0	0	4.2	0	0	0	0	1	1	9	127	110	7	0	10	0	0	1	0	70	0	0	19	495
82.48	561	0	6.4	2	10	2	11	0	0	8	0	77	0	0	0	1	51	0	10	1	10	0	0	0	0	0	5.2	0	2	0	0	3	0	8	122	110	13	0	5	0	0	0	0	60	0	0	18	535
82.58	623	0	8.2	2	6	5	5	0	1	10	0	73	1	0	0	0	55	1	5	4	11	0	0	2	0	0	6.2	1	0	0	0	2	0	18	145	123	10	1	6	0	0	0	3	71	2	0	25	602
82.68	514	0	12	1	6	1	6	0	1	5	0	58	0	0	0	0	34	0	5	1	5	0	0	1	0	0	3.8	0	2	0	0	1	1	19	123	139	7	0	6	0	0	0	2	86	0	0	31	557
82.78	606	0	11	0	5	1	1	0	1	10	0	20	1	0	0	0	45	2	1	0	6	0	0	3	0	0	11	0	1	0	0	0	0	28	84	115	23	0	7	0	1	0	0	71	0	0	13	461
82.88	681	0	4.4	2	5	0	5	0	0	4	0	20	0	0	0	0	13	0	6	5	4	0	0	0	0	0	8.4	0	0	0	0	0	1	10	93	131	9	0	2	0	0	0	0	42	0	1	13	379
82.98	639	0	6	1	4	6	2	0	0	7	0	27	0	0	0	0	31	0	10	2	1	0	0	2	0	0	1.2	0	0	0	0	0	0	15	107	83	9	0	5	0	0	0	1	52	0	0	24	396
83.08	646	0	18	1	2	2	8	0	0	17	0	56	0	0	0	0	38	2	2	3	5	0	0	0	0	0	6.4	0	0	0	0	0	0	34	128	154	11	0	7	0	1	3	4	61	0	1	14	578
83.18	685	0	7.4	1	4	0	10	0	0	6	0	64	1	0	0	5	21	4	14	10	4	0	0	0	0	0	2	0	0	0	0	1	0	22	158	167	21	0	11	0	0	0	1	65	0	0	12	611
83.28	719	0	10	2	11	3	5	0	0	8	0	51	1	0	0	7	38	1	8	6	6	0	0	1	0	0	7.8	0	0	0	0	1	0	25	145	152	8	1	10	0	0	0	2	66	0	0	16	592
83.38	609	0	7	1	7	1	2	0	0	4	0	33	0	1	0	0	15	0	8	2	7	0	0	1	0	0	4	0	0	1	0	0	0	13	92	113	7	0	10	0	0	1	3	50	0	0	13	396
83.48	651	0	5.8	2	4	0	3	0	0	9	0	43	0	0	0	0	10	0	7	4	9	0	0	2	0	0	4.6	0	1	0	0	2	0	20	155	106	17	1	6	0	0	1	3	70	0	0	25	510
83.58	656	0	7.4	0	10	0	0	0	1	5	0	32	0	0	0	0	18	0	4	1	1	0	0	2	0	0	5.2	0	0	0	1	2	0	8	106	99	6	1	4	0	1	0	1	61	2	0	9	388
83.68	657	0	16	1	4	0	3	0	1	6	0	41	0	0	0	0	16	0	10	7	7	0	0	3	0	0	1.2	0	0	0	0	1	0	17	164	160	4	1	7	0	1	1	0	64	1	0	30	567
83.78	749	0	5.8	3	6	0	1	0	0	0	0	29	0	0	0	0	23	1	4	3	6	0	0	1	0	0	2.6	0	1	0	0	1	0	11	100	126	13	0	3	0	1	0	1	61	1	0	22	426
83.88	668	0	6.6	1	3	0	1	0	2	3	0	18	0	0	0	0	18	0	13	0	6	0	0	0	0	0	3	0	0	0	0	0	0	20	101	115	12	0	2	0	0	0	0	52	0	0	12	389
83.98	667	0	9.2	0	6	0	9	0	0	3	0	42	0	0	0	4	22	1	7	1	4	0	0	2	0	0	2.4	0	1	0	0	0	0	12	85	166	15	0	6	0	0	1	2	71	0	0	11	482
84.08	713	0	6.2	1	9	0	7	0	0	3	0	39	0	0	0	0	31	2	16	0	6	0	0	0	0	0	0.8	0	0	0	0	1	0	16	121	187	4	0	3	0	3	0	3	75	0	0	12	546
84.18	662	0	3.6	3	7	0	3	0	1	8	0	45	0	0	0	2	23	0	6	2	2	0	0	0	0	0	4.2	0	2	0	0	0	0	18	101	190	1	0	7	0	2	0	2	70	0	0	6	509
84.28	753	0	9	2	10	0	11	0	1	3	0	58	0	0	0	8	33	3	13	2	7	0	0	3	0	0	2.2	0	1	0	0	0	0	22	106	200	1	1	6	0	0	1	1	82	0	0	11	597
84.38	651	0	5.8	2	7	1	4	0	0	3	0	48	0	0	0	0	44	2	7	1	7	0	0	1	0	3	1.2	0	1	0	0	1	0	26	72	179	5	0	5	0	0	3	1	50	0	0	9	489
84.48	657	0	5.2	1	3	2	3	0	2	6	0	52	0	0	0	6	52	1	45	2	13	0	0	4	0	0	2.2	0	0	0	0	0	0	33	106	295	6	0	6	0	2	0	0	75	0	0	12	734
84.58	644	0	7	1	5	1	1	0	1	5	0	34	1	0	0	0	49	0	27	3	11	0	0	1	0	0	3.2	0	0	0	0	0	0	27	37	138	0	0	2	0	0	1	2	60	0	0	15	432
84.68	688	0	5.2	0	7	0	4	0	0	6	0	42	1	0	0	4	47	0	25	1	11	0	0	0	0	0	1.8	0	0	0	0	0	0	26	46	190	2	0	1	0	0	2	1	59	0	0	9	491
84.78	713	0	5.4	1	5	2	1	0	0	4	0	39	0	0	0	6	30	0	15	0	12	0	0	2	0	0	2.4	0	0	0	0	0	0	18	21	171	3	0	3	0	3	0	0	57	0	0	6	407
84.88	867	0	3.6	0	4	0	3	0	0	5	0	44	0	0	0	0	32	0	21	0	2	0	0	1	0	0	0	0	0	0	0	0	0	17	35	197	2	0	0	0	0	0	0	49	0	0	14	430
84.98	784	0	2.2	0	3	0	3	0	2	3	0	35	0	0	0	0	58	0	8	0	5	0	0	0	0	0	2.2	0	0	0	0	0	0	16	8	145	2	0	0	0	0	0	0	77	0	0	5	374
85.08	843	0	3	0	2	0	3	0	1	6	0	55	0	0	0	0	44	1	17	3	6	0	0	2	0	0	4.8	0	0	0	0	0	0	23	9	212	14	0	6	0	1	0	1	87	0	0	14	515
85.11	754	0	6.4	0	4	0	5	0	0	4	0	62	1	0	0	0	36	3	14	3	4	0	0	0	0	0	2.6	0	1	0	0	0	0	28	10	209	3	0	5	0	1	0	0	63	0	0	16	481
85.18	750	0	7.8	0	2	0	0	0	0	3	0	42	0	0	0	1	48	1	23	0	9	0	0	2	0	0	0.2	0	0	0	0	0	0	15	9	217	1	0	6	0	0	0	0	81	0	1	7	476
85.21	851	0	7.8	0	2	0	9	0	0	7	1	77	0	0	0	0	47	0	24	2	5	0	0	5	0	0	3.4	0	1	0	0	0	0	34	21	241	0	1	6	0	0	1	4	91	0	0	34	624
85.31	869	0	13	0	4	1	4	0	0	7	0	89	0	2	0	6	54	4	25	2	14	0	0	3	0	0	2.6	0	0	0	0	0	0	33	19	255	8	1	7	1	0	0	0	94	1	0	28	678
85.41	917	0	7	0	7	0	6	0	0	6	0	88	0	0	0	5	56	0	22	1	8	0	0	7	0	0	3	0	0	0	0	0	0	47	22	339	4	1	12	1	0	0	1	90	0	0	37	770
85.51	995	0	8.8	2	7	2	6	0	0	6	0	98	0	0	0	0	45	0	24	0	14	0	0	3	0	0	1.4	0	1	0	0	0	1	54	12	349	7	2	15	0	0	0	3	82	0	0	33	776
85.61	829	0	4.6	0	2	0	0	0	0	10	0	51	0	0	0	0	38	0	20	0	2	0	0	2	0	0	2	0	0	0	0	0	0	29	7	230	4	0	2	0	0	0	0	72	1	0	8	485
85.71	884	0	6.8	4	5	1	3	0	1	6	0	94	0	0	0	3	58	2	20	0	9	0	0	5	0	0	1.6	0	3	0	0	0	0	32	4	287	3	4	15	0	1	1	0	112	0	1	32	715
85.81	825	0	9	1	5	0	6	0	0	7	0	71	0	0	0	2	44	1	19	2	10	0	0	3	0	0	1.2	0	0	0	0	0	0	43	1	289	3	1	5	0	1	2	0	101	0	0	32	660
85.91	800	0	10	1	3	0	4	0	0	2	0	70	0	0	0	3	43	1	19	0	7	0	0	4	0	0	0.6	0	1	0	0	0	0	43	7	258	15	0	3	0	0	1	1	80	0	3	25	605
86.01	826	0	17	0	6	0	7	0	0	9	0	107	0	0	0	0	48	2	25	1	5	0	0	1	0	0	0	0	0	0	0	0	0	54	5	101	8	0	9	0	3	0	1	107	0	0	32	548
86.11	836	0	8.6	1	2	1	4	0	1	8	0	83	0	0	0	3	47	1	15	0	4	0	0	5	0	0	2	0	0	0	0	0	0	55	9	187	5	2	5	0	0	0	1	120	0	0	35	605
86.21	566	0	5	1	5	1	1	0	0	9	0	33	0	0	0	1	29	0	14	1	4	0	0	0	0	0	2.2	0	1	0	0	1	0	50	9	176	5	1	1	0	0	1	3	58	1	0	6	419
86.31	601	0	5.2	2	8	1	2	0	0	5	0	40	0	0	0	2	25	3	11	1	3	0	0	2	0	0	2	0	0	0	0	0	0	44	5	252	0	2	1	0	2	0	3	75	0	0	11	507
86.41	540	0	6.8	0	4	0	0	0	0	2	0	39	0	0	0	0	24	2	13	7	3	0	0	1	0	0	3	0	2	0	0	0	0	40	1	201	4	0	0	0	1	0	1	75	0	3	10	443
86.51	499	0	5.8	0	6	1	11	0	0	7	0	81	0	0	3	1	42	0	11	7	6	0	0	0	0	0	3.2	0	1	0	0	0	0	39	12	217	5	1	0	0	3	2	0	97	0	6	18	586
86.61	581	0	3	0	3	1	5	0	0	5	0	51	0	0	0	1	31	1	11	5	3	0	0	1	0	0	1.4	0	0	0	0	1	0	49	1	148	4	0	2	0	0	1	0	82	0	0	11	421
86.71	828	0	8.6	1	5	1	11	0	2	4	0	74	0	0	0	1	50	2	16	0	4	0	0	1	0	0	3	0	0	0	0	0	0	53	4	76	1	0	4	0	2	6	0	124	2	0	40	496
86.81	793	0	8.8	0	7	2	0	0	1	2	1	41	0	0	0	1	33	3	27	2	2	0	0	1	0	0	2.8	0	0	1	0	0	0	53	5	97	1	0	2	0	1	2	1	112	0	0	23	433
86.91	949	0	8.4	0	13	2	3	0	0	2	0	114	0	0	0	0	64	2	37	0	4	0	0	2	0	0	4	0	1	0	0	0	0	105	7	158	2	0	17	0	3	1	4	162	1	0	57	773
87.01	698	0	2.8	0	4	0	0	0	0	4	0	31	0	0	0	1	28	0	7	0	4	0	0	0	0	0	0.6	0	0	0	0	0	0	35	7	85	2	0	2	0	1	0	0	62	0	0	12	288
87.11	766	0	2.2	0	2	0	0	0	0	0	0	20	0	0	0	0	24	0	9	0	3	0	0	0	0	0	0	0	0	0	0	0	0	14	3	21	24	0	0	0	0	0	0	64	0	0	8	195
87.21	796	0	6	0	6	1	0	0	1	3	0	46	1	0	0	0	25	1	7	4	10	0	0	1	0	0	1.2	0	0	0	0	0	0	73	1	79	4	0	2	0	0	0	0	102	0	0	11	385
87.31	791	0	7.4	1	9	0	3	0	0	10	0	68	0	0	0	0	32	3	13	2	6	0	0	2	0	0	3.4	0	0	0	0	0	0	43	6	141	7	0	1	0	0	0	1	101	0	0	15	475
87.41	703	0	7.8	1	8	2	0	0	1	6	0	53	0	0	0	0	26	0	10	1	3	0	0	0	0	0	0.4	0	0	0	0	0	0	58	2	50	3	0	4	0	0	0	0	117	0	0	12	366
87.51	816	0	1	0	4	1	2	0	0	7	0	49	0	0	0	0	20	3	4	1	4	0	0	2	0	0	1	0	0	0	0	0	0	83	0	51	0	0	0	0	0	0	0	116	0	0	7	356
87.61	803	0	2	0	2	0	0	0	0	2	0	27	0	0	0	0	24	0	8	0	2	0	0	0	0	0	2.4	0	0	0	0	0	0	31	7	59	3	0	0	0	0	0	0	74	0	0	6	249
87.71	909	0	6.4	0	4	0	0	0	0	9	0	79	0	0	0	2	44	1	13	3	3	0	0	2	0	0	2.4	0	0	0	0	0	0	88	2	60	4	0	3	0	1	0	0	136	0	0	4	467
87.81	835	0	6	0	4	0	0	0	0	4	0	34	0	0	0	0	28	4	7	3	1	0	0	1	0	0	0.2	0	0	0	0	0	0	58	1	33	5	0	0	0	1	0	0	105	0	0	8	303
87.91	803	0	4.6	0	2	0	0	0	0	7	0	26	0	0	0	0	33	0	14	4	0	0	0	1	0	0	1	0	0	0	0	0	0	54	4	66	1	0	0	0	0	0	0	104	0	0	4	325
88.01	734	0	5.4	0	2	0	0	0	0	4	0	25	0	0	0	0	23	0	10	0	4	0	0	0	0	0	1.2	0	0	0	0	0	0	37	6	69	9	0	0	0	0	0	0	78	0	0	5	278
88.11	773	0	2.6	0	1	0	0	0	0	0	0	4	0	0	0	0	23	0	8	0	2	0	0	0	0	0	2	0	0	0	0	0	0	20	11	76	17	0	0	0	0	0	0	72	0	0	4	243
88.21	779	0	6.2	0	7	0	0	0	0	2	0	11	0	0	0	2	26	0	25	0	1	0	0	1	0	0	2.8	0	0	0	0	0	0	36	2	75	7	0	0	0	0	0	0	68	0	0	2	274
88.31	781	0	10	0	3	0	0	0	0	4	0	30	0	0	0	0	27	0	18	2	5	0	0	0	0	0	1.2	0	0	0	0	0	0	28	4	42	6	0	1	2	2	0	1	99	0	0	10	295
88.41	863	0	4.4	0	2	0	0	0	0	1	0	10	0	0	0	0	11	0	5	0	3	0	0	0	0	0	0	0	0	0	0	0	0	4	3	37	3	0	0	0	0	0	0	68	0	0	10	161
88.51	968	0	7.8	0	4	0	0	0	0	3	0	23	0	0	0	0	36	0	18	2	3	0	0	0	0	0	6	0	0	0	0	0	0	28	11	98	2	0	0	0	0	0	0	122	0	0	10	373
88.61	963	0	3.4	0	0	0	0	0	0	1	0	11	0	0	0	0	16	0	7	0	0	0	0	0	0	0	0.4	0	0	0	0	0	0	22	4	53	1	0	0	0	0	0	0	85	0	0	5	208
88.71	655	0	5.6	0	1	0	0	0	0	1	0	10	0	0	0	2	9	0	0	0	1	0	0	0	0	0	0	0	0	0	0	0	0	15	8	20	3	0	0	0	0	0	0	53	0	0	6	135
88.81	976	0	7.8	0	5	0	0	0	2	4	0	30	0	0	0	1	21	0	8	2	5	0	0	0	0	0	5.4	0	0	0	0	0	0	50	8	5	5	0	0	0	1	0	0	115	0	0	12	287
88.91	900	0	3.2	0	5	0	0	0	1	2	0	18	0	0	0	0	14	0	10	0	0	0	0	0	0	0	1	0	0	0	0	0	0	47	2	0	4	0	0	0	1	0	0	85	0	0	10	203
89.01	614	0	1.8	0	0	0	4	0	0	1	0	8	0	0	0	2	16	0	5	0	2	0	0	0	0	0	2.4	0	0	0	0	0	0	31	4	0	0	0	2	0	0	0	0	52	0	0	4	135
89.11	936	0	4.4	0	1	0	0	0	0	2	0	31	0	0	0	3	18	0	8	1	1	0	0	0	0	0	1.2	0	0	0	0	0	0	49	5	0	6	1	0	0	0	0	0	80	0	0	1	212
89.21	841	0	3.4	0	3	2	1	0	0	3	0	40	0	0	0	4	38	1	13	4	2	0	0	0	0	0	0	0	0	0	0	1	0	46	3	28	3	0	0	0	2	0	1	94	0	0	7	299
89.31	671	0	3.8	0	5	1	0	0	0	3	0	21	0	0	0	2	14	0	2	0	3	0	0	0	0	0	1	0	0	0	0	0	0	35	5	18	2	0	1	0	0	0	1	53	0	0	5	176
89.37	661	0	6	0	5	0	4	0	0	3	0	30	0	0	0	3	24	0	4	0	4	0	0	1	0	0	0.6	0	0	0	0	0	0	40	6	40	1	0	6	0	2	0	0	85	0	0	3	268
89.41	588	0	4.2	1	9	0	4	0	0	2	0	25	0	0	0	3	19	0	2	4	4	0	0	0	0	0	1.2	0	0	0	0	0	0	22	7	71	2	0	9	0	0	0	0	81	0	0	2	273
89.47	587	0	7	0	5	0	1	0	0	4	0	25	0	0	0	0	12	0	11	1	2	0	0	0	0	0	3.2	0	0	0	0	0	0	27	12	56	1	0	5	0	0	0	1	61	0	0	2	236
89.51	625	0	8.8	0	8	0	2	0	0	6	0	19	0	0	0	0	7	0	3	1	4	0	0	1	0	0	2.8	0	1	0	0	0	0	49	5	114	1	0	5	0	0	4	4	69	0	0	11	325
89.57	673	0	2.6	0	2	0	0	0	0	3	0	19	0	0	0	0	23	0	7	0	3	0	0	0	0	0	1.8	0	0	0	0	0	0	36	5	52	4	0	2	0	1	1	0	76	0	0	7	245
89.61	662	0	12	0	2	0	0	0	0	6	0	25	0	0	0	0	17	1	8	1	3	0	0	1	0	0	1.6	0	0	0	0	0	0	37	1	46	5	0	2	0	1	0	0	72	0	0	6	247
89.67	673	0	7.2	0	2	1	3	0	0	6	0	26	0	1	0	0	14	1	8	1	2	0	0	0	0	0	1.8	0	2	0	0	0	0	51	1	61	3	0	3	0	3	0	0	86	0	0	2	286
89.71	615	0	5.2	0	0	0	0	0	0	4	0	42	0	0	0	0	12	0	6	2	1	0	0	2	0	0	2.2	0	1	0	0	0	1	43	2	77	0	0	1	0	3	2	0	59	0	0	3	268
89.77	781	0	8.6	1	9	1	2	0	0	4	0	38	2	0	0	1	20	0	7	1	1	0	0	1	0	0	3.2	0	2	0	0	0	0	58	2	110	1	1	13	0	4	1	0	111	0	0	10	412
89.87	633	0	4.8	0	3	0	16	0	0	2	0	49	0	0	0	6	21	0	5	1	3	0	0	0	0	0	1.6	0	0	0	0	0	0	43	10	101	0	6	5	0	3	0	0	75	1	0	11	367
89.97	680	0	4.2	1	2	0	3	0	0	2	0	30	0	0	0	14	25	0	3	1	2	0	0	0	0	0	1.4	0	0	0	0	0	0	60	3	113	4	0	5	0	0	2	0	77	0	0	5	358
90.07	712	0	7.8	1	7	0	6	0	0	6	0	38	0	0	0	3	15	0	10	0	4	0	0	1	0	0	2.2	0	0	0	0	0	0	54	5	137	0	1	12	0	0	1	1	97	1	0	7	417
90.17	538	0	2.8	1	4	0	11	0	0	2	0	27	1	0	0	1	15	0	4	1	3	0	0	1	0	0	1	0	2	0	0	0	0	41	3	111	2	1	9	0	2	0	1	86	0	0	3	335
90.27	660	0	2.6	0	1	0	12	0	0	3	0	47	0	0	0	1	9	0	13	0	4	0	0	0	0	0	3.6	0	1	0	0	0	0	37	5	119	1	0	5	0	0	1	1	99	1	0	8	374
90.37	733	0	4.2	1	5	0	5	0	0	1	0	42	0	0	0	0	11	0	14	1	5	0	0	1	0	0	1.8	0	2	0	0	0	0	41	6	115	1	0	2	0	0	0	0	74	0	0	8	341
90.47	696	0	6	0	6	1	8	0	0	0	0	48	0	0	0	0	15	0	6	0	2	0	0	1	0	0	1.2	0	1	0	0	0	0	44	11	161	0	0	5	0	1	0	2	82	0	0	5	406
90.57	688	0	8.2	0	3	0	7	0	0	4	0	46	0	0	0	4	18	0	7	2	2	0	0	0	0	0	2.2	0	0	0	0	0	0	51	7	182	5	0	3	0	0	0	0	83	1	0	4	439
90.67	609	0	6.6	0	3	0	9	0	1	4	0	38	0	1	0	4	13	0	9	0	8	0	0	1	0	0	0.2	0	2	0	0	0	0	49	7	149	1	0	5	0	1	0	0	87	0	0	9	408
90.77	717	0	2	0	5	0	14	0	0	1	0	45	0	0	0	3	8	0	11	0	2	0	0	0	0	0	1.2	0	0	0	0	0	0	55	13	135	1	0	6	0	0	0	1	101	0	0	9	413
90.87	674	0	2	0	4	0	32	0	0	2	0	28	0	0	0	8	5	0	11	0	3	0	0	1	0	0	0.2	0	0	0	0	0	0	53	3	132	1	0	13	0	2	0	1	90	1	0	15	407
90.97	618	0	6.2	0	1	0	14	0	0	0	0	32	0	1	0	1	9	0	5	2	1	0	0	1	0	0	1	0	0	0	0	0	0	54	7	78	3	0	4	0	0	2	0	80	0	0	3	305
91.07	654	0	7.6	0	3	0	15	0	0	3	0	63	0	1	0	17	20	0	17	0	8	0	0	0	0	0	3.4	0	0	0	0	0	0	93	10	172	19	0	10	0	2	1	3	154	0	0	11	633
91.17	613	0	1	0	1	0	0	0	0	0	0	10	0	0	0	0	7	0	2	0	3	0	0	0	0	0	0	0	0	0	0	0	0	29	1	55	0	0	0	0	0	0	0	66	0	0	2	177
91.27	679	0	3	0	1	0	0	0	0	0	0	16	0	0	0	0	2	0	4	0	0	0	0	0	0	0	0	0	0	0	0	0	0	23	0	48	1	0	0	0	0	0	0	57	0	0	1	156
91.37	712	0	3	0	0	0	1	0	0	2	0	37	0	1	0	1	24	0	14	2	6	0	0	1	0	0	1	0	0	0	0	0	0	63	3	42	3	0	8	0	2	0	0	123	0	0	6	343
91.47	663	0	0	0	0	0	2	0	0	3	0	20	0	0	0	0	6	0	7	0	0	0	0	0	0	0	0	0	0	0	0	0	0	25	2	70	1	0	3	0	2	0	0	83	0	0	2	226
91.57	768	0	2.6	0	2	0	4	0	0	1	0	52	0	1	1	2	14	0	13	1	1	0	0	1	0	0	0	0	1	0	0	0	0	42	7	106	0	0	3	0	1	1	1	78	0	0	7	343
91.67	626	0	6	0	2	0	6	0	0	1	0	37	0	0	0	5	20	0	6	1	0	0	0	4	0	0	1.2	0	0	0	0	0	0	33	5	125	2	0	3	0	0	1	1	92	2	0	4	357
91.77	781	0	9	0	2	0	10	0	1	2	0	89	1	0	0	3	45	0	9	0	9	0	0	1	0	0	1	0	4	0	0	0	0	52	3	109	1	0	9	0	1	1	0	133	10	0	6	511
91.87	724	0	1	0	2	0	12	0	0	6	0	53	0	1	0	0	32	0	5	2	13	0	0	5	0	0	0	0	1	0	0	0	0	45	4	97	1	0	1	0	0	1	0	112	0	0	11	405
91.97	605	0	2	2	2	0	13	0	0	4	0	34	0	0	0	1	25	0	13	2	4	0	0	1	0	0	1	0	3	0	0	0	0	59	3	96	0	0	3	0	1	0	3	107	0	0	20	399
92.07	703	0	4	0	4	0	15	0	0	5	0	70	0	1	0	3	34	0	15	0	6	0	0	1	0	0	1.2	0	3	0	0	0	0	73	15	124	3	0	5	0	0	0	2	102	0	0	8	494
92.17	724	0	4	0	1	0	7	0	0	6	0	50	0	1	0	0	28	0	16	0	3	0	0	3	0	0	2.2	0	1	0	0	0	0	79	4	158	1	0	3	0	0	0	4	176	0	0	19	566
92.27	607	0	2	1	2	0	8	0	0	4	0	59	0	1	0	0	25	0	12	2	7	0	0	2	0	0	1	0	3	0	1	0	0	56	3	115	3	0	6	0	0	0	2	104	0	0	12	431
92.37	738	0	1	0	2	0	8	0	0	6	0	46	0	0	0	3	27	0	10	0	3	0	0	1	0	0	1.6	0	1	0	0	0	0	79	4	130	1	0	5	0	0	0	2	109	0	0	21	461
92.47	711	0	4.2	0	7	0	7	0	0	1	0	35	0	0	0	7	16	0	10	0	3	0	0	1	0	0	1	0	1	0	0	0	0	61	13	175	2	0	2	0	0	0	0	104	0	0	21	471
92.57	638	0	7.2	0	2	0	7	0	0	1	0	28	0	0	0	0	24	0	6	0	0	0	0	1	0	0	0.4	0	0	0	0	0	0	61	10	96	0	0	2	0	0	0	2	120	0	0	14	382
92.67	747	0	4	0	7	0	4	0	0	3	0	24	0	0	0	1	33	0	8	0	2	0	0	3	0	0	0.2	0	0	0	0	0	0	48	9	135	0	0	8	0	0	0	6	111	0	0	18	424
92.77	678	0	1	0	7	0	7	0	0	2	0	33	0	0	0	1	15	0	6	2	4	0	0	1	0	0	0.8	0	1	0	0	0	0	39	9	129	1	0	2	0	0	0	2	78	0	0	9	350

APPENDIX D. NANNOFOSSIL ABSOLUTE ABUNDANCE WITH CALCULATED UNCERTAINTY

Depth	Blackities spinosus	Uncertainty	Braarudosphaera spp.	Uncertainty	Bramlettius serraculoides	Uncertainty	c.f. Bramlettius cerraculoides	Uncertainty	c.f. C. pelagicus	Uncertainty	Calcidiscus protoannulus	Uncertainty	Cepekiella lumina	Uncertainty	Chiasmolithus grandis	Uncertainty	Coccolithus formosus	Uncertainty	*Coccolithus minimus*	Uncertainty	*Coccolithus pelagicus*	Uncertainty	*Coronocyclus cf. bramletti*	Uncertainty
81.38	0	0	24233218	3239308	2425655	324242.7	0	0	0	0	32552083	4351309	0	0	0	0	32552083	4351309	3616898	483478.8	1.01E+08	13537407	0	0
81.48	0	0	24535124	3295858	9829415	1320407	0	0	0	0	32283058	4336655	0	0	0	0	10761019	1445552	0	0	1.23E+08	16479290	2152204	289110.3
81.58	0	0	15055339	2019015	6767578	907574.5	8138021	1091359	0	0	79345703	10640755	0	0	2034505	272839.9	0	0	4069010	545679.7	83414714	11186434	0	0
81.68	2798871	377491.8	31347352	4227908	0	0	8396612	1132475	0	0	78368380	10569770	0	0	0	0	16793224	2264951	0	0	1.51E+08	20384557	0	0
81.78	0	0	16592920	2233818	3220979	433623.5	2304572	310252.5	0	0	85269174	11479344	0	0	2304572	310252.5	9218289	1241010	6913717	930757.6	1.64E+08	22027930	6913717	930757.6
81.88	0	0	11904762	1598591	2552862	342802.5	10629252	1427313	0	0	61649660	8278417	0	0	0	0	27636054	3711015	0	0	1.25E+08	16842297	0	0
81.98	0	0	45566502	6157224	0	0	3078818	416028.7	4618227	624043	55418719	7488516	1539409	208014.3	0	0	13854680	1872129	0	0	1.45E+08	19553347	0	0
82.08	0	0	58992347	7981785	17821141	2411237	10629252	1438159	0	0	69090136	9348036	0	0	0	0	15943878	2157239	0	0	1.33E+08	17976993	5314626	719079.7
82.18	0	0	36789021	4935919	5424063	727737.1	8267196	1109195	4133598	554597.6	20667989	2772988	0	0	0	0	24801587	3327586	0	0	1.82E+08	24402295	0	0
82.28	0	0	26577503	3569763	2695512	362048.3	8573388	1151537	8573388	1151537	23576818	3166726	0	0	0	0	8573388	1151537	0	0	1.05E+08	14106323	0	0
82.38	0	0	17730496	2383960	5342276	718297.4	11081560	1489975	2216312	297994.9	11081560	1489975	0	0	0	0	13297872	1787970	0	0	1.11E+08	14899747	0	0
82.48	0	0	15797788	2131743	5854474	789998.9	24684044	3330849	4936809	666169.7	27152449	3663933	0	0	0	0	19747235	2664679	0	0	1.9E+08	25647534	0	0
82.58	0	0	20935458	2828421	5452743	736676.3	15318627	2069577	12765523	1724647	12765523	1724647	0	0	0	0	25531046	3449294	0	0	1.86E+08	25179849	2553105	344929.4
82.68	0	0	29147554	3928716	3092314	416804.2	14334862	1932155	2389144	322025.9	14334862	1932155	0	0	0	0	11945719	1610129	0	0	1.39E+08	18677502	0	0
82.78	0	0	26745495	3602739	0	0	11730480	1580149	2346096	316029.7	2346096	316029.7	0	0	0	0	23460961	3160297	0	0	46921922	6320594	2346096	316029.7
82.88	0	0	10912698	1472799	4845815	654000.4	12400794	1673635	0	0	12400794	1673635	0	0	0	0	9920635	1338908	0	0	49603175	6694539	0	0
82.98	0	0	16191710	2192055	2809604	380367.9	10794473	1461370	16191710	2192055	5397237	730685.2	0	0	0	0	18890328	2557398	0	0	72862694	9864250	0	0
83.08	0	0	48579109	6548867	2616477	352722.8	5520353	744189.4	5520353	744189.4	22081413	2976758	0	0	0	0	46923003	6325610	0	0	1.55E+08	20837304	0	0
83.18	0	0	17518939	2360597	2299270	309816.2	9469697	1275999	0	0	23674242	3189997	0	0	4734848	637999.3	14204545	1913998	0	0	1.52E+08	20415978	2367424	318999.7
83.28	0	0	26172529	3539184	4843410	654950.8	28789782	3893102	7851759	1061755	13086265	1769592	0	0	2617253	353918.4	20938023	2831347	0	0	1.33E+08	18049836	2617253	353918.4
83.38	0	0	16801075	2264924	2621961	353462.1	16801075	2264924	2400154	323560.6	4800307	647121.2	0	0	0	0	9600614	1294242	0	0	79205069	10677500	0	0
83.48	0	0	14880952	2010805	5243922	708590.7	10262726	1386762	0	0	7697044	1040072	0	0	0	0	23091133	3120215	0	0	1.1E+08	14907694	0	0
83.58	0	0	19465488	2632717	0	0	26304714	3557726	0	0	0	0	0	0	0	0	13152357	1778863	0	0	84175084	11384723	0	0
83.68	0	0	41158537	5559615	2572670	347511.2	10162602	1372744	0	0	7621951	1029558	0	0	0	0	15243902	2059117	0	0	1.04E+08	14070630	0	0
83.78	0	0	14453748	1951035	6640433	896356.8	14952153	2018312	0	0	2492026	336385.3	0	0	0	0	0	0	0	0	72268740	9755173	0	0
83.88	0	0	17903646	2424303	2701628	365822.9	8138021	1101956	0	0	2712674	367318.6	0	0	0	0	8138021	1101956	0	0	48828125	6611735	0	0
83.98	0	0	24447279	3307767	0	0	15943878	2157239	0	0	23915816	3235859	0	0	0	0	7971939	1078620	0	0	1.12E+08	15100674	0	0
84.08	0	0	13799858	1855715	2076815	279276.6	20032051	2693780	0	0	15580484	2095162	0	0	0	0	6677350	897926.7	0	0	86805556	11673047	0	0
84.18	0	0	9014423	1217016	7549239	1019205	17528045	2366421	0	0	7512019	1014180	0	0	0	0	20032051	2704481	0	0	1.13E+08	15212706	0	0
84.28	0	0	22536058	3042541	4424609	597356.3	25040064	3380601	0	0	27544071	3718661	0	0	0	0	7512019	1014180	0	0	1.45E+08	19607487	0	0
84.38	0	0	13920891	1876652	4905604	661316.1	16801075	2264924	2400154	323560.6	9600614	1294242	0	0	0	0	7200461	970681.8	0	0	1.15E+08	15530910	0	0
84.48	0	0	12538580	1690572	2441654	329207.3	7233796	975330.1	4822531	650220.1	7233796	975330.1	0	0	0	0	14467593	1950660	0	0	1.25E+08	16905721	0	0
84.58	0	0	16724006	2254181	2468089	332666.7	11945719	1610129	2389144	322025.9	2389144	322025.9	0	0	0	0	11945719	1610129	0	0	81230887	10948880	2389144	322025.9
84.68	0	0	12896825	1740580	0	0	17361111	2343089	0	0	9920635	1338908	0	0	0	0	14880952	2008362	0	0	1.04E+08	14058532	2480159	334726.9
84.78	0	0	13854680	1872129	2393964	323487.1	12828407	1733453	5131363	693381.1	2565681	346690.5	0	0	0	0	10262726	1386762	0	0	1E+08	13520931	0	0
84.88	0	0	9101942	1229257	0	0	10113269	1365841	0	0	7584951	1024381	0	0	0	0	12641586	1707301	0	0	1.11E+08	15024252	0	0
84.98	0	0	5672442	766633.4	0	0	7735149	1045409	0	0	7735149	1045409	0	0	0	0	7735149	1045409	0	0	90243399	12196440	0	0
85.08	0	0	7697044	1040072	0	0	5131363	693381.1	0	0	7697044	1040072	0	0	0	0	15394089	2080143	0	0	1.41E+08	19067980	0	0
85.11	0	0	15948963	2152866	0	0	9968102	1345541	0	0	12460128	1681926	0	0	0	0	9968102	1345541	0	0	1.55E+08	20855888	2492026	336385.3
85.18	0	0	19625604	2650063	0	0	5032206	679503.4	0	0	0	0	0	0	0	0	7548309	1019255	0	0	1.06E+08	14269572	0	0
85.21	0	0	19914216	2690450	0	0	5106209	689858.9	0	0	22977941	3104365	0	0	0	0	17871732	2414506	2553105	344929.4	1.97E+08	26559566	0	0
85.31	0	0	32051282	4327170	0	0	10016026	1352241	2504006	338060.1	10016026	1352241	0	0	2504006	338060.1	17528045	2366421	0	0	2.23E+08	30087351	0	0
85.41	0	0	15647353	2104441	0	0	15647353	2104441	0	0	13412017	1803807	0	0	0	0	13412017	1803807	0	0	1.97E+08	26455835	0	0
85.51	0	0	18707483	2512071	2842785	381733.9	14880952	1998239	4251701	570925.3	12755102	1712776	0	0	0	0	12755102	1712776	0	0	2.08E+08	27975340	0	0
85.61	0	0	12100168	1636554	0	0	5260943	711545.2	0	0	0	0	0	0	0	0	26304714	3557726	0	0	1.34E+08	18144402	0	0
85.71	0	0	17027244	2298809	7537852	1017668	12520032	1690301	2504006	338060.1	7512019	1014180	0	0	0	0	15024038	2028361	0	0	2.35E+08	31777652	0	0
85.81	0	0	24671053	3342019	2210526	299444.9	13706140	1856677	0	0	16447368	2228012	0	0	0	0	19188596	2599348	0	0	1.95E+08	26364814	0	0
85.91	0	0	22743814	3060563	1891376	254516.4	6823144	918168.8	0	0	9097525	1224225	0	0	0	0	4548763	612112.5	0	0	1.59E+08	21423938	0	0
86.01	0	0	42682927	5765526	0	0	15243902	2059117	0	0	17784553	2402303	0	0	0	0	22865854	3088675	0	0	2.72E+08	36720913	0	0
86.11	0	0	20641321	2782621	1910017	257486.1	4800307	647121.2	2400154	323560.6	9600614	1294242	0	0	0	0	19201229	2588485	0	0	1.99E+08	26855531	0	0
86.21	0	0	13152357	1778863	3091873	418177.4	13152357	1778863	2630471	355772.6	2630471	355772.6	0	0	0	0	23674242	3201953	0	0	86805556	11740495	0	0
86.31	0	0	12480799	1682515	5313724	716334.1	19201229	2588485	2400154	323560.6	4800307	647121.2	0	0	0	0	12000768	1617803	0	0	96006144	12942425	0	0
86.41	0	0	17276423	2333665	0	0	10162602	1372744	0	0	0	0	0	0	2540650	343186.1	5081301	686372.2	0	0	99085366	13384258	0	0
86.51	0	0	14523237	1960749	0	0	15024038	2028361	2504006	338060.1	27544071	3718661	0	0	0	0	17528045	2366421	0	0	2.03E+08	27382870	0	0
86.61	0	0	7440476	1004181	0	0	7440476	1004181	2480159	334726.9	12400794	1673635	0	0	0	0	12400794	1673635	0	0	1.26E+08	17071074	0	0
86.71	0	0	20546636	2769423	1919625	258740.8	11945719	1610129	2389144	322025.9	26280581	3542285	0	0	0	0	9556575	1288104	0	0	1.77E+08	23829916	0	0
86.81	0	0	23384354	3163951	0	0	18601190	2516779	5314626	719079.7	0	0	0	0	0	0	5314626	719079.7	2657313	359539.9	1.09E+08	14741134	0	0
86.91	0	0	19886364	2679597	0	0	30776515	4146996	4734848	637999.3	7102273	956999	0	0	0	0	4734848	637999.3	0	0	2.7E+08	36365961	0	0
87.01	0	0	7113821	960921.1	0	0	10162602	1372744	0	0	0	0	0	0	0	0	10162602	1372744	0	0	78760163	10638769	0	0
87.11	0	0	5787037	782699.7	0	0	5260943	711545.2	0	0	0	0	0	0	0	0	0	0	0	0	52609428	7115452	0	0
87.21	0	0	15703518	2123510	0	0	15703518	2123510	2617253	353918.4	0	0	0	0	0	0	7851759	1061755	0	0	1.2E+08	16280244	2617253	353918.4
87.31	0	0	18986043	2565510	2157897	291588.2	23091133	3120215	0	0	7697044	1040072	0	0	0	0	25656814	3466905	0	0	1.74E+08	23574957	0	0
87.41	0	0	19437799	2623805	2358314	318336.3	19936204	2691082	4984051	672770.6	0	0	0	0	0	0	14952153	2018312	0	0	1.32E+08	17828420	0	0
87.51	0	0	2578383	348469.7	0	0	10313531	1393879	2578383	348469.7	5156766	696939.4	0	0	0	0	18048680	2439288	0	0	1.26E+08	17075016	0	0
87.61	0	0	4822531	650220.1	0	0	4822531	650220.1	0	0	0	0	0	0	0	0	4822531	650220.1	0	0	65104167	8777971	0	0
87.71	0	0	14684288	1976583	0	0	9177680	1235364	0	0	0	0	0	0	2294420	308841.1	20649780	2779570	0	0	1.81E+08	24398444	0	0
87.81	0	0	15024038	2028361	0	0	10016026	1352241	0	0	0	0	0	0	7512019	1014180	10016026	1352241	0	0	85136218	11494044	0	0
87.91	0	0	11860561	1602961	0	0	5156766	696939.4	0	0	0	0	0	0	0	0	18048680	2439288	0	0	67037954	9060213	0	0
88.01	0	0	13992537	1891443	0	0	5182421	700534.4	0	0	0	0	0	0	0	0	10364842	1401069	0	0	64780265	8756680	0	0
88.11	0	0	6703795	906021.3	0	0	2578383	348469.7	0	0	0	0	0	0	0	0	0	0	0	0	10313531	1393879	0	0
88.21	0	0	15985974	2160512	0	0	18048680	2439288	0	0	0	0	0	0	0	0	5156766	696939.4	0	0	28362211	3833167	0	0
88.31	0	0	26967005	3647992	0	0	7931472	1072939	0	0	0	0	0	0	2643824	357646.3	10575296	1430585	0	0	79314721	10729389	0	0
88.41	0	0	11178862	1510019	0	0	5081301	686372.2	0	0	0	0	0	0	2540650	343186.1	2540650	343186.1	0	0	25406504	3431861	0	0
88.51	0	0	18721198	2523773	0	0	9600614	1294242	0	0	0	0	0	0	0	0	7200461	970681.8	0	0	55203533	7441894	0	0
88.61	0	0	8596278	1160965	0	0	0	0	0	0	0	0	0	0	0	0	2528317	341460.3	0	0	27811489	3756063	0	0
88.71	0	0	14367816	1941467	0	0	2565681	346690.5	0	0	0	0	0	0	0	0	2565681	346690.5	0	0	25656814	3466905	0	0
88.81	0	0	20111386	2718064	0	0	12891914	1742349	0	0	0	0	0	0	0	0	10313531	1393879	0	0	77351485	10454092	0	0
88.91	0	0	7936508	1071126	0	0	12400794	1673635	0	0	0	0	0	0	0	0	4960317	669453.9	0	0	44642857	6025085	0	0
89.01	0	0	4758883	643763.4	0	0	0	0	0	0	10575296	1430585	0	0	2643824	357646.3	2643824	357646.3	0	0	21150592	2861171	0	0
89.11	0	0	11070853	1494908	0	0	2516103	339751.7	0	0	0	0	0	0	0	0	5032206	679503.4	0	0	77999195	10532303	0	0
89.21	0	0	8898660	1203322	0	0	7851759	1061755	5234506	707836.7	2617253	353918.4	0	0	0	0	7851759	1061755	0	0	1.05E+08	14156734	0	0
89.31	0	0	9749589	1317424	0	0	12828407	1733453	2565681	346690.5	0	0	0	0	7697044	1040072	7697044	1040072	0	0	53879310	7280502	0	0
89.37	0	0	15318627	2069577	0	0	12765523	1724647	0	0	10212418	1379718	0	0	10212418	1379718	7659314	1034788	0	0	76593137	10347883	0	0
89.41	0	0	10416667	1405853	2806122	378719.6	22321429	3012543	0	0	9920635	1338908	0	0	9920635	1338908	4960317	669453.9	0	0	62003968	8368174	0	0
89.47	0	0	17361111	2343089	0	0	12400794	1673635	0	0	2480159	334726.9	0	0	4960317	669453.9	9920635	1338908	0	0	62003968	8368174	0	0
89.51	0	0	22357724	3020038	0	0	20325203	2745489	0	0	5081301	686372.2	0	0	10162602	1372744	15243902	2059117	0	0	48272358	6520536	0	0
89.57	0	0	6573625	887796.7	0	0	5056634	682920.6	0	0	0	0	0	0	7584951	1024381	7584951	1024381	0	0	48038026	6487745	0	0
89.61	0	0	30487805	4118233	0	0	5081301	686372.2	0	0	0	0	0	0	7621951	1029558	15243902	2059117	0	0	63516260	8579652	0	0
89.67	0	0	18203883	2458514	0	0	5056634	682920.6	2528317	341460.3	7584951	1024381	0	0	5056634	682920.6	15169903	2048762	0	0	65736246	8877967	0	0
89.71	0	0	13474295	1821390	0	0	0	0	0	0	0	0	0	0	2591211	350267.2	10364842	1401069	0	0	1.09E+08	14711223	0	0
89.77	0	0	22064860	2981539	2185527	295321.8	23091133	3120215	2565681	346690.5	5131363	693381.1	0	0	2565681	346690.5	10262726	1386762	0	0	97495895	13174241	5131363	693381.1
89.87	0	0	12315271	1664115	0	0	7697044	1040072	0	0	41050903	5547049	0	0	7697044	1040072	5131363	693381.1	0	0	1.26E+08	16987837	0	0
89.97	0	0	10416667	1405853	2426471	327481.1	4960317	669453.9	0	0	7440476	1004181	0	0	4960317	669453.9	4960317	669453.9	0	0	74404762	10041808	0	0
90.07	0	0	20517677	2775026	2457865	332427.5	18413300	2490408	0	0	15782828	2134635	0	0	10521886	1423090	15782828	2134635	0	0	99957912	13519358	0	0
90.17	0	0	7440476	1006712	3285980	444599.8	10629252	1438159	0	0	29230442	3954938	0	0	7971939	1078620	5314626	719079.7	0	0	71747449	9707576	2657313	359539.9
90.27	0	0	6703795	906021.3	0	0	2578383	348469.7	0	0	30940594	4181637	0	0	10313531	1393879	7735149	1045409	0	0	1.21E+08	16378077	0	0
90.37	0	0	10466507	1412818	2261794	305307.5	12460128	1681926	0	0	12460128	1681926	0	0	12460128	1681926	2492026	336385.3	0	0	1.05E+08	14128182	0	0
90.47	0	0	15169903	2048762	0	0	15169903	2048762	2528317	341460.3	20226537	2731682	0	0	5056634	682920.6	0	0	0	0	1.21E+08	16390093	0	0
90.57	0	0	19325038	2603564	0	0	7070136	952523.2	0	0	16496983	2222554	0	0	4713424	635015.5	9426848	1270031	0	0	1.08E+08	14605356	0	0
90.67	0	0	16686893	2253638	0	0	7584951	1024381	0	0	22754854	3073142	0	0	20226537	2731682	10113269	1365841	0	0	96076052	12975491	0	0
90.77	0	0	4913522	662917.6	0	0	12283805	1657294	0	0	34394654	4640423	0	0	4913522	662917.6	2456761	331458.8	0	0	1.11E+08	14915645	0	0
90.87	0	0	5056634	682920.6	0	0	10113269	1365841	0	0	80906149	10926729	0	0	7584951	1024381	5056634	682920.6	0	0	70792880	9560888	0	0
90.97	0	0	15675566	2117054	0	0	2528317	341460.3	0	0	35396440	4780444	0	0	2528317	341460.3	0	0	0	0	80906149	10926729	0	0
91.07	0	0	18849206	2543925	0	0	7440476	1004181	0	0	37202381	5020904	0	0	19841270	2677816	7440476	1004181	0	0	1.56E+08	21087798	0	0
91.17	0	0	2480159	334726.9	0	0	2480159	334726.9	0	0	0	0	0	0	7440476	1004181	0	0	0	0	24801587	3347269	0	0
91.27	0	0	730140.2	95405.44	0	0	243380.1	31801.81	0	0	0	0	0	0	0	0	0	0	0	0	3894081	508829	0	0
91.37	0	0	7070136	952523.2	0	0	0	0	0	0	2356712	317507.7	0	0	14140271	1905046	4713424	635015.5	0	0	87198341	11747787	0	0
91.47	0	0	0	0	0	0	0	0	0	0	5182421	700534.4	0	0	0	0	7773632	1050802	0	0	51824212	7005344	0	0
91.57	0	0	6770833	915416.7	0	0	5208333	704166.7	0	0	10416667	1408333	0	0	2604167	352083.3	2604167	352083.3	0	0	1.35E+08	18308333	0	0
91.67	0	0	15470297	2090818	0	0	5156766	696939.4	0	0	15470297	2090818	0	0	0	0	2578383	348469.7	0	0	95400165	12893380	0	0
91.77	0	0	20649780	2779570	0	0	4588840	617682.1	0	0	22944200	3088411	0	0	20649780	2779570	4588840	617682.1	0	0	2.04E+08	27486854	2294420	308841.1
91.87	0	0	2400154	323560.6	0	0	4800307	647121.2	0	0	28801843	3882727	0	0	31201997	4206288	14400922	1941364	0	0	1.27E+08	17148713	0	0
91.97	0	0	4509380	606642.3	4958678	667086	4509380	606642.3	0	0	29310967	3943175	0	0	9018759	1213285	9018759	1213285	0	0	76659452	10312920	0	0
92.07	0	0	9920635	1338908	0	0	9920635	1338908	0	0	37202381	5020904	0	0	14880952	2008362	12400794	1673635	0	0	1.74E+08	23430886	0	0
92.17	0	0	9512938	1282023	0	0	2378234	320505.6	0	0	16647641	2243539	0	0	7134703	961516.9	14269406	1923034	0	0	1.19E+08	16025282	0	0
92.27	0	0	4800307	647121.2	2630600	354626.7	4800307	647121.2	0	0	19201229	2588485	0	0	16801075	2264924	9600614	1294242	0	0	1.42E+08	19090076	0	0
92.37	0	0	2456761	331458.8	0	0	4913522	662917.6	0	0	19654088	2651670	0	0	7370283	994376.3	14740566	1988753	0	0	1.13E+08	15247104	0	0
92.47	0	0	10269953	1385364	0	0	17116588	2308939	0	0	17116588	2308939	0	0	7335681	989545.4	2445227	329848.5	0	0	85582942	11544697	0	0
92.57	0	0	17688679	2386503	0	0	4913522	662917.6	0	0	17197327	2320211	0	0	0	0	2456761	331458.8	0	0	68789308	9280846	0	0
92.67	0	0	10364842	1401069	0	0	18138474	2451871	0	0	10364842	1401069	0	0	5182421	700534.4	7773632	1050802	0	0	62189055	8406413	0	0
92.77	0	0	2540650	343186.1	0	0	17784553	2402303	0	0	17784553	2402303	0	0	10162602	1372744	5081301	686372.2	0	0	83841463	11325141	0	0
92.87	0	0	2540650	343186.1	0	0	12703252	1715930	0	0	10162602	1372744	0	0	12703252	1715930	7621951	1029558	0	0	58434959	7893280	0	0
92.97	0	0	12000768	1617803	0	0	12000768	1617803	0	0	4800307	647121.2	0	0	4800307	647121.2	4800307	647121.2	0	0	96006144	12942425	0	0
93.07	0	0	2591211	350267.2	0	0	7773632	1050802	0	0	7773632	1050802	0	0	15547264	2101603	20729685	2802138	0	0	1.01E+08	13660421	0	0
93.17	0	0	13083736	1766709	0	0	12580515	1698759	0	0	7548309	1019255	0	0	12580515	1698759	2516103	339751.7	0	0	1.08E+08	14609323	0	0
93.27	0	0	4913522	662917.6	0	0	17197327	2320211	0	0	12283805	1657294	0	0	19654088	2651670	9827044	1325835	0	0	66332547	8949387	0	0
93.37	0	0	7680492	1035394	7302321	984413.4	9600614	1294242	0	0	7200461	970681.8	0	0	12000768	1617803	4800307	647121.2	0	0	55203533	7441894	0	0
93.47	0	0	10775862	1456100	2570627	347358.9	15394089	2080143	0	0	23091133	3120215	0	0	15394089	2080143	2565681	346690.5	0	0	69273399	9360645	0	0

Depth	*Coronocyclus nitiscens*	Uncertainty	*Coronocyclus spp.*	Uncertainty	*Cyclicargolithus floridanus*	Uncertainty	*Discoaster barbadiensis*	Uncertainty	*Discoaster nodifer*	Uncertainty	*Discoaster saipanensis*	Uncertainty	*Discoaster spp.*	Uncertainty	*Discoaster tanii*	Uncertainty	*Ericsonia sp.*	Uncertainty	*Helicosphaera salebrosa*	Uncertainty	*Helicosphaeracompacta*	Uncertainty	*Lanternithus procerus*	Uncertainty	*Markalius inversus*	Uncertainty
81.38	0	0	0	0	30743634	4109570	52445023	7010443	5425347	725218.2	28935185	3867831	9042245	1208697	12659144	1692176	3616898	483478.8	1808449	241739.4	0	0	0	0	0	0
81.48	0	0	0	0	49500689	6649538	1.12E+08	15033738	4304408	578220.7	4304408	578220.7	6456612	867331	15065427	2023772	0	0	10761019	1445552	2152204	289110.3	2152204	289110.3	0	0
81.58	0	0	0	0	30517578	4092598	40690104	5456797	0	0	16276042	2182719	6103516	818519.6	14241536	1909879	0	0	0	0	2034505	272839.9	0	0	0	0
81.68	0	0	2798871	377491.8	47580802	6417361	1.2E+08	16232148	0	0	50379673	6794852	11195483	1509967	5597741	754983.6	0	0	11195483	1509967	2798871	377491.8	0	0	0	0
81.78	0	0	0	0	46091445	6205051	32264012	4343535	0	0	23045723	3102525	9218289	1241010	16132006	2171768	0	0	2304572	310252.5	2304572	310252.5	0	0	0	0
81.88	0	0	0	0	59523810	7992954	40391156	5423790	0	0	36139456	4852865	2125850	285462.7	10629252	1427313	0	0	4251701	570925.3	0	0	0	0	0	0
81.98	0	0	0	0	35406404	4784330	1.14E+08	15393060	0	0	60036946	8112559	1539409	208014.3	15394089	2080143	0	0	0	0	0	0	0	0	0	0
82.08	0	0	0	0	31887755	4314478	69090136	9348036	0	0	31887755	4314478	23915816	3235859	10629252	1438159	5314626	719079.7	5314626	719079.7	0	0	2657313	359539.9	2657313	359539.9
82.18	0	0	0	0	12400794	1663793	1.45E+08	19410916	6200397	831896.4	16534392	2218390	8267196	1109195	20667989	2772988	0	0	0	0	4133598	554597.6	0	0	0	0
82.28	0	0	0	0	4286694	575768.3	68587106	9212293	0	0	6430041	863652.4	4286694	575768.3	19290123	2590957	0	0	0	0	0	0	0	0	0	0
82.38	0	0	0	0	6648936	893984.8	93085106	12515788	0	0	13297872	1787970	2216312	297994.9	15514184	2085965	0	0	0	0	0	0	0	0	0	0
82.48	0	0	0	0	2468404	333084.9	1.26E+08	16987328	0	0	24684044	3330849	2468404	333084.9	24684044	3330849	0	0	0	0	0	0	0	0	0	0
82.58	0	0	0	0	0	0	1.4E+08	18971119	2553105	344929.4	12765523	1724647	10212418	1379718	28084150	3794224	0	0	0	0	5106209	689858.9	0	0	0	0
82.68	0	0	0	0	0	0	81230887	10948880	0	0	11945719	1610129	2389144	322025.9	11945719	1610129	0	0	0	0	2389144	322025.9	0	0	0	0
82.78	0	0	0	0	0	0	1.06E+08	14221337	4692192	632059.4	2346096	316029.7	0	0	14076577	1896178	0	0	0	0	7038288	948089.1	0	0	0	0
82.88	0	0	0	0	0	0	32242063	4351450	0	0	14880952	2008362	12400794	1673635	9920635	1338908	0	0	0	0	0	0	0	0	0	0
82.98	0	0	0	0	0	0	83657168	11325620	0	0	26986183	3653426	5397237	730685.2	2698618	365342.6	0	0	0	0	5397237	730685.2	0	0	0	0
83.08	0	0	0	0	0	0	1.05E+08	14139599	5520353	744189.4	5520353	744189.4	8280530	1116284	13800883	1860474	0	0	0	0	0	0	0	0	0	0
83.18	0	0	0	0	11837121	1594998	49715909	6698993	9469697	1275999	33143939	4465995	23674242	3189997	9469697	1275999	0	0	0	0	0	0	0	0	0	0
83.28	0	0	0	0	18320771	2477428	99455611	13448898	2617253	353918.4	20938023	2831347	15703518	2123510	15703518	2123510	0	0	0	0	2617253	353918.4	0	0	0	0
83.38	2621961	353462.1	0	0	0	0	36002304	4853409	0	0	19201229	2588485	4800307	647121.2	16801075	2264924	0	0	0	0	2400154	323560.6	0	0	0	0
83.48	0	0	0	0	0	0	25656814	3466905	0	0	17959770	2426834	10262726	1386762	23091133	3120215	0	0	0	0	5131363	693381.1	0	0	0	0
83.58	0	0	0	0	0	0	47348485	6403906	0	0	10521886	1423090	2630471	355772.6	2630471	355772.6	0	0	0	0	5260943	711545.2	0	0	0	0
83.68	0	0	0	0	0	0	40650407	5490978	0	0	25406504	3431861	17784553	2402303	17784553	2402303	0	0	0	0	7621951	1029558	0	0	0	0
83.78	0	0	0	0	0	0	57316587	7736862	2492026	336385.3	9968102	1345541	7476077	1009156	14952153	2018312	0	0	0	0	2492026	336385.3	0	0	0	0
83.88	0	0	0	0	0	0	48828125	6611735	0	0	35264757	4775142	0	0	16276042	2203912	0	0	0	0	0	0	0	0	0	0
83.98	0	0	0	0	10629252	1438159	58460884	7909877	2657313	359539.9	18601190	2516779	2657313	359539.9	10629252	1438159	0	0	0	0	5314626	719079.7	0	0	0	0
84.08	0	0	0	0	0	0	68999288	9278576	4451567	598617.8	35612536	4788942	0	0	13354701	1795853	0	0	0	0	0	0	0	0	0	0
84.18	0	0	0	0	5008013	676120.3	57592147	7775383	0	0	15024038	2028361	5008013	676120.3	5008013	676120.3	0	0	0	0	0	0	0	0	0	0
84.28	0	0	0	0	20032051	2704481	82632212	11155984	7512019	1014180	32552083	4394782	5008013	676120.3	17528045	2366421	0	0	0	0	7512019	1014180	0	0	0	0
84.38	0	0	0	0	0	0	1.06E+08	14236667	4800307	647121.2	16801075	2264924	2400154	323560.6	16801075	2264924	0	0	0	0	2400154	323560.6	0	0	7200461	970681.8
84.48	0	0	0	0	14467593	1950660	1.25E+08	16905721	2411265	325110	1.09E+08	14629951	4822531	650220.1	31346451	4226430	0	0	0	0	9645062	1300440	0	0	0	0
84.58	0	0	0	0	0	0	1.17E+08	15779269	0	0	64506881	8694699	7167431	966077.7	26280581	3542285	0	0	0	0	2389144	322025.9	0	0	0	0
84.68	0	0	0	0	9920635	1338908	1.17E+08	15732166	0	0	62003968	8368174	2480159	334726.9	27281746	3681996	0	0	0	0	0	0	0	0	0	0
84.78	0	0	0	0	15394089	2080143	76970443	10400716	0	0	38485222	5200358	0	0	30788177	4160287	0	0	0	0	5131363	693381.1	0	0	0	0
84.88	0	0	0	0	0	0	80906149	10926729	0	0	53094660	7170666	0	0	5056634	682920.6	0	0	0	0	2528317	341460.3	0	0	0	0
84.98	0	0	0	0	0	0	1.5E+08	20211244	0	0	20627063	2787758	0	0	12891914	1742349	0	0	0	0	0	0	0	0	0	0
85.08	0	0	0	0	0	0	1.13E+08	15254384	2565681	346690.5	43616585	5893739	7697044	1040072	15394089	2080143	0	0	0	0	5131363	693381.1	0	0	0	0
85.11	0	0	0	0	0	0	89712919	12109870	7476077	1009156	34888357	4709394	7476077	1009156	9968102	1345541	0	0	0	0	0	0	0	0	0	0
85.18	0	0	0	0	2516103	339751.7	1.21E+08	16308082	2516103	339751.7	57870370	7814289	0	0	22644928	3057765	0	0	0	0	5032206	679503.4	0	0	0	0
85.21	0	0	0	0	0	0	1.2E+08	16211683	0	0	61274510	8278306	5106209	689858.9	12765523	1724647	0	0	0	0	12765523	1724647	0	0	0	0
85.31	3833982	517617.1	0	0	15024038	2028361	1.35E+08	18255247	10016026	1352241	62600160	8451503	5008013	676120.3	35056090	4732842	0	0	0	0	7512019	1014180	0	0	0	0
85.41	0	0	0	0	11176681	1503172	1.25E+08	16835531	0	0	49177396	6613959	2235336	300634.5	17882690	2405076	0	0	0	0	15647353	2104441	0	0	0	0
85.51	0	0	0	0	0	0	95663265	12845819	0	0	51020408	6851104	0	0	29761905	3996477	0	0	0	0	6377551	856388	0	0	0	0
85.61	0	0	0	0	0	0	99957912	13519358	0	0	52609428	7115452	0	0	5260943	711545.2	0	0	0	0	5260943	711545.2	0	0	0	0
85.71	0	0	0	0	7512019	1014180	1.45E+08	19607487	5008013	676120.3	50080128	6761203	0	0	22536058	3042541	0	0	0	0	12520032	1690301	0	0	0	0
85.81	0	0	0	0	5482456	742670.8	1.21E+08	16338758	2741228	371335.4	52083333	7055373	5482456	742670.8	27412281	3713354	0	0	0	0	8223684	1114006	0	0	0	0
85.91	0	0	0	0	6823144	918168.8	97798399	13160419	2274381	306056.3	43213246	5815069	0	0	15920670	2142394	0	0	0	0	9097525	1224225	0	0	0	0
86.01	0	0	0	0	0	0	1.22E+08	16472933	5081301	686372.2	63516260	8579652	2540650	343186.1	12703252	1715930	0	0	0	0	2540650	343186.1	0	0	0	0
86.11	0	0	0	0	7200461	970681.8	1.13E+08	15207349	2400154	323560.6	36002304	4853409	0	0	9600614	1294242	0	0	0	0	12000768	1617803	0	0	0	0
86.21	0	0	0	0	2630471	355772.6	76283670	10317405	0	0	36826599	4980816	2630471	355772.6	10521886	1423090	0	0	0	0	0	0	0	0	0	0
86.31	0	0	0	0	4800307	647121.2	60003840	8089015	7200461	970681.8	26401690	3559167	2400154	323560.6	7200461	970681.8	0	0	0	0	4800307	647121.2	0	0	0	0
86.41	0	0	0	0	0	0	60975610	8236466	5081301	686372.2	33028455	4461419	17784553	2402303	7621951	1029558	0	0	0	0	2540650	343186.1	0	0	0	0
86.51	0	0	7512019	1014180	2504006	338060.1	1.05E+08	14198525	0	0	27544071	3718661	17528045	2366421	15024038	2028361	0	0	0	0	0	0	0	0	0	0
86.61	0	0	0	0	2480159	334726.9	76884921	10376535	2480159	334726.9	27281746	3681996	12400794	1673635	7440476	1004181	0	0	0	0	2480159	334726.9	0	0	0	0
86.71	0	0	0	0	2389144	322025.9	1.19E+08	16101294	4778287	644051.8	38226300	5152414	0	0	9556575	1288104	0	0	0	0	2389144	322025.9	0	0	0	0
86.81	0	0	0	0	2657313	359539.9	87691327	11864815	7971939	1078620	71747449	9707576	5314626	719079.7	5314626	719079.7	0	0	0	0	2657313	359539.9	0	0	0	0
86.91	0	0	0	0	0	0	1.52E+08	20415978	4734848	637999.3	87594697	11802987	0	0	9469697	1275999	0	0	0	0	4734848	637999.3	0	0	0	0
87.01	0	0	0	0	2540650	343186.1	71138211	9609211	0	0	17784553	2402303	0	0	10162602	1372744	0	0	0	0	0	0	0	0	0	0
87.11	0	0	0	0	0	0	63131313	8538542	0	0	23674242	3201953	0	0	7891414	1067318	0	0	0	0	0	0	0	0	0	0
87.21	0	0	0	0	0	0	65431323	8847959	2617253	353918.4	18320771	2477428	10469012	1415673	26172529	3539184	0	0	0	0	2617253	353918.4	0	0	0	0
87.31	0	0	0	0	0	0	82101806	11094098	7697044	1040072	33353859	4506977	5131363	693381.1	15394089	2080143	0	0	0	0	5131363	693381.1	0	0	0	0
87.41	0	0	0	0	0	0	64792663	8746018	0	0	24920255	3363853	2492026	336385.3	7476077	1009156	0	0	0	0	0	0	0	0	0	0
87.51	0	0	0	0	0	0	51567657	6969394	7735149	1045409	10313531	1393879	2578383	348469.7	10313531	1393879	0	0	0	0	5156766	696939.4	0	0	0	0
87.61	0	0	0	0	0	0	57870370	7802641	0	0	19290123	2600880	0	0	4822531	650220.1	0	0	0	0	0	0	0	0	0	0
87.71	0	0	0	0	4588840	617682.1	1.01E+08	13589007	2294420	308841.1	29827460	4014934	6883260	926523.2	6883260	926523.2	0	0	0	0	4588840	617682.1	0	0	0	0
87.81	0	0	0	0	0	0	70112179	9465684	10016026	1352241	17528045	2366421	7512019	1014180	2504006	338060.1	0	0	0	0	2504006	338060.1	0	0	0	0
87.91	0	0	0	0	0	0	85086634	11499501	0	0	36097360	4878576	10313531	1393879	0	0	0	0	0	0	2578383	348469.7	0	0	0	0
88.01	0	0	0	0	0	0	59597844	8056146	0	0	25912106	3502672	0	0	10364842	1401069	0	0	0	0	0	0	0	0	0	0
88.11	0	0	0	0	0	0	59302805	8014803	0	0	20627063	2787758	0	0	5156766	696939.4	0	0	0	0	0	0	0	0	0	0
88.21	0	0	0	0	5156766	696939.4	67037954	9060213	0	0	64459571	8711743	0	0	2578383	348469.7	0	0	0	0	2578383	348469.7	0	0	0	0
88.31	0	0	0	0	0	0	71383249	9656451	0	0	47588832	6437634	5287648	715292.6	13219120	1788232	0	0	0	0	0	0	0	0	0	0
88.41	0	0	0	0	0	0	27947154	3775047	0	0	12703252	1715930	0	0	7621951	1029558	0	0	0	0	0	0	0	0	0	0
88.51	0	0	0	0	0	0	86405530	11648182	0	0	43202765	5824091	4800307	647121.2	7200461	970681.8	0	0	0	0	0	0	0	0	0	0
88.61	0	0	0	0	0	0	40453074	5463364	0	0	17698220	2390222	0	0	0	0	0	0	0	0	0	0	0	0	0	0
88.71	0	0	0	0	5131363	693381.1	23091133	3120215	0	0	0	0	0	0	2565681	346690.5	0	0	0	0	0	0	0	0	0	0
88.81	0	0	0	0	2578383	348469.7	54146040	7317864	0	0	20627063	2787758	5156766	696939.4	12891914	1742349	0	0	0	0	0	0	0	0	0	0
88.91	0	0	0	0	0	0	34722222	4686177	0	0	24801587	3347269	0	0	0	0	0	0	0	0	0	0	0	0	0	0
89.01	0	0	0	0	5287648	715292.6	42301184	5722341	0	0	13219120	1788232	0	0	5287648	715292.6	0	0	0	0	0	0	0	0	0	0
89.11	0	0	0	0	7548309	1019255	45289855	6115531	0	0	20128824	2718014	2516103	339751.7	2516103	339751.7	0	0	0	0	0	0	0	0	0	0
89.21	0	0	0	0	10469012	1415673	99455611	13448898	2617253	353918.4	34024288	4600939	10469012	1415673	5234506	707836.7	0	0	0	0	0	0	0	0	0	0
89.31	0	0	0	0	5131363	693381.1	35919540	4853668	0	0	5131363	693381.1	0	0	7697044	1040072	0	0	0	0	0	0	0	0	0	0
89.37	0	0	0	0	7659314	1034788	61274510	8278306	0	0	10212418	1379718	0	0	10212418	1379718	0	0	0	0	2553105	344929.4	0	0	0	0
89.41	0	0	0	0	7440476	1004181	47123016	6359812	0	0	4960317	669453.9	9920635	1338908	9920635	1338908	0	0	0	0	0	0	0	0	0	0
89.47	0	0	0	0	0	0	29761905	4016723	0	0	27281746	3681996	2480159	334726.9	4960317	669453.9	0	0	0	0	0	0	0	0	0	0
89.51	0	0	0	0	0	0	17784553	2402303	0	0	7621951	1029558	2540650	343186.1	10162602	1372744	0	0	0	0	2540650	343186.1	0	0	0	0
89.57	0	0	0	0	0	0	58151294	7853586	0	0	17698220	2390222	0	0	7584951	1024381	0	0	0	0	0	0	0	0	0	0
89.61	0	0	0	0	0	0	43191057	5834164	2540650	343186.1	20325203	2745489	2540650	343186.1	7621951	1029558	0	0	0	0	2540650	343186.1	0	0	0	0
89.67	2499315	337543.4	0	0	0	0	35396440	4780444	2528317	341460.3	20226537	2731682	2528317	341460.3	5056634	682920.6	0	0	0	0	0	0	0	0	0	0
89.71	0	0	0	0	0	0	31094527	4203207	0	0	15547264	2101603	5182421	700534.4	2591211	350267.2	0	0	0	0	5182421	700534.4	0	0	0	0
89.77	0	0	0	0	2565681	346690.5	51313629	6933811	0	0	17959770	2426834	2565681	346690.5	2565681	346690.5	0	0	0	0	2565681	346690.5	0	0	0	0
89.87	0	0	0	0	15394089	2080143	53879310	7280502	0	0	12828407	1733453	2565681	346690.5	7697044	1040072	0	0	0	0	0	0	0	0	0	0
89.97	0	0	0	0	34722222	4686177	62003968	8368174	0	0	7440476	1004181	2480159	334726.9	4960317	669453.9	0	0	0	0	0	0	0	0	0	0
90.07	0	0	0	0	7891414	1067318	39457071	5336589	0	0	26304714	3557726	0	0	10521886	1423090	0	0	0	0	2630471	355772.6	0	0	0	0
90.17	0	0	0	0	2657313	359539.9	39859694	5393098	0	0	10629252	1438159	2657313	359539.9	7971939	1078620	0	0	0	0	2657313	359539.9	0	0	0	0
90.27	0	0	0	0	2578383	348469.7	23205446	3136227	0	0	33518977	4530106	0	0	10313531	1393879	0	0	0	0	0	0	0	0	0	0
90.37	0	0	0	0	0	0	27412281	3700238	0	0	34888357	4709394	2492026	336385.3	12460128	1681926	0	0	0	0	2492026	336385.3	0	0	0	0
90.47	0	0	0	0	0	0	37924757	5121904	0	0	15169903	2048762	0	0	5056634	682920.6	0	0	0	0	2528317	341460.3	0	0	0	0
90.57	0	0	0	0	9426848	1270031	42420814	5715139	0	0	16496983	2222554	4713424	635015.5	4713424	635015.5	0	0	0	0	0	0	0	0	0	0
90.67	2761969	373015.9	0	0	10113269	1365841	32868123	4438984	0	0	22754854	3073142	0	0	20226537	2731682	0	0	0	0	2528317	341460.3	0	0	0	0
90.77	0	0	0	0	7370283	994376.3	19654088	2651670	0	0	27024371	3646047	0	0	4913522	662917.6	0	0	0	0	0	0	0	0	0	0
90.87	0	0	0	0	20226537	2731682	12641586	1707301	0	0	27811489	3756063	0	0	7584951	1024381	0	0	0	0	2528317	341460.3	0	0	0	0
90.97	2721746	367583.6	0	0	2528317	341460.3	22754854	3073142	0	0	12641586	1707301	5056634	682920.6	2528317	341460.3	0	0	0	0	2528317	341460.3	0	0	0	0
91.07	2522936	340500.2	0	0	42162698	5690358	49603175	6694539	0	0	42162698	5690358	0	0	19841270	2677816	0	0	0	0	0	0	0	0	0	0
91.17	0	0	0	0	0	0	17361111	2343089	0	0	4960317	669453.9	0	0	7440476	1004181	0	0	0	0	0	0	0	0	0	0
91.27	0	0	0	0	0	0	486760.1	63603.63	0	0	973520.2	127207.3	0	0	0	0	0	0	0	0	0	0	0	0	0	0
91.37	2202069	296673.5	0	0	2356712	317507.7	56561086	7620186	0	0	32993967	4445108	4713424	635015.5	14140271	1905046	0	0	0	0	2356712	317507.7	0	0	0	0
91.47	0	0	0	0	0	0	15547264	2101603	0	0	18138474	2451871	0	0	0	0	0	0	0	0	0	0	0	0	0	0
91.57	2255859	304992.2	2604167	352083.3	5208333	704166.7	36458333	4929167	0	0	33854167	4577083	2604167	352083.3	2604167	352083.3	0	0	0	0	2604167	352083.3	0	0	0	0
91.67	0	0	0	0	12891914	1742349	51567657	6969394	0	0	15470297	2090818	2578383	348469.7	0	0	0	0	0	0	10313531	1393879	0	0	0	0
91.77	0	0	0	0	6883260	926523.2	1.03E+08	13897848	0	0	20649780	2779570	0	0	20649780	2779570	0	0	0	0	2294420	308841.1	0	0	0	0
91.87	2205489	297318.2	0	0	0	0	76804916	10353940	0	0	12000768	1617803	4800307	647121.2	31201997	4206288	0	0	0	0	12000768	1617803	0	0	0	0
91.97	0	0	0	0	2254690	303321.2	56367244	7583029	0	0	29310967	3943175	4509380	606642.3	9018759	1213285	0	0	0	0	2254690	303321.2	0	0	0	0
92.07	2347084	316766.9	0	0	7440476	1004181	84325397	11380716	0	0	37202381	5020904	0	0	14880952	2008362	0	0	0	0	2480159	334726.9	0	0	0	0
92.17	2185348	294511	0	0	0	0	66590563	8974158	0	0	38051750	5128090	0	0	7134703	961516.9	0	0	0	0	7134703	961516.9	0	0	0	0
92.27	2630600	354626.7	0	0	0	0	60003840	8089015	0	0	28801843	3882727	4800307	647121.2	16801075	2264924	0	0	0	0	4800307	647121.2	0	0	0	0
92.37	0	0	0	0	7370283	994376.3	66332547	8949387	0	0	24567610	3314588	0	0	7370283	994376.3	0	0	0	0	2456761	331458.8	0	0	0	0
92.47	0	0	0	0	17116588	2308939	39123631	5277576	0	0	24452269	3298485	0	0	7335681	989545.4	0	0	0	0	2445227	329848.5	0	0	0	0
92.57	0	0	0	0	0	0	58962264	7955011	0	0	14740566	1988753	0	0	0	0	0	0	0	0	2456761	331458.8	0	0	0	0
92.67	0	0	0	0	2591211	350267.2	85509950	11558818	0	0	20729685	2802138	0	0	5182421	700534.4	0	0	0	0	7773632	1050802	0	0	0	0
92.77	0	0	0	0	2540650	343186.1	38109756	5147791	0	0	15243902	2059117	5081301	686372.2	10162602	1372744	0	0	0	0	2540650	343186.1	0	0	0	0
92.87	0	0	0	0	2540650	343186.1	71138211	9609211	0	0	33028455	4461419	0	0	12703252	1715930	0	0	0	0	5081301	686372.2	0	0	0	0
92.97	2401164	323696.9	0	0	2400154	323560.6	69604455	9383258	0	0	21601382	2912046	0	0	4800307	647121.2	0	0	0	0	0	0	0	0	0	0
93.07	4775293	645500.8	0	0	2591211	350267.2	51824212	7005344	2591211	350267.2	20729685	2802138	0	0	15547264	2101603	0	0	0	0	5182421	700534.4	0	0	0	0
93.17	0	0	0	0	2516103	339751.7	80515298	10872055	0	0	27677134	3737269	0	0	12580515	1698759	0	0	0	0	2516103	339751.7	0	0	0	0
93.27	2435818	328633.2	0	0	17197327	2320211	39308176	5303340	0	0	29481132	3977505	2456761	331458.8	19654088	2651670	0	0	0	0	4913522	662917.6	0	0	0	0
93.37	0	0	0	0	0	0	48003072	6471212	0	0	14400922	1941364	0	0	12000768	1617803	0	0	0	0	2400154	323560.6	0	0	0	0
93.47	2570627	347358.9	0	0	0	0	61576355	8320573	0	0	25656814	3466905	0	0	15394089	2080143	0	0	0	0	2565681	346690.5	0	0	0	0
93.57	0	0	0	0	5106209	689858.9	40849673	5518871	0	0	15318627	2069577	0	0	2553105	344929.4	0	0	0	0	5106209	689858.9	0	0	0	0

Depth	*Micrantholithus spp.*	Uncertainty	*Neococcolithes protenus*	Uncertainty	*Pedinocyclus larvalis*	Uncertainty	*Pontosphaera plana*	Uncertainty	*Pontosphaera sp.*	Uncertainty	*Pyrocyclus orogensis*	Uncertainty	*Pyrocyclus sp.*	Uncertainty	*Reticulofenestra bisecta*	Uncertainty	*Reticulofenestra reticulata*	Uncertainty	*Reticulofenestra sp. (0-7μ)*	Uncertainty	*Reticulofenestra sp. (7-13μ)*	Uncertainty	*Sphenolithus editus*	Uncertainty
81.38	43402778	5801746	0	0	0	0	0	0	0	0	3616898	483478.8	0	0	25318287	3384352	2.84E+08	37953087	3.74E+08	50040057	10850694	1450436	1808449	241739.4
81.48	33574380	4510121	0	0	0	0	0	0	0	0	0	0	0	0	23674242	3180214	2.24E+08	30067476	2.93E+08	39319007	10761019	1445552	2152204	289110.3
81.58	4475911	600247.7	0	0	2034505	272839.9	2034505	272839.9	0	0	2034505	272839.9	0	0	20345052	2728399	2.73E+08	36560542	3.72E+08	49929695	10172526	1364199	0	0
81.68	13434579	1811961	0	0	5597741	754983.6	0	0	0	0	8396612	1132475	0	0	78368380	10569770	5.35E+08	72100934	5.12E+08	69081000	25189836	3397426	0	0
81.78	6452802	868707.1	0	0	4609145	620505.1	0	0	0	0	4609145	620505.1	0	0	25350295	3412778	4.26E+08	57396718	4.38E+08	58947981	9218289	1241010	0	0
81.88	6802721	913480.5	2125850	285462.7	14880952	1998239	0	0	0	0	10629252	1427313	0	0	44642857	5994716	3.72E+08	49955965	5.14E+08	69081962	4251701	570925.3	2125850	285462.7
81.98	16009852	2163349	0	0	3078818	416028.7	0	0	1539409	208014.3	3078818	416028.7	0	0	32327586	4368301	2.37E+08	32034207	2.57E+08	34738393	52339901	7072487	0	0
82.08	13818027	1869607	5314626	719079.7	5314626	719079.7	0	0	0	0	7971939	1078620	0	0	58460884	7909877	3.72E+08	50335581	3.88E+08	52492820	18601190	2516779	0	0
82.18	14880952	1996551	0	0	4133598	554597.6	0	0	0	0	6200397	831896.4	0	0	43402778	5823275	3.74E+08	50191084	2.83E+08	37989936	33068783	4436781	0	0
82.28	7716049	1036383	0	0	4286694	575768.3	0	0	0	0	0	0	0	0	21433471	2878841	2.87E+08	38576475	2.81E+08	37712823	6430041	863652.4	0	0
82.38	9308511	1251579	0	0	0	0	0	0	0	0	2216312	297994.9	2216312	297994.9	19946809	2681955	2.81E+08	37845358	2.44E+08	32779444	15514184	2085965	0	0
82.48	12835703	1732041	0	0	4936809	666169.7	0	0	0	0	7405213	999254.6	0	0	19747235	2664679	3.01E+08	40636352	2.72E+08	36639334	32089258	4330103	0	0
82.58	15829248	2138562	2553105	344929.4	0	0	0	0	0	0	5106209	689858.9	0	0	45955882	6208730	3.7E+08	50014768	3.14E+08	42426320	25531046	3449294	2553105	344929.4
82.68	9078746	1223698	0	0	4778287	644051.8	0	0	0	0	2389144	322025.9	2389144	322025.9	45393731	6118492	2.94E+08	39609184	3.32E+08	44761599	16724006	2254181	0	0
82.78	25807057	3476327	0	0	2346096	316029.7	0	0	0	0	0	0	0	0	65690691	8848832	1.97E+08	26546496	2.7E+08	36343417	53960210	7268683	0	0
82.88	20833333	2811706	0	0	0	0	0	0	0	0	0	0	2480159	334726.9	24801587	3347269	2.31E+08	31129606	3.25E+08	43849230	22321429	3012543	0	0
82.98	3238342	438411.1	0	0	0	0	0	0	0	0	0	0	0	0	40479275	5480139	2.89E+08	39091656	2.24E+08	30323434	24287565	3288083	0	0
83.08	17665131	2381406	0	0	0	0	0	0	0	0	0	0	0	0	93846006	12651220	3.53E+08	47628123	4.25E+08	57302585	30361943	4093042	0	0
83.18	4734848	637999.3	0	0	0	0	0	0	0	0	2367424	318999.7	0	0	52083333	7017992	3.74E+08	50401946	3.95E+08	53272942	49715909	6698993	0	0
83.28	20414573	2760563	0	0	0	0	0	0	0	0	2617253	353918.4	0	0	65431323	8847959	3.8E+08	51318162	3.98E+08	53795590	20938023	2831347	2617253	353918.4
83.38	9600614	1294242	0	0	0	0	2400154	323560.6	0	0	0	0	0	0	31201997	4206288	2.21E+08	29767577	2.71E+08	36562350	16801075	2264924	0	0
83.48	11802135	1594777	0	0	2565681	346690.5	0	0	0	0	5131363	693381.1	0	0	51313629	6933811	3.98E+08	53737035	2.72E+08	36749198	43616585	5893739	2565681	346690.5
83.58	13678451	1850017	0	0	0	0	0	0	2630471	355772.6	5260943	711545.2	0	0	21043771	2846181	2.79E+08	37711894	2.6E+08	35221486	15782828	2134635	2630471	355772.6
83.68	3048780	411823.3	0	0	0	0	0	0	0	0	2540650	343186.1	0	0	43191057	5834164	4.17E+08	56282520	4.07E+08	54909776	10162602	1372744	2540650	343186.1
83.78	6479266	874601.8	0	0	2492026	336385.3	0	0	0	0	2492026	336385.3	0	0	27412281	3700238	2.49E+08	33638529	3.14E+08	42384546	32396332	4373009	0	0
83.88	8138021	1101956	0	0	0	0	0	0	0	0	0	0	0	0	54253472	7346372	2.74E+08	37099180	3.12E+08	42241640	32552083	4407823	0	0
83.98	6377551	862895.7	0	0	2657313	359539.9	0	0	0	0	0	0	0	0	31887755	4314478	2.26E+08	30560888	4.41E+08	59683617	39859694	5393098	0	0
84.08	1780627	239447.1	0	0	0	0	0	0	0	0	2225783	299308.9	0	0	35612536	4788942	2.69E+08	36216377	4.16E+08	55970765	8903134	1197236	0	0
84.18	10516827	1419853	0	0	5008013	676120.3	0	0	0	0	0	0	0	0	45072115	6085082	2.53E+08	34144073	4.76E+08	64231424	2504006	338060.1	0	0
84.28	5508814	743732.3	0	0	2504006	338060.1	0	0	0	0	0	0	0	0	55088141	7437323	2.65E+08	35834373	5.01E+08	67612025	2504006	338060.1	2504006	338060.1
84.38	2880184	388272.7	0	0	2400154	323560.6	0	0	0	0	2400154	323560.6	0	0	62403994	8412576	1.73E+08	23296364	4.3E+08	57917350	12000768	1617803	0	0
84.48	5304784	715242.1	0	0	0	0	0	0	0	0	0	0	0	0	79571759	10728631	2.56E+08	34461663	7.11E+08	95907457	14467593	1950660	0	0
84.58	7645260	1030483	0	0	0	0	0	0	0	0	0	0	0	0	64506881	8694699	88398318	11914958	3.3E+08	44439573	0	0	0	0
84.68	4464286	602508.5	0	0	0	0	0	0	0	0	0	0	0	0	64484127	8702901	1.14E+08	15397440	4.71E+08	63598120	4960317	669453.9	0	0
84.78	6157635	832057.3	0	0	0	0	0	0	0	0	0	0	0	0	46182266	6240430	53879310	7280502	4.39E+08	59284084	7697044	1040072	0	0
84.88	0	0	0	0	0	0	0	0	0	0	0	0	0	0	42981392	5804825	88491100	11951110	4.98E+08	67267675	5056634	682920.6	0	0
84.98	5672442	766633.4	0	0	0	0	0	0	0	0	0	0	0	0	41254125	5575515	20627063	2787758	3.74E+08	50528109	5156766	696939.4	0	0
85.08	12315271	1664115	0	0	0	0	0	0	0	0	0	0	0	0	59010673	7973883	23091133	3120215	5.44E+08	73498396	35919540	4853668	0	0
85.11	6479266	874601.8	0	0	2492026	336385.3	0	0	0	0	0	0	0	0	69776715	9418788	24920255	3363853	5.21E+08	70304526	7476077	1009156	0	0
85.18	503220.6	67950.34	0	0	0	0	0	0	0	0	0	0	0	0	37741546	5096276	22644928	3057765	5.46E+08	73726120	2516103	339751.7	0	0
85.21	8680556	1172760	0	0	2553105	344929.4	0	0	0	0	0	0	0	0	86805556	11727601	53615196	7243518	6.15E+08	83127994	0	0	2553105	344929.4
85.31	6510417	878956.3	0	0	0	0	0	0	0	0	0	0	0	0	82632212	11155984	47576122	6423142	6.39E+08	86205332	20032051	2704481	2504006	338060.1
85.41	6706009	901903.5	0	0	0	0	0	0	0	0	0	0	0	0	1.05E+08	14129821	49177396	6613959	7.58E+08	1.02E+08	8941345	1202538	2235336	300634.5
85.51	2976190	399647.7	0	0	2125850	285462.7	0	0	0	0	0	0	2125850	285462.7	1.15E+08	15414983	25510204	3425552	7.42E+08	99626466	14880952	1998239	4251701	570925.3
85.61	5260943	711545.2	0	0	0	0	0	0	0	0	0	0	0	0	76283670	10317405	18413300	2490408	6.05E+08	81827694	10521886	1423090	0	0
85.71	4006410	540896.2	0	0	7512019	1014180	0	0	0	0	0	0	0	0	80128205	10817924	10016026	1352241	7.19E+08	97023256	7512019	1014180	10016026	1352241
85.81	3289474	445602.5	0	0	0	0	0	0	0	0	0	0	0	0	1.18E+08	15967423	2741228	371335.4	7.92E+08	1.07E+08	8223684	1114006	2741228	371335.4
85.91	1364629	183633.8	0	0	2274381	306056.3	0	0	0	0	0	0	0	0	97798399	13160419	15920670	2142394	5.87E+08	78962513	34115721	4590844	0	0
86.01	0	0	0	0	0	0	0	0	0	0	0	0	0	0	1.37E+08	18532049	12703252	1715930	2.57E+08	34661796	20325203	2745489	0	0
86.11	4800307	647121.2	0	0	0	0	0	0	0	0	0	0	0	0	1.32E+08	17795834	21601382	2912046	4.49E+08	60505835	12000768	1617803	4800307	647121.2
86.21	5787037	782699.7	0	0	2630471	355772.6	0	0	0	0	2630471	355772.6	0	0	1.32E+08	17788629	23674242	3201953	4.63E+08	62615975	13152357	1778863	2630471	355772.6
86.31	4800307	647121.2	0	0	0	0	0	0	0	0	0	0	0	0	1.06E+08	14236667	12000768	1617803	6.05E+08	81537275	0	0	4800307	647121.2
86.41	7621951	1029558	0	0	5081301	686372.2	0	0	0	0	0	0	0	0	1.02E+08	13727444	2540650	343186.1	5.11E+08	68980406	10162602	1372744	0	0
86.51	8012821	1081792	0	0	2504006	338060.1	0	0	0	0	0	0	0	0	97656250	13184345	30048077	4056722	5.43E+08	73359048	12520032	1690301	2504006	338060.1
86.61	3472222	468617.7	0	0	0	0	0	0	0	0	2480159	334726.9	0	0	1.22E+08	16401620	2480159	334726.9	3.67E+08	49539588	9920635	1338908	0	0
86.71	7167431	966077.7	0	0	0	0	0	0	0	0	0	0	0	0	1.27E+08	17067372	9556575	1288104	1.82E+08	24473968	2389144	322025.9	0	0
86.81	7440476	1006712	0	0	0	0	2657313	359539.9	0	0	0	0	0	0	1.41E+08	19055613	13286565	1797699	2.58E+08	34875367	2657313	359539.9	0	0
86.91	9469697	1275999	0	0	2367424	318999.7	0	0	0	0	0	0	0	0	2.49E+08	33494964	16571970	2232998	3.74E+08	50401946	4734848	637999.3	0	0
87.01	1524390	205911.7	0	0	0	0	0	0	0	0	0	0	0	0	88922764	12011513	17784553	2402303	2.16E+08	29170818	5081301	686372.2	0	0
87.11	0	0	0	0	0	0	0	0	0	0	0	0	0	0	36826599	4980816	7891414	1067318	55239899	7471224	63131313	8538542	0	0
87.21	3140704	424702	0	0	0	0	0	0	0	0	0	0	0	0	1.91E+08	25836040	2617253	353918.4	2.07E+08	27959550	10469012	1415673	0	0
87.31	8723317	1178748	0	0	0	0	0	0	0	0	0	0	0	0	1.1E+08	14907694	15394089	2080143	3.62E+08	48883367	17959770	2426834	0	0
87.41	996810.2	134554.1	0	0	0	0	0	0	0	0	0	0	0	0	1.45E+08	19510347	4984051	672770.6	1.25E+08	16819264	7476077	1009156	0	0
87.51	2578383	348469.7	0	0	0	0	0	0	0	0	0	0	0	0	2.14E+08	28922987	0	0	1.31E+08	17771956	0	0	0	0
87.61	5787037	780264.1	0	0	0	0	0	0	0	0	0	0	0	0	74749228	10078411	16878858	2275770	1.42E+08	19181491	7233796	975330.1	0	0
87.71	5506608	741218.5	0	0	0	0	0	0	0	0	0	0	0	0	2.02E+08	27178013	4588840	617682.1	1.38E+08	18530463	9177680	1235364	0	0
87.81	500801.3	67612.03	0	0	0	0	0	0	0	0	0	0	0	0	1.45E+08	19607487	2504006	338060.1	82632212	11155984	12520032	1690301	0	0
87.91	2578383	348469.7	0	0	0	0	0	0	0	0	0	0	0	0	1.39E+08	18817365	10313531	1393879	1.7E+08	22999001	2578383	348469.7	0	0
88.01	3109453	420320.7	0	0	0	0	0	0	0	0	0	0	0	0	95874793	12959887	15547264	2101603	1.79E+08	24168438	23320896	3152405	0	0
88.11	5156766	696939.4	0	0	0	0	0	0	0	0	0	0	0	0	51567657	6969394	28362211	3833167	1.96E+08	26483698	43832508	5923985	0	0
88.21	7219472	975715.2	0	0	0	0	0	0	0	0	0	0	0	0	92821782	12544910	5156766	696939.4	1.93E+08	26135229	18048680	2439288	0	0
88.31	3172589	429175.6	0	0	0	0	0	0	0	0	0	0	0	0	74027073	10014097	10575296	1430585	1.11E+08	15021145	15862944	2145878	0	0
88.41	0	0	0	0	0	0	0	0	0	0	0	0	0	0	10162602	1372744	7621951	1029558	94004065	12697886	7621951	1029558	0	0
88.51	14400922	1941364	0	0	0	0	0	0	0	0	0	0	0	0	67204301	9059697	26401690	3559167	2.35E+08	31708940	4800307	647121.2	0	0
88.61	1011327	136584.1	0	0	0	0	0	0	0	0	0	0	0	0	55622977	7512126	10113269	1365841	1.34E+08	18097395	2528317	341460.3	0	0
88.71	0	0	0	0	0	0	0	0	0	0	0	0	0	0	38485222	5200358	20525452	2773524	51313629	6933811	7697044	1040072	0	0
88.81	13923267	1881736	0	0	0	0	0	0	0	0	0	0	0	0	1.29E+08	17423486	20627063	2787758	12891914	1742349	12891914	1742349	0	0
88.91	2480159	334726.9	0	0	0	0	0	0	0	0	0	0	0	0	1.17E+08	15732166	4960317	669453.9	0	0	9920635	1338908	0	0
89.01	6345178	858351.2	0	0	0	0	0	0	0	0	0	0	0	0	81958545	11087036	10575296	1430585	0	0	0	0	0	0
89.11	3019324	407702	0	0	0	0	0	0	0	0	0	0	0	0	1.23E+08	16647834	12580515	1698759	0	0	15096618	2038510	2516103	339751.7
89.21	0	0	0	0	0	0	0	0	0	0	2617253	353918.4	0	0	1.2E+08	16280244	7851759	1061755	73283082	9909714	7851759	1061755	0	0
89.31	2565681	346690.5	0	0	0	0	0	0	0	0	0	0	0	0	89798851	12134169	12828407	1733453	46182266	6240430	5131363	693381.1	0	0
89.37	1531863	206957.7	0	0	0	0	0	0	0	0	0	0	0	0	1.02E+08	13797177	15318627	2069577	1.02E+08	13797177	2553105	344929.4	0	0
89.41	2976190	401672.3	0	0	0	0	0	0	0	0	0	0	0	0	54563492	7363993	17361111	2343089	1.76E+08	23765613	4960317	669453.9	0	0
89.47	7936508	1071126	0	0	0	0	0	0	0	0	0	0	0	0	66964286	9037628	29761905	4016723	1.39E+08	18744709	2480159	334726.9	0	0
89.51	7113821	960921.1	0	0	2540650	343186.1	0	0	0	0	0	0	0	0	1.24E+08	16816119	12703252	1715930	2.9E+08	39123215	2540650	343186.1	0	0
89.57	4550971	614628.5	0	0	0	0	0	0	0	0	0	0	0	0	91019417	12292570	12641586	1707301	1.31E+08	17755934	10113269	1365841	0	0
89.61	4065041	549097.8	0	0	0	0	0	0	0	0	0	0	0	0	94004065	12697886	2540650	343186.1	1.17E+08	15786561	12703252	1715930	0	0
89.67	4550971	614628.5	0	0	5056634	682920.6	0	0	0	0	0	0	0	0	1.29E+08	17414474	2528317	341460.3	1.54E+08	20829077	7584951	1024381	0	0
89.71	5700663	770587.9	0	0	2591211	350267.2	0	0	0	0	0	0	2591211	350267.2	1.11E+08	15061490	5182421	700534.4	2E+08	26970576	0	0	0	0
89.77	8210181	1109410	0	0	5131363	693381.1	0	0	0	0	0	0	0	0	1.49E+08	20108052	5131363	693381.1	2.82E+08	38135960	2565681	346690.5	2565681	346690.5
89.87	4105090	554704.9	0	0	0	0	0	0	0	0	0	0	0	0	1.1E+08	14907694	25656814	3466905	2.59E+08	35015745	0	0	15394089	2080143
89.97	3472222	468617.7	0	0	0	0	0	0	0	0	0	0	0	0	1.49E+08	20083617	7440476	1004181	2.8E+08	37824145	9920635	1338908	0	0
90.07	5787037	782699.7	0	0	0	0	0	0	0	0	0	0	0	0	1.42E+08	19211719	13152357	1778863	3.6E+08	48740844	0	0	2630471	355772.6
90.17	2657313	359539.9	0	0	5314626	719079.7	0	0	0	0	0	0	0	0	1.09E+08	14741134	7971939	1078620	2.95E+08	39908925	5314626	719079.7	2657313	359539.9
90.27	9282178	1254491	0	0	2578383	348469.7	0	0	0	0	0	0	0	0	95400165	12893380	12891914	1742349	3.07E+08	41467896	2578383	348469.7	0	0
90.37	4485646	605493.5	0	0	4984051	672770.6	0	0	0	0	0	0	0	0	1.02E+08	13791797	14952153	2018312	2.87E+08	38684308	2492026	336385.3	0	0
90.47	3033981	409752.3	0	0	2528317	341460.3	0	0	0	0	0	0	0	0	1.11E+08	15024252	27811489	3756063	4.07E+08	54975105	0	0	0	0
90.57	5184766	698517	0	0	0	0	0	0	0	0	0	0	0	0	1.2E+08	16192895	16496983	2222554	4.29E+08	57786410	11783560	1587539	0	0
90.67	505663.4	68292.06	0	0	5056634	682920.6	0	0	0	0	0	0	0	0	1.24E+08	16731554	17698220	2390222	3.77E+08	50877581	2528317	341460.3	0	0
90.77	2948113	397750.5	0	0	0	0	0	0	0	0	0	0	0	0	1.35E+08	18230233	31937893	4308964	3.32E+08	44746935	2456761	331458.8	0	0
90.87	505663.4	68292.06	0	0	0	0	0	0	0	0	0	0	0	0	1.34E+08	18097395	7584951	1024381	3.34E+08	45072757	2528317	341460.3	0	0
90.97	2528317	341460.3	0	0	0	0	0	0	0	0	0	0	0	0	1.37E+08	18438855	17698220	2390222	1.97E+08	26633902	7584951	1024381	0	0
91.07	8432540	1138072	0	0	0	0	0	0	0	0	0	0	0	0	2.31E+08	31129606	24801587	3347269	4.27E+08	57573035	47123016	6359812	0	0
91.17	0	0	0	0	0	0	0	0	0	0	0	0	0	0	71924603	9707081	2480159	334726.9	1.36E+08	18409982	0	0	0	0
91.27	0	0	0	0	0	0	0	0	0	0	0	0	0	0	5597741	731441.7	0	0	11682243	1526487	243380.1	31801.81	0	0
91.37	2356712	317507.7	0	0	0	0	0	0	0	0	0	0	0	0	1.48E+08	20002988	7070136	952523.2	98981900	13335325	7070136	952523.2	0	0
91.47	0	0	0	0	0	0	0	0	0	0	0	0	0	0	64780265	8756680	5182421	700534.4	1.81E+08	24518705	2591211	350267.2	0	0
91.57	0	0	0	0	2604167	352083.3	0	0	0	0	0	0	0	0	1.09E+08	14787500	18229167	2464583	2.76E+08	37320833	0	0	0	0
91.67	3094059	418163.7	0	0	0	0	0	0	0	0	0	0	0	0	85086634	11499501	12891914	1742349	3.22E+08	43558715	5156766	696939.4	0	0
91.77	2294420	308841.1	0	0	9177680	1235364	0	0	0	0	0	0	0	0	1.19E+08	16059735	6883260	926523.2	2.5E+08	33663675	2294420	308841.1	0	0
91.87	0	0	0	0	2400154	323560.6	0	0	0	0	0	0	0	0	1.08E+08	14560228	9600614	1294242	2.33E+08	31385380	2400154	323560.6	0	0
91.97	2254690	303321.2	0	0	6764069	909963.5	0	0	0	0	0	0	0	0	1.33E+08	17895949	6764069	909963.5	2.16E+08	29118832	0	0	0	0
92.07	2976190	401672.3	0	0	7440476	1004181	0	0	0	0	0	0	0	0	1.81E+08	24435067	37202381	5020904	3.08E+08	41506141	7440476	1004181	0	0
92.17	5232116	705112.4	0	0	2378234	320505.6	0	0	0	0	0	0	0	0	1.88E+08	25319945	9512938	1282023	3.76E+08	50639891	2378234	320505.6	0	0
92.27	2400154	323560.6	0	0	7200461	970681.8	0	0	2400154	323560.6	0	0	0	0	1.34E+08	18119394	7200461	970681.8	2.76E+08	37209471	7200461	970681.8	0	0
92.37	3930818	530334	0	0	2456761	331458.8	0	0	0	0	0	0	0	0	1.94E+08	26185243	9827044	1325835	3.19E+08	43089641	2456761	331458.8	0	0
92.47	2445227	329848.5	0	0	2445227	329848.5	0	0	0	0	0	0	0	0	1.49E+08	20120757	31787950	4288030	4.28E+08	57723485	4890454	659697	0	0
92.57	982704.4	132583.5	0	0	0	0	0	0	0	0	0	0	0	0	1.5E+08	20218985	24567610	3314588	2.36E+08	31820043	0	0	0	0
92.67	518242.1	70053.44	0	0	0	0	0	0	0	0	0	0	0	0	1.24E+08	16812826	23320896	3152405	3.5E+08	47286074	0	0	0	0
92.77	2032520	274548.9	0	0	2540650	343186.1	0	0	0	0	0	0	0	0	99085366	13384258	22865854	3088675	3.28E+08	44271007	2540650	343186.1	0	0
92.87	0	0	0	0	0	0	0	0	0	0	0	0	0	0	1.5E+08	20247980	27947154	3775047	2.69E+08	36377727	0	0	0	0
92.97	9600614	1294242	0	0	2400154	323560.6	0	0	0	0	0	0	0	0	1.68E+08	22649243	48003072	6471212	3.26E+08	44004244	4800307	647121.2	2400154	323560.6
93.07	1036484	140106.9	0	0	0	0	0	0	0	0	0	0	0	0	1.61E+08	21716567	46641791	6304810	2.12E+08	28721912	5182421	700534.4	5182421	700534.4
93.17	0	0	0	0	0	0	0	0	0	0	0	0	0	0	95611916	12910565	17612721	2378262	2.26E+08	30577654	2516103	339751.7	7548309	1019255
93.27	4422170	596625.8	0	0	0	0	0	0	0	0	0	0	0	0	1.25E+08	16904398	27024371	3646047	2.56E+08	34471713	2456761	331458.8	0	0
93.37	4800307	647121.2	0	0	0	0	0	0	0	0	0	0	0	0	1.2E+08	16178031	28801843	3882727	2.26E+08	30414698	2400154	323560.6	4800307	647121.2
93.47	7697044	1040072	0	0	0	0	0	0	0	0	0	0	0	0	1.1E+08	14907694	20525452	2773524	2.8E+08	37789270	2565681	346690.5	5131363	693381.1
93.57	2553105	344929.4	0	0	2553105	344929.4	0	0	0	0	2553105	344929.4	0	0	99571078	13452248	17871732	2414506	2.71E+08	36562520	2553105	344929.4	2553105	344929.4
93.67	0	0	0	0	2504006	338060.1	0	0	0	0	0	0	0	0	1.03E+08	13860465	32552083	4394782	2.53E+08	34144073	0	0	7512019	1014180
93.77	0	0	0	0	0	0	0	0	0	0	0	0	0	0	92364532	12480860	0	0	1.87E+08	25308410	5131363	693381.1	2565681	346690.5
93.87	0	0	0	0	2893519	392811.2	0	0	0	0	0	0	0	0	1.01E+08	13748392	5787037	785622.4	2.03E+08	27496785	11574074	1571245	5787037	785622.4
93.97	2022654	273168.2	0	0	0	0	0	0	0	0	0	0	0	0	1.09E+08	14682792	27811489	3756063	2.81E+08	37902091	0	0	5056634	682920.6
94.07	2553105	344929.4	0	0	0	0	0	0	0	0	0	0	0	0	1.1E+08	14831966	35743464	4829012	2.71E+08	36562520	5106209	689858.9	2553105	344929.4
94.13	2604167	352083.3	0	0	2604167	352083.3	0	0	2604167	352083.3	0	0	0	0	88541667	11970833	39062500	5281250	2.94E+08	39785417	2604167	352083.3	5208333	704166.7
94.17	2630471	355772.6	0	0	2630471	355772.6	0	0	0	0	0	0	0	0	97327441	13163586	23674242	3201953	3.03E+08	40913847	26304714	3557726	5260943	711545.2
94.23	2630471	355772.6	0	0	2630471	355772.6	0	0	0	0	0	0	0	0	76283670	10317405	26304714	3557726	3.68E+08	49808162	2630471	355772.6	2630471	355772.6
94.33	0	0	0	0	0	0	0	0	0	0	0	0	0	0	65761785	8894315	34196128	4625044	3.87E+08	52298570	10521886	1423090	2630471	355772.6
94.43	1031353	139387.9	0	0	2578383	348469.7	0	0	0	0	0	0	0	0	1.47E+08	19862774	10313531	1393879	2.71E+08	36589320	2578383	348469.7	2578383	348469.7

Depth	*Sphenolithus moriformis*	Uncertainty	*Sphenolithus obtusus*	Uncertainty	*Sphenolithus radians*	Uncertainty	*Sphenolithus sp. 1*	Uncertainty	*Sphenolithus spiniger*	Uncertainty	*Total pemma*	Uncertainty	*Unidentified sp. 1*	Uncertainty	*Zygodiscus sp.*	Uncertainty	*Zygryhablithus bijugatus*	Uncertainty	Total Nannos	Uncertainty
81.38	19892940	2659133	0	0	5425347.2	725218.2	1808449.1	241739.4	7233796.3	966957.6	78486689.81	10491490.24	1808449.1	241739.4	0	0	9042245.37	1208697	1207682292	161433576
81.48	23674242	3180214	0	0	0	0	8608815.4	1156441	0	0	145488980.7	19543859.42	0	0	0	0	8608815.43	1156441.4	1178546832	158316826
81.58	26448568	3546918	0	0	2034505.2	272839.9	8138020.8	1091359	4069010.4	545679.7	139567057.3	18716814.68	0	0	0	0	10172526	1364199.3	1180419922	158301689
81.68	36385319	4907393	0	0	0	0	11195483	1509967	13994354	1887459	227268302.2	30652334.36	0	0	0	0	19592095	2642442.6	2029741044	273757055
81.78	25350295	3412778	0	0	2304572.3	310252.5	4609144.5	620505.1	0	0	152101769.9	20476667.12	0	0	0	0	13827433.6	1861515.2	1537149705	206938439
81.88	34013605	4567402	0	0	0	0	0	0	6377551	856388	151360544.2	20324941	2125850.3	285462.7	0	0	25510204.1	3425551.9	1583758503	212669678
81.98	40024631	5408373	0	0	1539408.9	208014.3	3078817.7	416028.7	3078817.7	416028.7	183497536.9	24795308.06	0	0	0	0	12315270.9	1664114.6	1391933498	188086557
82.08	15943878	2157239	0	0	5314625.9	719079.7	5314625.9	719079.7	7971938.8	1078620	128082483	17329821.34	0	0	0	0	7971938.78	1078619.6	1574723639	213063322
82.18	4133597.9	554597.6	0	0	4133597.9	554597.6	4133597.9	554597.6	4133597.9	554597.6	204199735.4	27397121.97	0	0	0	0	10333994.7	1386494	1502149471	201540772
82.28	17146776	2303073	2143347	287884.1	0	0	2143347.1	287884.1	2143347.1	287884.1	128600823	17273048.65	0	0	0	0	10716735.3	1439420.7	1088820302	146245145
82.38	22163121	2979949	0	0	0	0	2216312.1	297994.9	0	0	155141844	20859646.14	0	0	0	0	13297872.3	1787969.7	1097517730	147567097
82.48	12342022	1665424	0	0	0	0	0	0	0	0	147610584.5	19918474.33	0	0	0	0	7405213.27	999254.57	1321583728	178333631
82.58	15318627	2069577	0	0	0	0	0	0	7659313.7	1034788	181270424.8	24489989.83	5106209.2	689858.9	0	0	20424836.6	2759435.5	1537990196	207785491
82.68	14334862	1932155	0	0	0	0	0	0	4778287.5	644051.8	205466360.9	27694226.43	0	0	0	0	11945718.7	1610129.4	1330753058	179368420
82.78	16422673	2212208	0	0	2346096.1	316029.7	0	0	0	0	165634384.4	22311697.68	0	0	0	0	14076576.6	1896178.3	1081550300	145689697
82.88	4960317.5	669453.9	0	0	0	0	0	0	0	0	104166666.7	14058531.75	0	0	2480158.7	334726.9	19841269.8	2677815.6	939484127	126794567
82.98	13493092	1826713	0	0	0	0	0	0	2698618.3	365342.6	140328152	18997814.26	0	0	0	0	29684801.4	4018768.4	1069192573	144748731
83.08	19321237	2604663	0	0	2760176.7	372094.7	8280530	1116284	11040707	1488379	168370775.7	22697777.19	0	0	2760176.7	372094.7	27601766.5	3720947.1	1595382104	215070741
83.18	26041667	3508996	0	0	0	0	0	0	2367424.2	318999.7	153409090.9	20671177.69	0	0	0	0	7102272.73	956998.97	1446969697	194972590
83.28	26172529	3539184	0	0	0	0	0	0	5234505.9	707836.7	173785594.6	23500178.87	0	0	0	0	31407035.2	4247020.3	1549937186	209590451
83.38	24001536	3235606	0	0	0	0	2400153.6	323560.6	7200460.8	970681.8	119527649.8	16113318.66	0	0	0	0	9600614.44	1294242.5	949980798.8	128065292
83.48	15394089	2080143	0	0	0	0	2565681.4	346690.5	7697044.3	1040072	179084564.9	24199000.32	0	0	0	0	38485221.7	5200358.2	1309010673	176881518
83.58	10521886	1423090	0	0	2630471.4	355772.6	0	0	2630471.4	355772.6	161510942.8	21844436.58	5260942.8	711545.2	0	0	18413299.7	2490408.1	1020622896	138039762
83.68	17784553	2402303	0	0	2540650.4	343186.1	2540650.4	343186.1	0	0	161331300.8	21792317.32	2540650.4	343186.1	0	0	30487804.9	4118233.2	1440294715	194552200
83.78	7476076.6	1009156	0	0	2492025.5	336385.3	0	0	2492025.5	336385.3	151265949	20418587.08	2492025.5	336385.3	0	0	34888357.3	4709394.1	1061852073	143333772
83.88	5425347.2	734637.2	0	0	0	0	0	0	0	0	142144097.2	19247495.3	0	0	0	0	2712673.61	367318.61	1055230035	142886940
83.98	15943878	2157239	0	0	0	0	2657312.9	359539.9	5314625.9	719079.7	187606292.5	25383514.25	0	0	0	0	5314625.85	719079.72	1281356293	173370121
84.08	6677350.4	897926.7	0	0	6677350.4	897926.7	0	0	6677350.4	897926.7	167378917.4	22508029.56	0	0	0	0	11128917.4	1496544.5	1215722934	163482523
84.18	17528045	2366421	0	0	5008012.8	676120.3	0	0	5008012.8	676120.3	176282051.3	23799432.94	0	0	0	0	2504006.41	338060.13	1275040064	172140217
84.28	15024038	2028361	0	0	0	0	2504006.4	338060.1	2504006.4	338060.1	205328525.6	27720930.41	0	0	0	0	15024038.5	2028360.8	1495392628	201889508
84.38	12000768	1617803	0	0	0	0	7200460.8	970681.8	2400153.6	323560.6	119527649.8	16113318.66	0	0	0	0	12000768	1617803.1	1173195084	158156429
84.48	14467593	1950660	0	0	4822530.9	650220.1	0	0	0	0	180121527.8	24285718.88	0	0	0	0	14467592.6	1950660.2	1770109954	238663269
84.58	4778287.5	644051.8	0	0	0	0	2389143.7	322025.9	4778287.5	644051.8	143826452.6	19385958.5	0	0	0	0	19113149.8	2576207.1	1033065749	139243994
84.68	2480158.7	334726.9	0	0	0	0	4960317.5	669453.9	2480158.7	334726.9	146329365.1	19748889.83	0	0	0	0	4960317.46	669453.89	1217757937	164350931
84.78	7697044.3	1040072	0	0	7697044.3	1040072	0	0	0	0	147270114.9	19900037.51	0	0	0	0	2565681.44	346690.55	1044745484	141172392
84.88	0	0	0	0	0	0	0	0	0	0	124393203.9	16799845.65	0	0	0	0	12641585.8	1707301.4	1086670712	146759627
84.98	0	0	0	0	0	0	0	0	0	0	197504125.4	26692780.32	0	0	0	0	0	0	964315181.5	130327674
85.08	15394089	2080143	0	0	2565681.4	346690.5	0	0	2565681.4	346690.5	222701149.4	30092739.65	0	0	0	0	17959770.1	2426833.8	1320299672	178406957
85.11	12460128	1681926	0	0	2492025.5	336385.3	0	0	0	0	156000797.4	21057719.13	0	0	0	0	17444178.6	2354697	1197667464	161666770
85.18	15096618	2038510	0	0	0	0	0	0	0	0	204810789	27655788.84	0	0	2516103.1	339751.7	2516103.06	339751.71	1198671498	161857713
85.21	15318627	2069577	0	0	0	0	2553104.6	344929.4	10212418	1379718	231311274.5	31250606.74	0	0	0	0	30637254.9	4139153.2	1592626634	215166981
85.31	17528045	2366421	2504006	338060.1	0	0	0	0	0	0	236378205.1	31912875.99	2504006.4	338060.1	0	0	42568109	5747022.2	1697215545	229137154
85.41	26824034	3607614	2235336	300634.5	0	0	0	0	2235336.2	300634.5	201627324.7	27117231.01	0	0	0	0	58118741.1	7816496.7	1721655937	231548684
85.51	31887755	4281940	0	0	0	0	0	0	6377551	856388	173469387.8	23293752.6	0	0	0	0	29761904.8	3996477.2	1649234694	221461927
85.61	5260942.8	711545.2	0	0	0	0	0	0	0	0	189920033.7	25686780.47	2630471.4	355772.6	0	0	15782828.3	2134635.5	1275252525	172478548
85.71	37560096	5070902	0	0	2504006.4	338060.1	2504006.4	338060.1	0	0	281450320.5	37997958.27	0	0	2504006.4	338060.1	42568109	5747022.2	1789863782	241645379
85.81	13706140	1856677	0	0	2741228.1	371335.4	5482456.1	742670.8	0	0	277686403.5	37616277.12	0	0	0	0	41118421.1	5570031.2	1807839912	244895703
85.91	6823144.1	918168.8	0	0	0	0	2274381.4	306056.3	2274381.4	306056.3	181950509.5	24484500.04	0	0	6823144.1	918168.8	43213246	5815068.8	1375090975	185041609
86.01	22865854	3088675	0	0	7621951.2	1029558	0	0	2540650.4	343186.1	272357723.6	36789549.87	0	0	0	0	55894308.9	7550094.2	1392276423	188065983
86.11	12000768	1617803	0	0	0	0	0	0	2400153.6	323560.6	288498463.9	38891986.01	0	0	0	0	55203533	7441894.2	1451612903	195689460
86.21	2630471.4	355772.6	0	0	0	0	2630471.4	355772.6	7891414.1	1067318	152041245.8	20563655.28	2630471.4	355772.6	0	0	10521885.5	1423090.3	1102167508	149068712
86.31	2400153.6	323560.6	0	0	4800307.2	647121.2	0	0	7200460.8	970681.8	180491551.5	24331758.3	0	0	0	0	7200460.83	970681.85	1217837942	164174656
86.41	0	0	0	0	2540650.4	343186.1	0	0	2540650.4	343186.1	190548780.5	25738957.47	0	0	7621951.2	1029558	5081300.81	686372.2	1125000000	151962805
86.51	0	0	0	0	7512019.2	1014180	5008012.8	676120.3	0	0	242387820.5	32724220.29	0	0	15024038	2028361	37560096.2	5070901.9	1466846955	198035622
86.61	4960317.5	669453.9	0	0	0	0	2480158.7	334726.9	0	0	202380952.4	27313718.82	0	0	0	0	12400793.7	1673634.7	1044146825	140920044
86.71	9556574.9	1288104	0	0	4778287.5	644051.8	14334862	1932155	0	0	296253822.6	39931210.2	4778287.5	644051.8	0	0	54950305.8	7406595.4	1184059633	159596030
86.81	5314625.9	719079.7	0	0	2657312.9	359539.9	5314625.9	719079.7	2657312.9	359539.9	298150510.2	40340372.5	0	0	0	0	50488945.6	6831257.4	1150085034	155608852
86.91	40246212	5422994	0	0	7102272.7	956999	2367424.2	318999.7	9469697	1275999	383049242.4	51614144.28	2367424.2	318999.7	0	0	118371212	15949983	1830492424	246650534
87.01	5081300.8	686372.2	0	0	2540650.4	343186.1	0	0	0	0	157520325.2	21277538.17	0	0	0	0	25406504.1	3431861	732723577.2	98974871.1
87.11	0	0	0	0	0	0	0	0	0	0	169402356.9	22911754.33	0	0	0	0	15782828.3	2134635.5	511889730.6	69233344.6
87.21	5234505.9	707836.7	0	0	0	0	0	0	0	0	267221524.3	36135064.19	0	0	0	0	28789782.2	3893101.9	1008427554	136364743
87.31	2565681.4	346690.5	0	0	0	0	0	0	2565681.4	346690.5	259133825.9	35015745.45	0	0	0	0	38485221.7	5200358.2	1218185550	164608673
87.41	9968102.1	1345541	0	0	0	0	0	0	0	0	292563795.9	39491632.99	0	0	0	0	27412280.7	3700238.2	911084529.5	122982462
87.51	0	0	0	0	0	0	0	0	0	0	298576732.7	40352793.23	0	0	0	0	18048679.9	2439288	917388613.9	123985525
87.61	0	0	0	0	0	0	0	0	0	0	177469135.8	23928097.85	0	0	0	0	14467592.6	1950660.2	600405092.6	80952396.3
87.71	6883259.9	926523.2	0	0	2294420	308841.1	0	0	0	0	312500000	42064151.98	0	0	0	0	6883259.91	926523.17	1071494126	144228774
87.81	0	0	0	0	2504006.4	338060.1	0	0	0	0	262920673.1	35496313.33	0	0	0	0	20032051.3	2704481	759214743.6	102499830
87.91	0	0	0	0	0	0	0	0	0	0	266862623.8	36066615.71	0	0	0	0	10313531.4	1393878.9	838232260.7	113287505
88.01	0	0	0	0	0	0	0	0	0	0	201596185.7	27250789.48	0	0	0	0	12956053.1	1751336.1	721393034.8	97514393.2
88.11	0	0	0	0	0	0	0	0	0	0	186159240.9	25159513.57	0	0	0	0	10313531.4	1393878.9	626031353.1	84608447.3
88.21	0	0	0	0	0	0	0	0	0	0	176103547.9	23800481.67	0	0	0	0	5156765.68	696939.43	707250412.5	95585243.4
88.31	2643824	357646.3	5287648	715292.6	5287648.1	715292.6	0	0	2643824	357646.3	261738578.7	35406985.17	0	0	0	0	26438240.3	3576463.1	780985617.6	105648721
88.41	0	0	0	0	0	0	0	0	0	0	171747967.5	23199380.33	0	0	0	0	25406504.1	3431861	409044715.4	55252962
88.51	0	0	0	0	0	0	0	0	0	0	291858679	39344970.87	0	0	0	0	21601382.5	2912045.5	896217357.9	120817534
88.61	0	0	0	0	0	0	0	0	0	0	213895631.1	28887539.47	0	0	0	0	12641585.8	1707301.4	526901294.5	71160321.8
88.71	0	0	0	0	0	0	0	0	0	0	135981116.6	18374599.1	0	0	0	0	15394088.7	2080143.3	345340722.5	46664547.9
88.81	0	0	0	0	2578382.8	348469.7	0	0	0	0	296514026.4	40074017.46	0	0	0	0	25783828.4	3484697.2	740511551.2	100080503
88.91	0	0	0	0	2480158.7	334726.9	0	0	0	0	211309523.8	28518735.83	0	0	0	0	24801587.3	3347269.5	504464285.7	68083460.9
89.01	5287648.1	715292.6	0	0	0	0	0	0	0	0	138007614.2	18669137.64	0	0	0	0	10575296.1	1430585.3	357973773.3	48425311
89.11	0	0	0	0	0	0	0	0	0	0	200281803.5	27044235.77	0	0	0	0	2516103.06	339751.71	533917069.2	72095311.9
89.21	0	0	0	0	5234505.9	707836.7	0	0	2617252.9	353918.4	245498325	33197541.83	0	0	0	0	18320770.5	2477428.5	783082077.1	105892372
89.31	2565681.4	346690.5	0	0	0	0	0	0	2565681.4	346690.5	135467980.3	18305260.99	0	0	0	0	7697044.33	1040071.6	450533661.7	60878860.4
89.37	15318627	2069577	0	0	5106209.2	689858.9	0	0	0	0	218035130.7	29456973.68	0	0	0	0	5106209.15	689858.87	684232026.1	92441088.4
89.41	22321429	3012543	0	0	0	0	0	0	0	0	201884920.6	27246773.43	0	0	0	0	4960317.46	669453.89	676587301.6	91313511
89.47	12400794	1673635	0	0	0	0	0	0	2480158.7	334726.9	150793650.8	20351398.34	0	0	0	0	2480158.73	334726.95	585317460.3	78995559.3
89.51	12703252	1715930	0	0	0	0	10162602	1372744	10162602	1372744	174288617.9	23542566.43	0	0	0	0	25406504.1	3431861	826219512.2	111604120
89.57	5056634.3	682920.6	0	0	2528317.2	341460.3	2528317.2	341460.3	0	0	192152103.6	25950981.09	0	0	0	0	12641585.8	1707301.4	620449029.1	83794352.1
89.61	5081300.8	686372.2	0	0	2540650.4	343186.1	0	0	0	0	181656504.1	24537806.12	0	0	0	0	7621951.22	1029558.3	627794715.4	84801285.2
89.67	7584951.5	1024381	0	0	7584951.5	1024381	0	0	0	0	218446601.9	29502167.97	0	0	0	0	5056634.3	682920.55	724110032.4	97794223.5
89.71	2591210.6	350267.2	0	0	7773631.8	1050802	5182421.2	700534.4	0	0	152363184.1	20595712.36	0	0	0	0	7773631.84	1050801.7	694962686.6	93941667.6
89.77	33353859	4506977	0	0	10262726	1386762	2565681.4	346690.5	0	0	283764367.8	38343974.72	0	0	0	0	12828407.2	1733452.7	1058087028	142975182
89.87	12828407	1733453	0	0	7697044.3	1040072	0	0	0	0	191399835.8	25863114.95	2565681.4	346690.5	0	0	17959770.1	2426833.8	941605090.3	127235431
89.97	12400794	1673635	0	0	0	0	4960317.5	669453.9	0	0	190972222.2	25773974.87	0	0	0	0	7440476.19	1004180.8	886904761.9	119698356
90.07	31565657	4269271	0	0	0	0	2630471.4	355772.6	2630471.4	355772.6	255155723.9	34509940.52	2630471.4	355772.6	0	0	13152356.9	1778862.9	1096906566	148357167
90.17	23915816	3235859	0	0	5314625.9	719079.7	0	0	2657312.9	359539.9	227200255.1	30740658.19	0	0	0	0	7971938.78	1078619.6	890997023.8	120553716
90.27	12891914	1742349	0	0	0	0	2578382.8	348469.7	2578382.8	348469.7	254744224.4	34428808.04	2578382.8	348469.7	0	0	12891914.2	1742348.6	964315181.5	130327674
90.37	4984051	672770.6	0	0	0	0	0	0	0	0	183413078.1	24757957.31	0	0	0	0	19936204.1	2691082.3	848783891.5	114572830
90.47	12641586	1707301	0	0	2528317.2	341460.3	0	0	5056634.3	682920.6	207322006.5	27999742.75	0	0	0	0	12641585.8	1707301.4	1027002427	138701165
90.57	7070135.7	952523.2	0	0	0	0	0	0	0	0	195135746.6	26289641.39	2356711.9	317507.7	0	0	9426847.66	1270031	1035067873	139449402
90.67	12641586	1707301	0	0	2528317.2	341460.3	0	0	0	0	220722087.4	29809482.22	0	0	0	0	22754854.4	3073142.5	1031806230	139349939
90.77	14740566	1988753	0	0	0	0	0	0	2456761	331458.8	248624213.8	33543628.37	0	0	0	0	22110849.1	2983129	1015625000	137025059
90.87	32868123	4438984	0	0	5056634.3	682920.6	0	0	2528317.2	341460.3	228054207.1	30799717.02	2528317.2	341460.3	0	0	32868123	4438983.6	1030036408	139110917
90.97	10113269	1365841	0	0	0	0	5056634.3	682920.6	0	0	202771035.6	27385114.25	0	0	0	0	7584951.46	1024380.8	772148058.3	104281969
91.07	24801587	3347269	0	0	4960317.5	669453.9	2480158.7	334726.9	7440476.2	1004181	380952381	51414058.96	0	0	0	0	24801587.3	3347269.5	1568948413	211748266
91.17	0	0	0	0	0	0	0	0	0	0	162698412.7	21958087.68	0	0	0	0	4960317.46	669453.89	437996031.7	59112778.7
91.27	0	0	0	0	0	0	0	0	0	0	13823987.54	1806342.985	0	0	0	0	243380.062	31801.813	37918613.71	4954722.48
91.37	18853695	2540062	0	0	4713423.8	635015.5	0	0	0	0	290346908	39116954.33	0	0	0	0	11783559.6	1587538.7	808823529.4	108968659
91.47	7773631.8	1050802	0	0	5182421.2	700534.4	0	0	0	0	215070480.9	29072179.01	0	0	0	0	5182421.23	700534.43	585613598.7	79160391
91.57	7812500	1056250	0	0	2604166.7	352083.3	2604166.7	352083.3	2604166.7	352083.3	203125000	27462500	0	0	0	0	13020833.3	1760416.7	892187500	120623750
91.67	7735148.5	1045409	0	0	0	0	2578382.8	348469.7	2578382.8	348469.7	236695544.6	31989520.02	5156765.7	696939.4	0	0	10313531.4	1393878.9	920482673.3	124403689
91.77	20649780	2779570	0	0	2294420	308841.1	2294420	308841.1	0	0	306075624.1	41199397.02	22944200	3088411	0	0	11472099.9	1544205.3	1173366373	157941317
91.87	2400153.6	323560.6	0	0	0	0	2400153.6	323560.6	0	0	268337173.6	36174076.84	0	0	0	0	21601382.5	2912045.5	971582181.3	130977337
91.97	6764069.3	909963.5	0	0	2254689.8	303321.2	0	0	6764069.3	909963.5	241702741.7	32516029.18	0	0	0	0	45093795.1	6066423.4	900072150.1	121085810
92.07	12400794	1673635	0	0	0	0	0	0	4960317.5	669453.9	251984127	34008257.75	0	0	0	0	19841269.8	2677815.6	1224702381	165288166
92.17	7134703.2	961516.9	0	0	0	0	0	0	9512937.6	1282023	419044901.1	56473093.16	0	0	0	0	45186453.6	6089607.1	1347031963	181534393
92.27	14400922	1941364	0	0	0	0	0	0	4800307.2	647121.2	248655914	33520879.79	0	0	0	0	28801843.3	3882727.4	1033506144	139325201
92.37	12283805	1657294	0	0	0	0	0	0	4913522	662917.6	268769654.1	36261590.35	0	0	0	0	51591981.1	6960634.3	1132566824	152802497
92.47	4890453.8	659697	0	0	0	0	0	0	0	0	253325508.6	34172302.86	0	0	0	0	48904538.3	6596969.7	1151212833	155292666
92.57	4913522	662917.6	0	0	0	0	0	0	4913522	662917.6	295794025.2	39907636.91	0	0	0	0	34394654.1	4640422.9	938482704.4	126617253
92.67	20729685	2802138	0	0	0	0	0	0	15547264	2101603	288142620.2	38949714.53	0	0	0	0	46641791	6304809.9	1099709784	148653407
92.77	5081300.8	686372.2	0	0	0	0	0	0	5081300.8	686372.2	198170731.7	26768515.76	0	0	0	0	22865853.7	3088674.9	888719512.2	120046498
92.87	5081300.8	686372.2	0	0	0	0	0	0	5081300.8	686372.2	254573170.7	34387247.17	0	0	0	0	35569105.7	4804605.4	963414634.1	130136169
92.97	16801075	2264924	0	0	4800307.2	647121.2	0	0	2400153.6	323560.6	217453917.1	29314591.78	0	0	0	0	21601382.5	2912045.5	1059907834	142884368
93.07	20729685	2802138	0	0	5182421.2	700534.4	0	0	7773631.8	1050802	294361525.7	39790355.85	0	0	0	0	49233001.7	6655077.1	1054622720	142558757
93.17	7548309.2	1019255	0	0	5032206.1	679503.4	0	0	2516103.1	339751.7	220410628	29762249.41	0	0	0	0	57870370.4	7814289.2	920390499.2	124281174
93.27	7370283	994376.3	0	0	4913522	662917.6	0	0	17197327	2320211	195066823.9	26317827	0	0	0	0	46678459.1	6297716.8	911949685.5	123037499
93.37	2400153.6	323560.6	0	0	0	0	0	0	2400153.6	323560.6	182891705.1	24655318.92	0	0	0	0	28801843.3	3882727.4	773809523.8	104315943
93.47	10262726	1386762	0	0	2565681.4	346690.5	0	0	5131362.9	693381.1	205254515.6	27735243.92	0	0	0	0	23091133	3120214.9	903633004.9	122104411
93.57	2553104.6	344929.4	0	0	5106209.2	689858.9	0	0	2553104.6	344929.4	212928921.6	28767114.81	0	0	0	0	45955882.4	6208729.8	921670751.6	124519526
93.67	7512019.2	1014180	0	0	2504006.4	338060.1	0	0	2504006.4	338060.1	165264423.1	22311968.38	0	0	0	0	37560096.2	5070901.9	773737980.8	104460579
93.77	0	0	0	0	0	0	0	0	2565681.4	346690.5	160611658.5	21702828.37	0	0	0	0	17959770.1	2426833.8	571633825.9	77242654.3
93.87	17361111	2356867	0	0	0	0	0	0	0	0	201967592.6	27418222.74	0	0	0	0	37615740.7	5106545.8	755208333.3	102523727
93.97	10113269	1365841	0	0	0	0	0	0	2528317.2	341460.3	186084142.4	25131476.42	0	0	0	0	53094660.2	7170665.8	823220064.7	111179466
94.07	7659313.7	1034788	0	0	0	0	0	0	10212418	1379718	215482026.1	29112044.25	0	0	0	0	40849673.2	5518870.9	855290032.7	115551360
94.13	7812500	1056250	0	0	0	0	0	0	0	0	226041666.7	30560833.33	0	0	0	0	28645833.3	3872916.7	932812500	126116250
94.17	2630471.4	355772.6	0	0	2630471.4	355772.6	0	0	10521886	1423090	193076599.3	26113707.57	0	0	0	0	39457070.7	5336588.7	958543771	129643529
94.23	13152357	1778863	0	0	0	0	0	0	0	0	203598484.8	27536797.9	0	0	0	0	28935185.2	3913498.4	957491582.5	129501220
94.33	13152357	1778863	0	0	0	0	0	0	0	0	279356060.6	37783048.29	0	0	0	0	47348484.8	6403906.5	1081123737	146222532
94.43	15470297	2090818	0	0	2578382.8	348469.7	0	0	0	0	273308580.9	36937790	0	0	0	0	48989273.9	6620924.6	1018976898	137715232

APPENDIX E. PLATES

Plate 1: Major Taxa. The 5µm scale bar is for all the pictures. All pictures in all the plates are taken from 81.38 mcd except for *Blackities spinosus* and unindentified sp. Which are from 81.48 mcd.

Small *reticulofenestr*

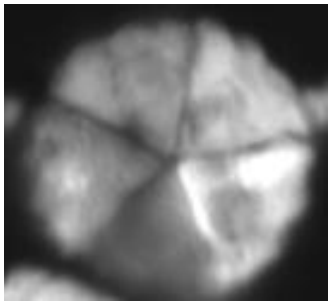

Pemma

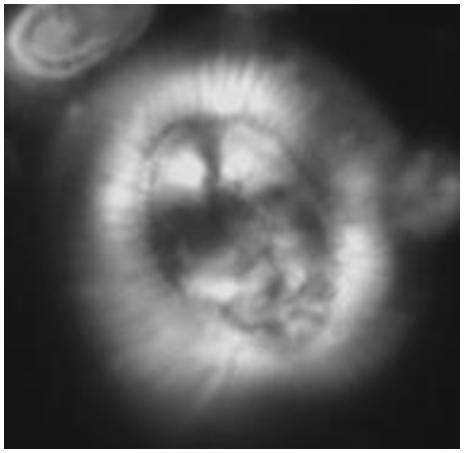

Coccolithus pelagicus

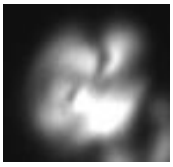

Reticulofenestra bisecta

Reticulofenestra reticulatum

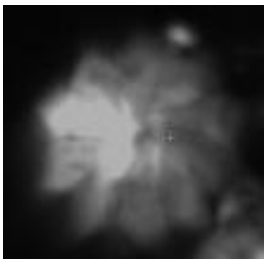

Discoaster barbadiensis

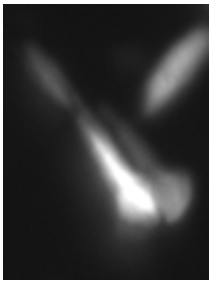

Zygryhablithus bijugatus

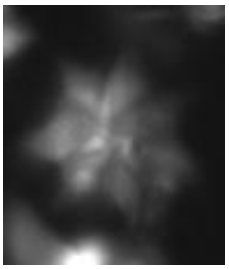

Discoaster saipanensis

5 µm

Plate 2: Minor Taxa

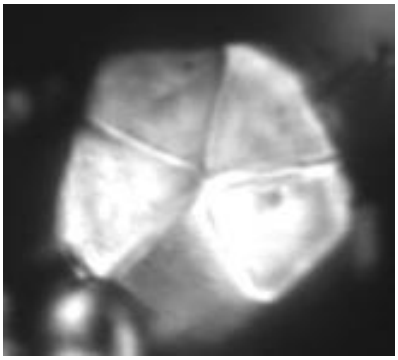

***Braarudosphaera* spp.**

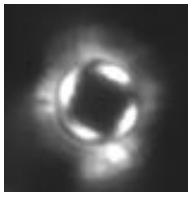

Calcidiscus protoannulus

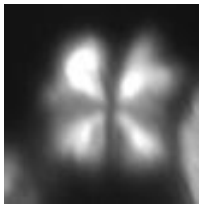

Sphenolithus moriformis

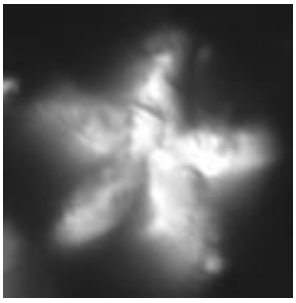

Discoaster tanii

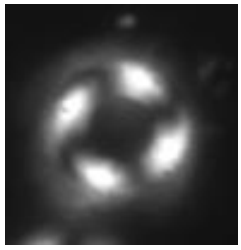

Coccolithus formosus

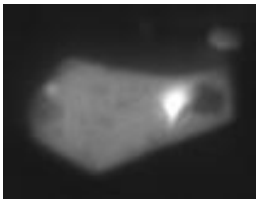

Bramletteius serraculoides

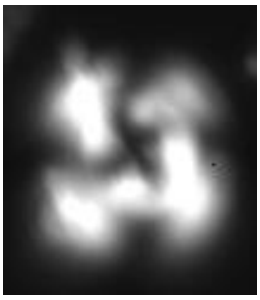

Cyclicargolithus floridanus

5 µm

Plate 3: Rare Taxa

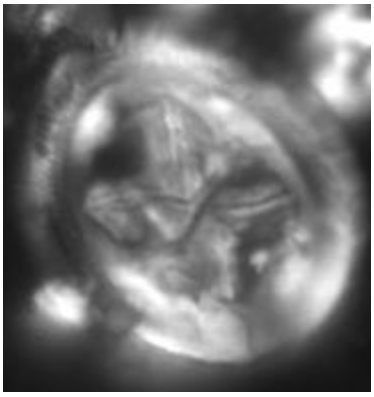

Chiasmolithus grandis

Blackities spinosus

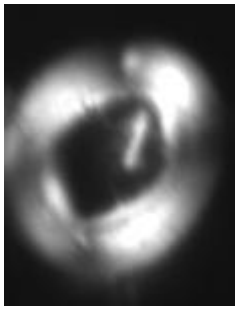

Reticulofenestra (7 -13 µm)

Coccolithus minimus

c.f. Bramletteius serraculoides

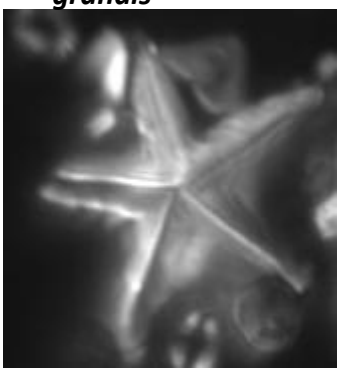

***Micrantholithus* spp.**

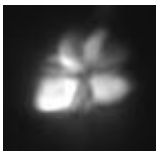

Sphenolithus spiniger

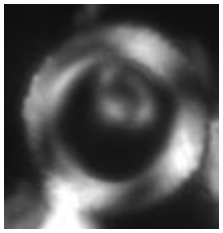

Ericsonia sp.

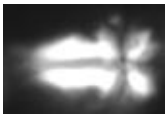

Sphenolithus radians

5 µm

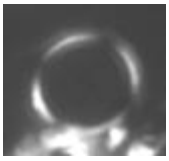

Coronocyclus bramletti

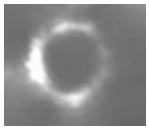

Coronocyclus sp.

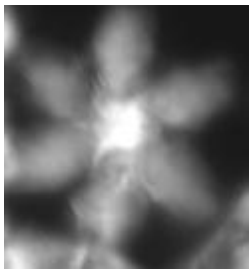

Discoaster nodifer

Pyrocyclus orogensis

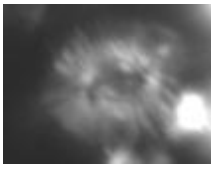

c.f. *Coccolithus pelagicus*

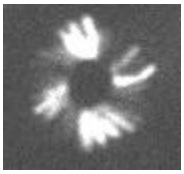

Pedinocyclus larvalis

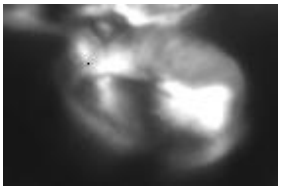

Helicosphaera compacta

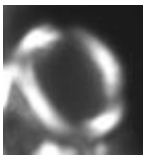

***Unidentified* sp.**

VITA

Name:	Chioma Uche Okafor
Address:	c/o Department of Geology and Geophysics Texas A&M University College Station, TX 77843-3115
Email Address:	chiudeze@gmail.com
Education:	B.A., Geology, University of Nigeria-Nsukka, 2001
	M.S., Geology, University of Missouri-Rolla, 2003
	Ph.D., Geology, Texas A&M University, 2009